DESIGN OF A DEPLOYABLE STRUCTURE TO BE USED AS TEMPORARY RAMP

A Thesis Submitted to the
Graduate School of Engineering and Sciences of
İzmir Institute of Technology
in Partial Fulfillment of the Requirements for the Degree of

MASTER OF SCIENCE

in Mechanical Engineering

By
Elvan DOĞAN KUMTEPE

December 2017
İZMİR

We approve the thesis of **Elvan DOĞAN KUMTEPE**

Examining Committee Members:

Assoc. Prof. Dr. Gökhan KİPER

Department of Mechanical Engineering, Izmir Institute of Technology

Prof. Dr. Bülent YARDIMOĞLU

Department of Mechanical Engineering, Izmir Institute of Technology

Assist. Prof. Dr. Erkin GEZGİN

Department of Mechatronics Engineering, Izmir Katip Celebi University

29 December 2017

Assoc. Prof. Dr. Gökhan KİPER

Supervisor,

Department of Mechanical Engineering,

Izmir Institute of Technology

Prof. Dr. Metin TANOĞLU
Head of the Department of
Mechanical Engineering

Prof. Dr. Aysun SOFUOĞLU
Dean of the Graduate School of
Engineering and Sciences

ACKNOWLEDGMENTS

First and foremost, I would like to express my sincere gratitude to my supervisor Assoc. Prof. Dr. Gökhan Kiper for his insightful guidance and considerable encouragements to complete this study.

I am also grateful to Prof. Dr. Metin Tanoğlu and Prof. Dr. Bülent Yardımoğlu for sharing their knowledge during structural design and experimental stage of this thesis.

I would like to thank the jury members; Assist. Prof. Dr. Özgür Kilit and Assist. Prof. Dr. Erkin Gezgin for their attendance at my thesis defence seminar and valuable recommendations.

I would like to thank my dear friends in RAML and my partners in crime, Mert Kanık and Emre Uzunoğlu for their friendship.

I would like to thank my lovely family for their endless support. Finally, I would especially like to express my gratitude to my beloved husband Erdem Kumtepe who has always supported and helped me to overcome the difficulties without complaining.

This study is financially supported by 1512 – Entrepreneurship Multi-phase Programme (Teknogirişim Sermaye Desteği Programı) of The Scientific and Technological Research Council of Turkey (TÜBİTAK).

ABSTRACT

DESIGN OF A DEPLOYABLE STRUCTURE TO BE USED AS TEMPORARY RAMP

Portable ramps, used generally by wheelchair users, offer temporary solution to increase accessibility and mobility. It is expected that these ramps should be compact and lightweight in terms of ease of handling and storage. Different types of portable ramps in the market, which can be used by wheelchair users, are generally made of aluminum and their compactness is convenient to be redesigned and developed in the matter of increasing compactness.

In this context, the main objectives of the thesis are to determine the wheelchair users' inclinations and design a product to achieve better compactness and lightness by comparison with similar products in the market. To this end, a case study addresses challenges of designing of a deployable structure to be used as temporary ramp. The design approach and its implementation are described briefly and example of parametric analyses are illustrated in this study.

First, the geometrical design is performed considering several alternative forms. The link lengths are optimized for compact rolling. Then load bearing capacity of the assembly is analyzed analytically and also verified with finite-element analyses. Material selection is performed for the composite panels and the panel thickness is determined according to strength of materials calculations. Finally, prototypes are manufactured and tested according to standards. The final design is 15,1% more compact and has 20,25% less weight compared to the best rival product available in the market. Also the product was tested by some wheelchair users and their opinions about the product are asked. Positive feedbacks are taken.

ÖZET

GEÇİCİ RAMPA OLARAK KULLANILABİLEN KATLANABİLİR YAPI TASARIMI

Taşınabilir rampalar, genellikle tekerlekli sandalye kullanıcılarının ulaşılabilirlik ve erişilebilirliğini geçici olarak arttırmaya yönelik kullandığı ürünlerdir. Bu tür rampaların, taşıma ve depolama kolaylığı sunması açısından kompakt ve hafif olması beklenmektedir. Pazarda bulunan tekerlekli sandalye kullanıcılarına yönelik değişik tipteki rampalar genellikle alüminyum malzemeden imal edilmekte ve kompaktlık açısından yeniden tasarlanma ve geliştirilmeye uygun yapıdadırlar.

Bu bağlamda, tezin ana hedefleri başta tekerlekli sandalye kullanıcılarının eğilimlerini ortaya çıkarmak ve pazarda konumlanan ürünlere göre daha kompakt ve hafif bir ürün tasarlamaktır. Bu amaçla, bir vaka çalışması yürütülerek tasarım süreci zorluklarının da ele alındığı geçici rampa tasarımı yapılmıştır. Bu çalışmada, tasarım aşamasında kullanılan yaklaşımlar ve uygulamaları detaylı şekilde açıklanmış ve parametrik analizler örneklerle ortaya konmuştur.

Öncelikle çeşitli formlar ele alınarak geometric tasarım yapıldı. Uzuv boyutları, kompakt katlanma için eniyilendi. Sonra sistemin yük taşıma kapasitesi analitik olarak analiz edildi ve sonlu eleman analizleri ile doğrulandı. Kompozit paneller için malzeme seçimi yapıldı ve panel kalınlıkları mukavemet hesapları ile belirlendi. Son olarak prototipler imal edilerek standartlar uyarınca test edildi. Tasarlanan rampa piyasadaki en iyi rakibinden %15,1 daha kompakt ve %20,25 daha hafiftir. Ayrıca tekerlekli sandalye kullanıcılarına ürün test ettirilerek fikirleri alındı. Olumlu geribildirimler alındı.

TABLE OF CONTENTS

LIST OF FIGURES

LIST OF TABLES

CHAPTER 1

INTRODUCTION

The term accessibility refers to products and/or services which are specifically designed for people with disabilities to provide equal accesses with people who have no disability. Although the term directly refers to disabled people, the overall benefits of increased accessibility may affect positively everyone.

The increasing mobility in the globalized world, has led to need of accessibility for wheelchair users. The main objective of this study is to design a light and compact unilateral deployable ramp which offers temporary solution to increase accessibility for wheelchair users.

Table 1.1 presents the design methodology and design tools which are guiding throughout the design process to reduce complexity and development time. This dissertation presents numerical, analytical and empirical methodology for the design of a unilateral ramp and its implementation with parametric study with the integration of Design Thinking approach. Several design tools are adapted as methods of the thesis while following steps of design thinking approach. These tools are semi-structured interview, morphologic chart, convex hull and smallest enclosing circle algorithm.

The study in Chapter 2 presents a patent survey for deployable ramps. Furthermore, patents are categorized according to their deployment types. In Chapter 3, the conceptual design starts with implementation of design thinking approach to the selected problem to reduce development time and uncover the users' expectations. Chapter 4 gives brief information about detailed design process, which includes geometric and strength calculations. Moreover, CAD models of alternative designs are presented. Chapter 5 comprises prototyping and testing steps of the study. Finally, Chapter 6 presents conclusion and discussions for the success of the final assembly, future studies of the product and design challenges, which are experienced during application of whole design process.

Table 1.1 Design Methodology

CHAPTER 2. LITERATURE AND PATENT SURVEY

- TELESCOPIC RAMPS
- ROLLABLE RAMPS
- FOLDABLE RAMPS
- SCISSOR RAMPS

CHAPTER 3. CONCEPTUAL DESIGN

- UNDERSTAND
- OBSERVE
- DEFINE
  - Semi-Structured Face to Face Interview
- IDEATE
  - Morphologic Chart
- FIRST PROTOTYPE AND TEST

CHAPTER 4. DETAILED DESIGN

- GEOMETRIC CALCULATIONS
- KINEMATIC ANALYSIS AND DESIGN
  - Convex Hull Algorithm
  - Smallest Enclosing Circle Algorithm
- MATERIAL SELECTION
  - Aluminium 6061 T6 and 7075 T6
  - Sandwich Composites
    - Flexural Test ASTM C-393
- STRENGTH ANALYSIS
  - Use of Singularity Function to Determine the Maximum Deflection
  - Deflection of a Simply-Supported Sandwich Beam with Antiplane Core and Thin Faces (Symmetrical Load)

CHAPTER 5. PROTOTYPE AND TEST

- DESIGN VERIFICATIONS
- FIELD TEST

CHAPTER 6. CONCLUSION

CHAPTER 2

LITERATURE AND PATENT SURVEY

This chapter presents a patent review for deployable ramps. Furthermore, patents are categorized according to their deployment types.

2.1. Survey on Deployable Ramps

Deployable ramps can be categorized into four main types according to their deployment method in consideration of patent survey. As illustrated in Fig 2.1, these deployment types can be listed as telescopic, rollable, foldable and scissors.

TELESCOPIC	ROLLABLE	FOLDABLE	SCISSORS
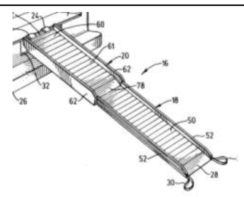	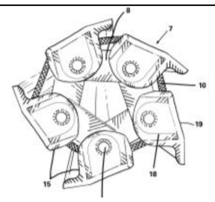	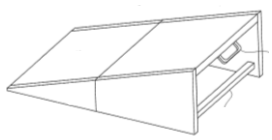	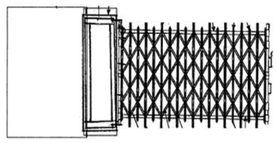

Figure 2.1 Categorization of Deployable Ramps

2.1.1. Telescopic Ramps

Telescopic structures consist of hollow cross-sectional profiles that slide into another member to achieve deployment. This type of ramps can be categorized under the title of telescopic ramps.

2.1.1.1. Telescoping and Magnetic Tailgate Ramp

The ramp members comprise a plurality of aligned, telescoping members that form an extendable ramp, wherein the members form into one another and are extendable by separation of a first ramp end from an opposing second ramp end, the members being connected there between (Fig. 2.2). The first ramp end connects to upstanding portions of the frame and within a slotted channel. The channel allows the first ramp end to be moved horizontally and vertically within the frame to position the condensed ramp within the frame interior, while also allowing the extended ramp to clear the frame and facilitate a smooth transition between the ramp and the frame when loading objects thereacross. The ramp members are box structures that condense into one another and include progressively tapering cross sections (U.S. Patent No. 20,130,028,693 A1, 2013).

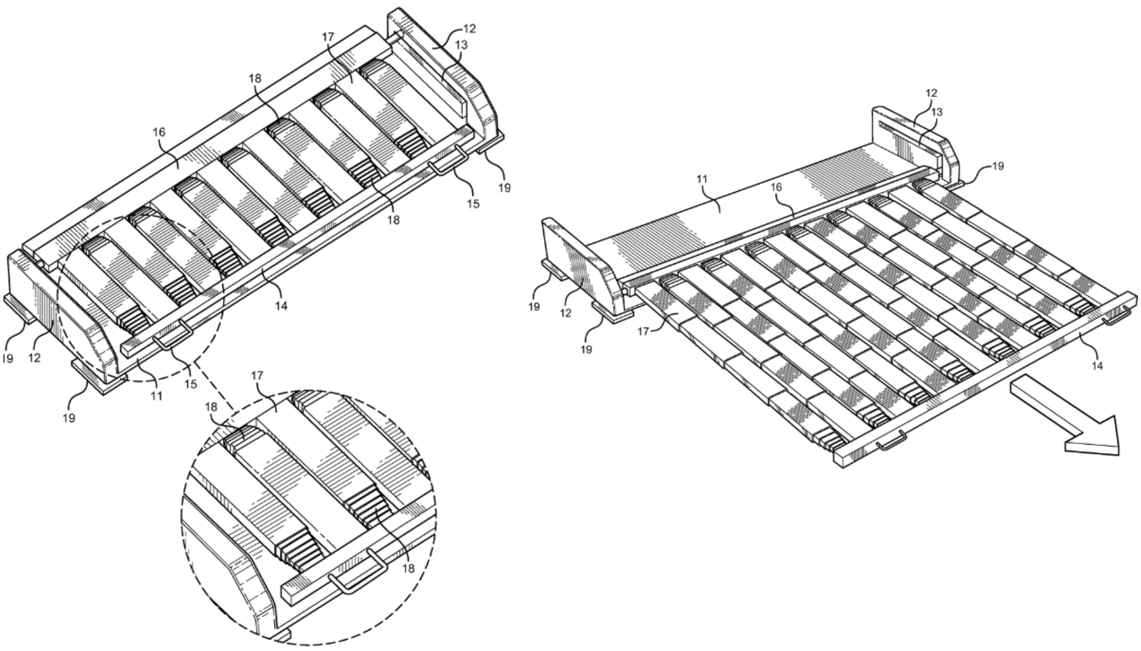

Figure 2.2 Telescoping and magnetic tailgate ramp

2.1.1.2. Telescoping Truck Loading Ramp Assembly

A ramp assembly (Fig. 2.3) facilitating the loading and unloading of a truck comprises two telescoping ramp sections including a forward section and a rearward section movable relative to each other between a full-length ramp operating configuration and a stowed configuration. In one embodiment, the side rails of the rearward section of the ramp are slidably received within sleeve-like side rails of the forward section. In the stowed configuration of the ramp assembly, the ramp assembly is approximately half its fully extended length and fits between the existing longitudinal chassis frame members under the cargo deck of the truck without interfering with the housing of the truck differential. Accordingly, the invention makes possible the use of a full-length ramp with virtually all truck sizes (U.S. Patent No. US5813071 A, 1998).

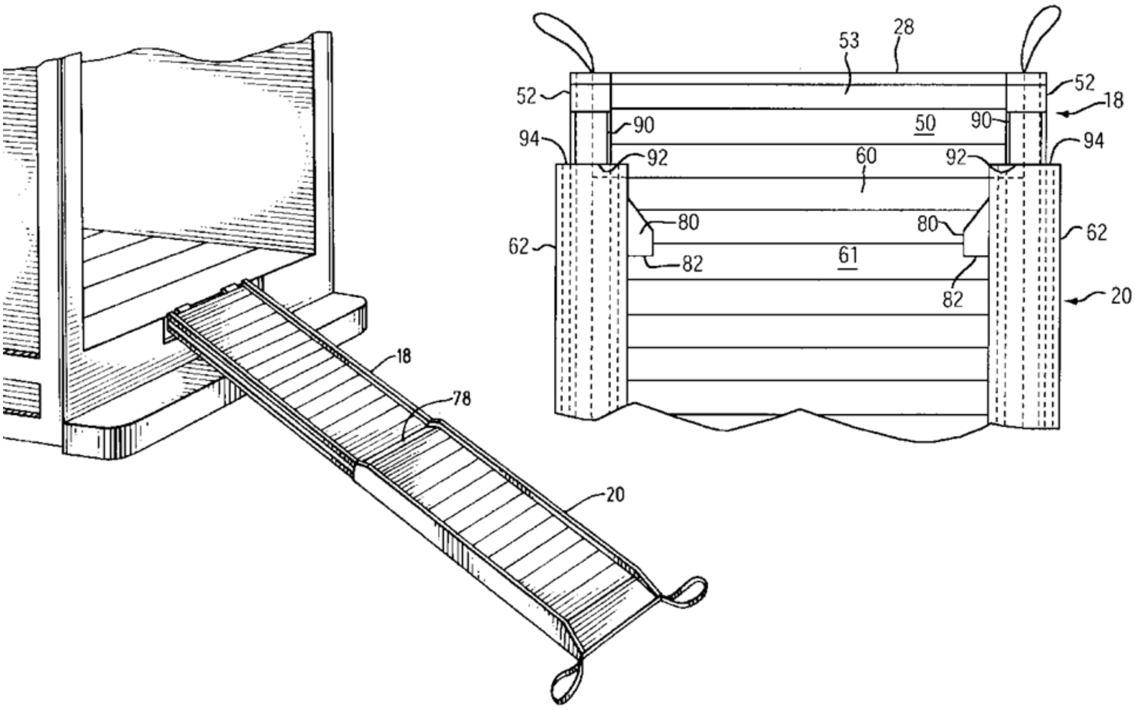

Figure 2.3 Telescoping truck loading ramp assembly

2.1.1.3. Tailgate Enclosed Telescopic Ramp Structure

A conventional pickup truck equipped with a tailgate for closing the rear end of the load bed of the pickup truck is provided and the upper margin of the hollow/tailgate is provided with at least one elongated slot extending along the upper margin from which a loading ramp structure consisting of at least three telescopically engaged ramp sections may be extended and disposed at a rearwardly and downwardly inclined position when the tailgate is in its horizontally rearwardly projecting position, the telescopically engaged ramp sections including an outer wide ramp section, at least one intermediate and somewhat narrower ramp section and an inner narrow ramp section with the ramp sections inwardly of the outer wide ramp section being progressively narrower in width and thickness toward the innermost narrow ramp section (Fig. 2.4). The smaller transverse area of the inner ramp section received through the slot in the free margin of the tailgate enabling the inner end of the narrow ramp section to be rearwardly and downwardly inclined relative to the tailgate when the latter is in its rearwardly projecting position without interference with the opposite side edges of the slot in which the ramp structure may be telescopically received, the outer wide ramp section being snugly received in the slot when the ramp structure is in the fully retracted position (U.S. Patent No. US5312149, 1994).

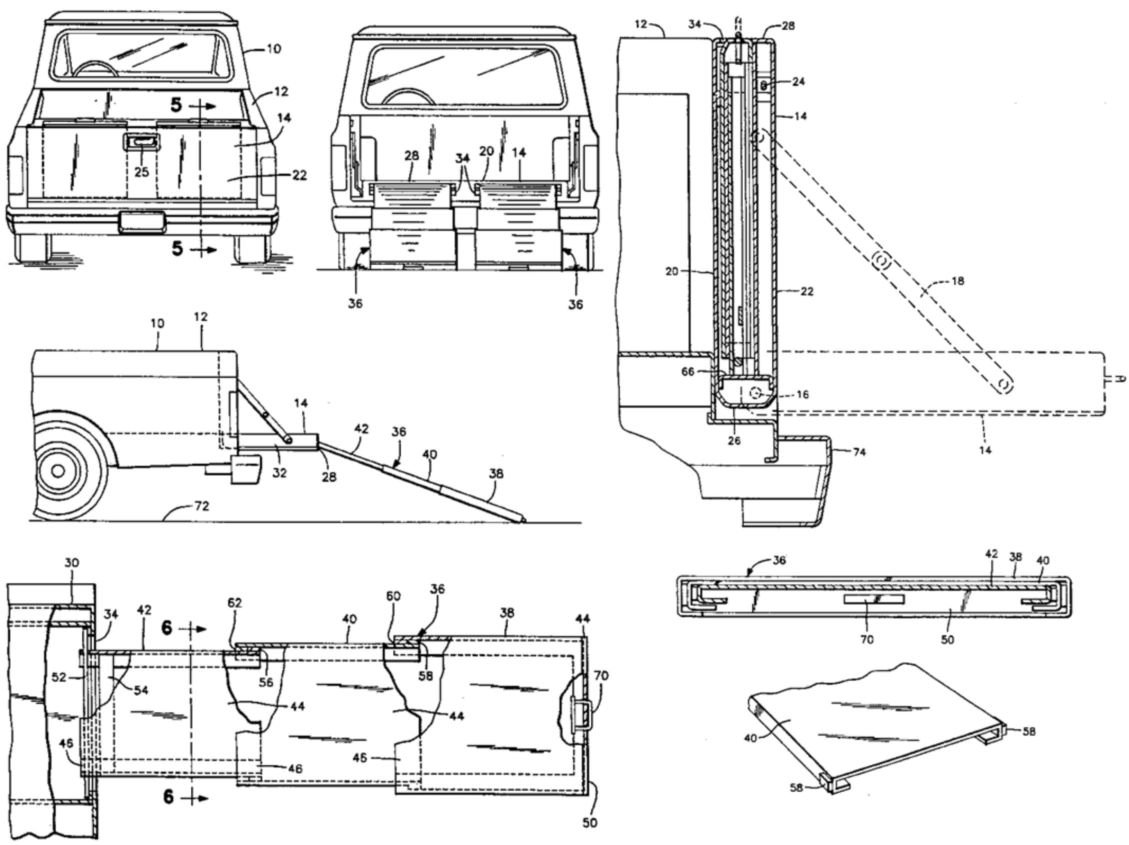

Figure 2.4 Tailgate enclosed telescopic ramp structure

2.1.2. Rollable Ramps

Rollable ramps consist of serial chain members which are able to rotate about the connection axes. Thus, they can be rolled out like carpet on one side and carry load on the other side due the constructional design of the load-bearing members with mechanical motion limits.

2.1.2.1. Multi Tread Segmented Self-Deploying Roll up Ramp

A roll out multi-tread ramp design is supported by its arched design and the identical shape and angle of each of its multiple treads adjacent one another for creating a surface area that distributes stress from weight placed on the surface of the ramp. Rectangular links comprise two holes per link and hold each tread that about one another together, a cylindrical pin inserts smoothly through an end of each ramp tread, passes through the link hole, then preferably re-enters tread of the ramp which connects multiple treads together and creates strength. When weight is placed on ramp and allows the ramp to be rolled up. Ramp length is adjustable by using varying numbers of treads in each ramp assembly. An elastic cord runs through all treads to assist with self-deployment of ramp and assists in holding ramp treads in place (Fig 2.5) (U.S. Patent No. 7,958,586 B1, 2011).

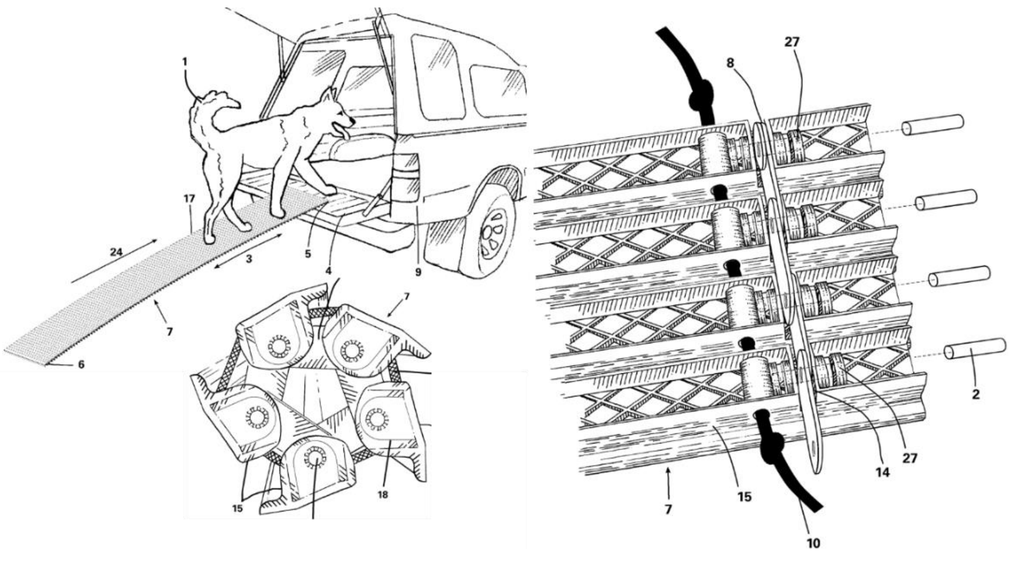

Figure 2.5 Multi tread segmented self-deploying roll up ramp

2.1.2.2. Roll up Ramp System

The roll up ramp system includes a plurality of load-bearing links which are connected to one another on the side plates. Each side plate has at least two apertures appointed for receiving and housing a pin, for pivotally connecting the load bearing links to one another. The load-bearing links are adapted to rotate about the pin to form an unrolled and a rolled configuration. The roll up configuration achieved by the ramp structure provides for convenient storage usefully.

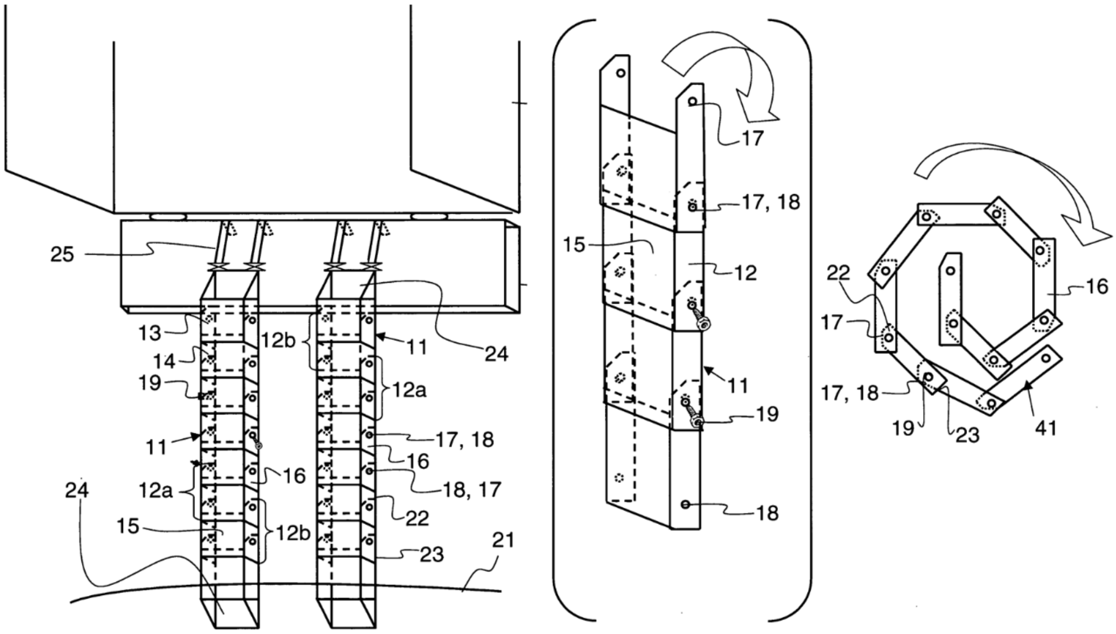

Figure 2.6 Roll up ramp system

Chain link rigidity is provided when the links are flexed in one direction but not in the opposite direction, whereupon the flexible connection is achieved. As a result, the structure has sufficient flexibility to be rolled-up, for storage conveniently (Fig 2.6). When the links are in the unrolled position the ramp structure endows the ramp configuration with sufficient rigidity to securely hold heavy objects. The system provides a ramp which is readily attachable to various vehicles, such as trucks. (U.S. Patent No. 20,060,214,456 A1, 2006).

2.1.2.3. Loading Ramp Device Which Rolls Up for Convenient Storage

A loading ramp (Fig. 2.7) structure is provided which is constructed out of a plurality of relatively small and rectangular links that are joined end to end to form a span of any desired length. The manner in which these links are joined together allows the span to be rolled up for storage when it is not in use and to be unrolled to form a ridged span when it is to be employed in the loading or unloading of wheeled load materials such as small supplementary vehicles. It is an additional objective of this invention to provide such a loading device that can be rolled up for easy and compact storage when the device is not in use and which is constructed in a manner and of a material that makes it light weight enough for almost all individuals of a large variety of physical capabilities. When the invention is in unrolled and deployed orientation, is strong enough to easily support the weight of the vehicles and their occupants that are typically loaded and transported in this manner.

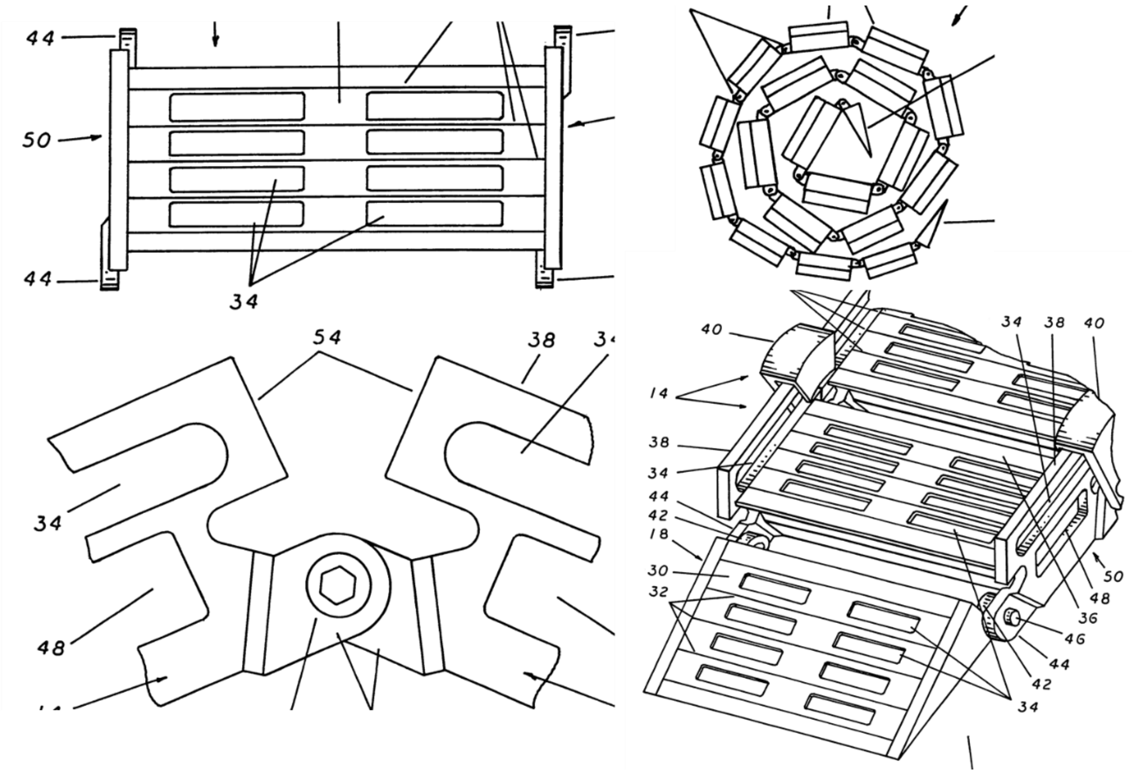

Figure 2.7 Loading ramp device which rolls up for convenient storage

It is a still further objective of the present invention to provide such a loading device that is relatively simple and inexpensive in its design and construction which allows it to be used by average people without the need for specialized tools or knowledge (U.S. Patent No. 6,643,878 B2, 2003).

2.1.2.4. Loading Ramp Device Which Rolls Up for Storage

A loading ramp (Fig. 2.8) structure is provided which is constructed out of a plurality of relatively small and rectangular links that are joined end to end to form a span of any desired length. Moreover, the manner in which these links are joined together allows the span to be rolled up for storage when it is not in use and to be easily unrolled to form a ridged span when it is to be employed in the loading or unloading of wheeled load materials such as small supplementary vehicles (Patent No. 20,020,088,065 A1, 2003).

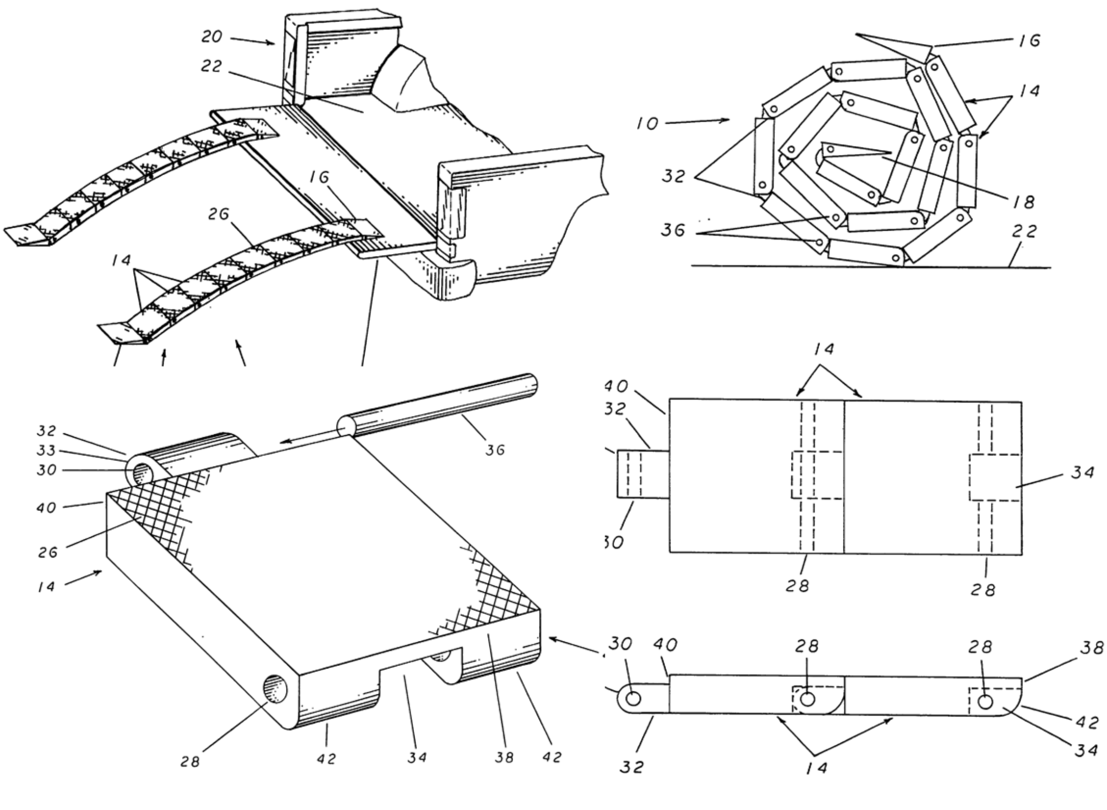

Figure 2.8 Loading ramp device which rolls up for storage

2.1.3. Foldable Ramps

Foldable ramps generally consist of hinges and load bearing panels. These two main members provide jackknife-like deployment.

2.1.3.1. Portable Ramp with Transport Facilitators

It is designed for practicing wheeled sport especially skateboarding. A portable ramp (Fig. 2.9) with transport facilitators including a ramp portion consisting of an upper section and a foldable and collapsible lower section. The side plates of ramp have triangular configurations; thus, it creates a slope for the base plate. When the side plates are in collapsed position, they form a triangular shape on the base plate. The side plates are hinged with the opposed side edges, the side plates having a removable crossbar when it is in an extended orientation, the front edge having the handle member extending outwardly therefrom, the upper plate having a pair of hooks extending outwardly from the front edge (U.S. Patent No. 20,020,108,190 A1, 2002).

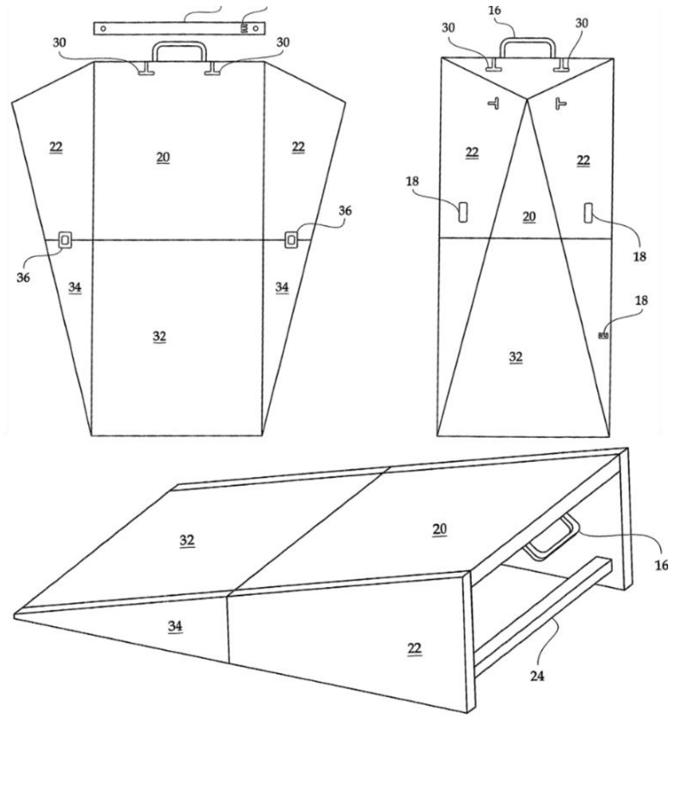

Figure 2.9 Portable ramp with transport facilitators

2.1.3.2. Portable Wheelchair Ramp

The ramp (Fig. 2.10) provides a mobile wheelchair ramp comprising: a main body comprising first and second ends and sides; at least one wheel secured beneath the main body; hand rails; and at least one pair of legs for grounding the ramp; where the ramp can be transformed from an extended position to a stowed position. When the ramp is in the stowed position the ramp is folded so that the hand rails are substantially parallel and adjacent to the plane of the main body. In the extended position the ramp is extended so that the hand rails are substantially parallel and spaced from the plane of the main body. The main body portion further comprising at least one telescoping extension from at least one of the first and second ends. There is a braking mechanism for the wheels. The legs are retractable and they are both telescoping (U.S. Patent No. 20,090,300,860 A1, 2009).

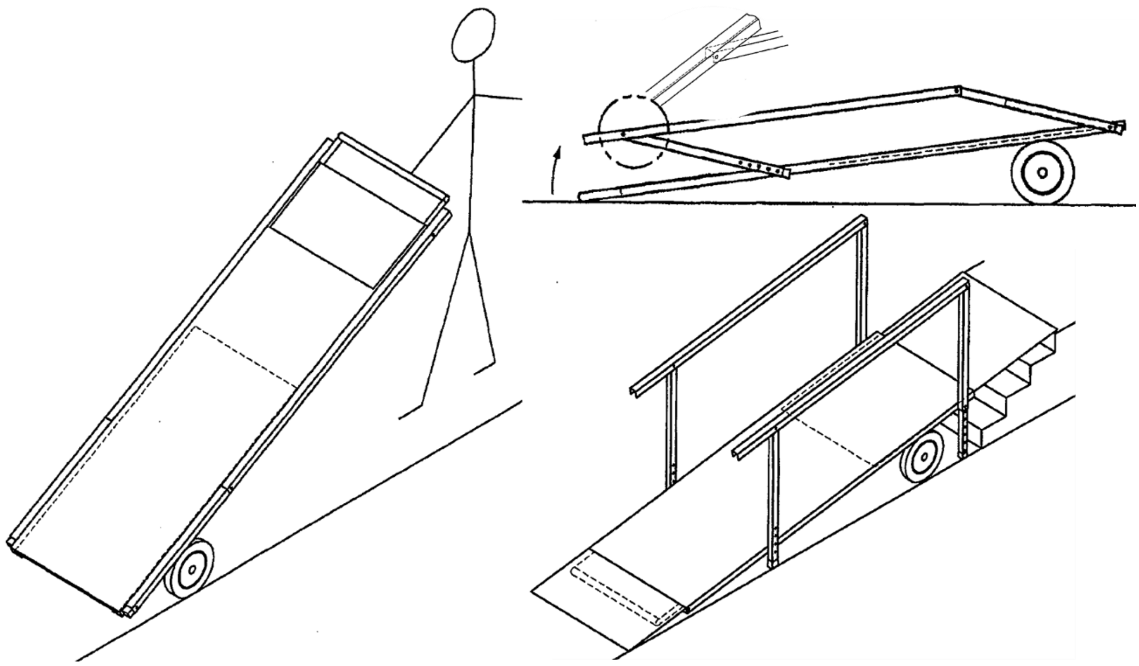

Figure 2.10 Portable wheelchair ramp

2.1.3.3. Stowable Load Ramp for Vehicles

A stowable load ramp (Fig. 2.11) for a vehicle includes a tailgate operable between a closed vertical position and an open horizontal position, an upper panel hingedly attached to the tailgate, a lower panel hingedly attached to the upper panel, and wherein the upper and lower panels are operable between a stowed horizontal position and an extended downwardly angled ramp position (U.S. Patent No. 6,378,927 B1, 2002).

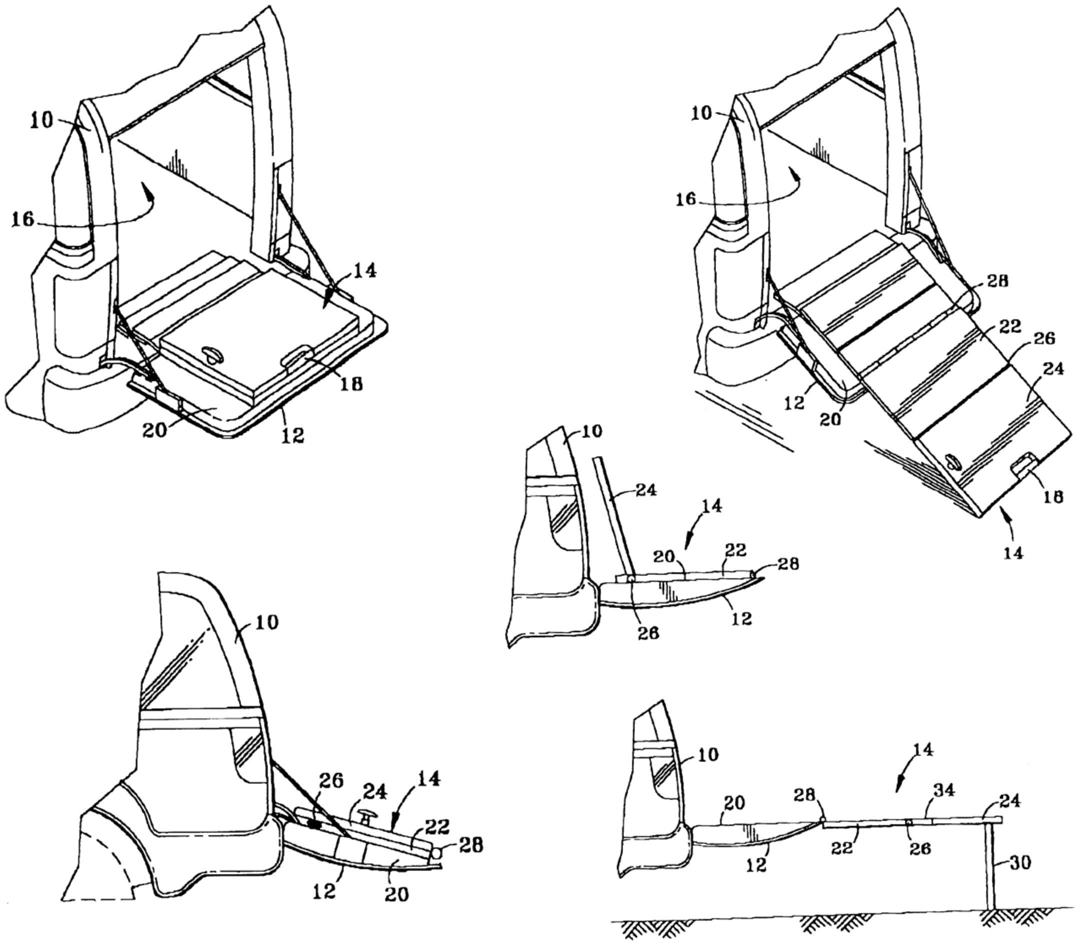

Figure 2.11 Stowable load ramp for vehicles

2.1.4. Scissor Ramps

These types of ramps consist of scissor members to achieve deployment. Somehow, there is only one patented example was found in the literature and have no real-life product in the market.

2.1.4.1. Extendable Ramp for Storage in a Tailgate or Flat Bed

An extendable ramp system (Fig. 2.12) extending a ramp from a storage position on a vehicle tailgate or flatbed is provided. A collection box is shown having a collection box channel with a sliding member which are engaged and moving within the collection box channel and coupling an end of the ramp to the collection box. The sliding member is being coupled to the end of the ramp closest to the collection box when the ramp is extended. An at least two folding structural members are provided having an at least one coupling member coupling the at least two folding structural members and the at least two folding structural members coupling to the at least one sliding member (Patent No. 20,110,072,596 A1, 2011).

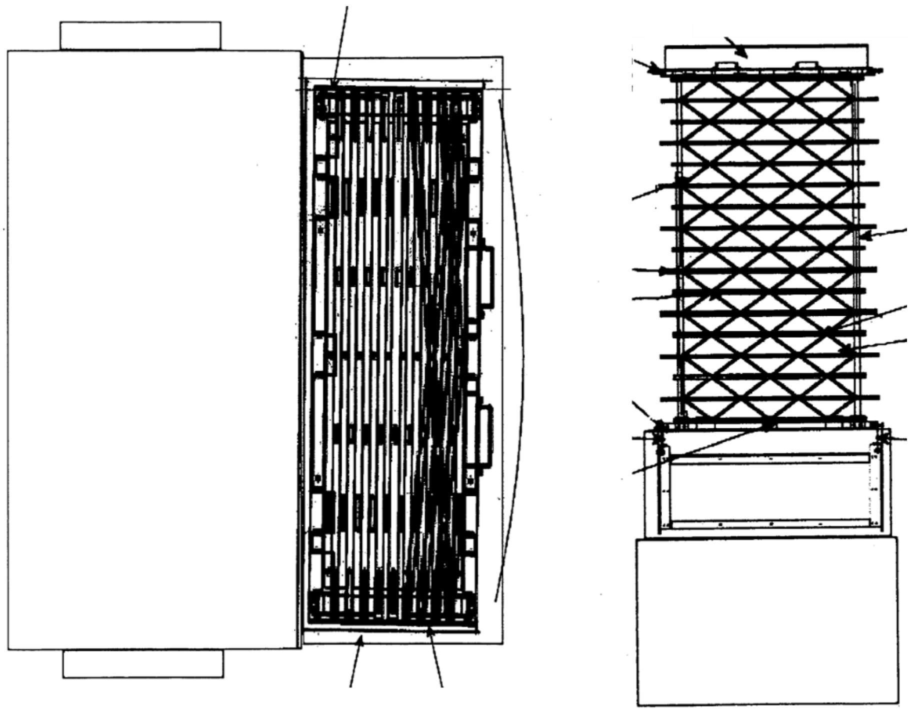

Figure 2.12 Extendable ramp for storage in a tailgate or flat bed

CHAPTER 3

CONCEPTUAL DESIGN

In the most general sense, conceptual design is the generating suitable solutions for achieving desired functions (Pahl and Beitz, 1996). It is generally accepted that conceptual design is one of the most critical phases of the product development process. (O'Sullivan, 2002).

In this Chapter, concept of design is presented not only by offering a design alternative but researching potential users' inclinations. First of all, problem definition has been clarified by focusing on a specific target group for which design parameters, constraints and design challenges are determined. In order to achieve this aim, design thinking approach is adapted in conceptual design process to simplify the complexity, and also to reduce the development time. Another reason for this selection is that, design thinking, which can fit almost all design or problem-solving cases, is a holistic approach and one of the core ideas of design research developed in recent years.

3.1. Design Thinking Approach

In recent years, "design thinking" has entered in the design literature and continues to draw attention increasingly (Brown, 2009; Lockwood, 2009). Although the term "design" is commonly associated with quality and/or aesthetic sides of the product, the main goal of design as a discipline should be offering wellbeing in people's lives (Vianna et al., 2012).

Recently, design thinking has attracted the attention of business and management, opening new paths to business innovation (Ingle, 2013). Its potential to deliver competitive advantage through helping business realm to be more innovative and bring more user-centered products to market (Brown, 2008). It is not only for whom product and/or industrial design are considered their job description. Design thinking approach can be learned and practiced easily by professionals from other disciplines (Vianna et al., 2012; Chen et al., 2013). Nowadays, managers benefit from design thinking as a problem-solving tool throughout the pioneer companies such as GE Healthcare, Procter & Gamble, and Philips Electronics (Wong,2009). Applied design thinking in engineering or business problem empowers strategic innovation which is used to uncover hidden value in existing products without necessarily reinventing it (Mootee, 2013).

This Chapter outlines each of the six steps (Fig. 3.1) of design thinking approach, while subsequent Chapters elaborate specific stages of the design process in more detail.

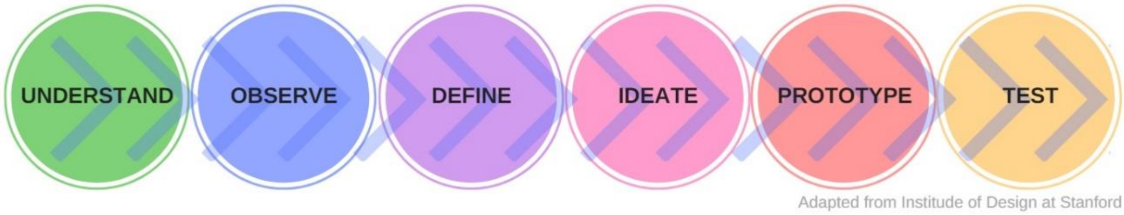

Figure 3.1 Design Thinking Steps

The first step is understanding the design challenge which designer should understand, define and frame the problem before what appropriate solutions might be like. Following step is observing that designer should observe how people behave and try to develop sense of empathy with possible users thereby, it creates awareness to better understand the difference between looking and seeing. In the define step, semi-structured face to face interview method was conducted to uncover users' inclinations and expectations. Ideate step provides a guideline for decision making process which can be considered as one of the most fundamental part of the conceptual design. A morphologic chart is created to reveal possible design solutions.

3.1.1. Understand

Understanding the design challenge is one of the most crucial steps of design thinking to create a solution or solutions. Furthermore, the degree of understanding is relevant to be able to think well beyond the current possible solutions with similar nature which does not mean reinventing available solutions (Ingle, 2013).

According to World Health Organization (WHO), about 10% of the global population have disabilities and 10% of these require a wheelchair (Sheldon et al., 2007). Moreover, several researches reveal that the majority of wheelchair users face with accessibility problems constantly in their daily lives (Frost et al., 2015; Silva et al., 2015;

Kim et al., 20014; Meyers et al., 2002). Another research indicates the maneuvering freedom of wheelchair users in Turkey. The results show that accessibility difficulties affect lives of disabled people with the reduction of life quality. Figure 3.2 shows the percentage of wheelchair users' residence types and ownership status (Çınar, 2008). These pie charts give a foresight about whether wheelchair users are able to increase their accessibility permanently or not.

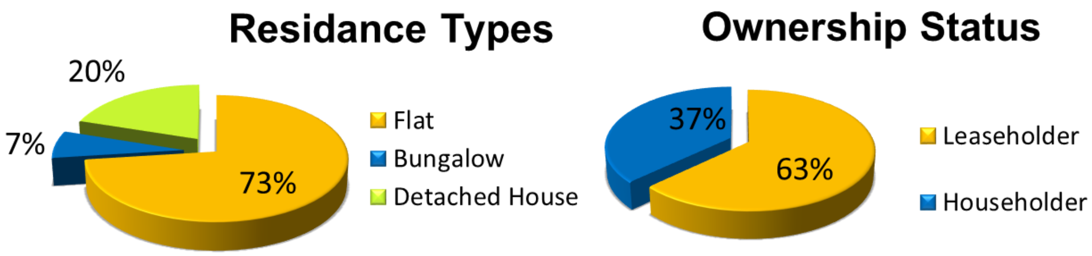

Figure 3.2 Residence types and ownership status

According to Table 3.1, most of the wheelchair users live in detached houses which do not have any ramps or lifts to provide them accessibility. Moreover, most of the wheelchair users are leaseholders which means they are not able to modify their residence permanently to increase their accessibility.

Table 3.1 Accessibility in and out the residence

Accessibility	**Leaseholder**				**Householder**			
	Interior		**Exterior**		**Interior**		**Exterior**	
	Yes	**No**	**Yes**	**No**	**Yes**	**No**	**Yes**	**No**
Staircase	0	100	93	7	0	100	50	50
Lift	9	91	5	95	10	90	73	27
Ramp	0	0	2	98	13	87	100	0

To this end, possible solutions for the main problem have been examined in Chapter 2. In the define step of design thinking, advantages and disadvantages of these current products or solutions are examined in Section 3.1.3 while proceeding to the next steps.

3.1.2. Observe

In this step designer should observe how people behave and try to develop sense of empathy with possible users thereby. This creates awareness to better understand the difference between looking and seeing.

Observation helps to build bridges of insight through empathy to see the world through the eyes of others, to understand the world through their experiences, and to feel the world through their emotions (Brown, 2009). Thus, it encourages the use of tools such as interview or questionnaire to help designers communicate with people in order to better understand their behaviors to uncover their expectations and needs through the insight (Mootee, 2013).

In this context, great number of problems was observed with respect to what kind of difficulties wheelchair users get in their daily life routine in terms of accessibility (Figs. 3.3 and 3.4). These difficulties can be listed as follows:

- Historical buildings
- Public spaces (banks, hospitals, etc.)
- Public transportation
- Residence
- Road repairment and cable or pipe installation (excavation works)

Figure 3.3 Rail installation

Figure 3.4 Excavation work

3.1.3. Define

Define step simply asks what the users' expectations and inclinations to achieve better solution through design job are, and it is important that these expectations are fully understood. Briefly, objectives need to be specified so that the designer knows what is to be achieved and what the project boundaries are (Ambrose & Harris, 2010).

To this end, interview questions were prepared according to diverse literature survey about wheelchair users and their accessibility to uncover their expectations and needs. A basic qualitative research method was used to examine the expectations of wheelchair users. The study was conducted in İzmir.

8 wheelchair users with ages ranging in between 13-40 and who have been used wheelchair at least for 1 year were selected in the middle class. This frame was chosen because upper class in society generally is able to find more expensive and permanent solutions to increase their mobility and accessibility in their daily lives.

Interviews were carried out with semi-structured interview questions. Discussions were recorded and written with participants' consent, translated and transcribed. Individual semi-structured interviews were carried out at a location convenient to each participant and conductor. Interviews started with a general question with regard to their feelings about being a wheelchair user and the struggles in their daily lives. Afterward, further questions were addressed to explore their expectations and needs.

Interviews lasted approximately 50-55 minutes, and four main themes and two or three sub-themes formed according to answers were identified during the interview, as shown in Table 3.2.

Table 3.2 Main and sub-themes of the interview questions

CONCEPT OF BEING A WHEELCHAIR USER	DAILY STRUGLES
	ACCESSIBILITY
	FAMILY AND ENTOURAGE
PUBLIC SPACES	SUFFICIENCY AND EFFICIENCY OF PUBLIC RAMP
	DEFICIENCIES OF PUBLIC RAMPS
	STANDARDIZATION OF PUBLIC RAMPS
TRANSPORTAION	PUBLIC TRANSPORTATION
	PERSONAL TRANSPORTATION
SUGGESTIONS	PERSONAL RAMPS
	PREFERENCES

The questions begin with identifying potential users' accessibility and usability problems they encountered in everyday life. All attendees have complained about accessibility problems due to the inadequacy or the absence of ramps in public places such as hospitals, historical buildings and their relatives' houses. And they emphasized that they do not prefer to leave their houses unless it is necessary, rather than to face and struggle accessibility problems in their daily lives.

It was asked whether they are able to use effectively the fixed ramps placed in public spaces and whether these ramps were in conformity with the dimensional standards. All eight attendees have pointed out they are not able to use these public ramps without any assistance because of ill-designed ramps not meeting the dimensional standards in terms of slope, width, nonskid surface.

It is generally stated by attendees that they have difficulty in using public transportation. Moreover, most of the participants complained that the bus ramps have no barrier on sides that causes danger of falling.

When participants were asked whether they had their own portable ramp, it was revealed that some of the participants surprisingly were not aware of the existence of portable-foldable ramps in the market.

It was revealed that all of the participants are dwelling on the ground floor and only three of the participants have a fixed ramp at the entrance of their apartment or the balcony of their own house. The remaining five participants mentioned about why they are not using a fixed ramp at their apartment. According to their responses, the main reasons are as following:

- The narrowness of the apartment entrance to locate a fixed ramp (blocking the entrance and stairs permanently)
- The lack of the necessary distance to provide the appropriate angle of inclination for a wheelchair user
- Being faced with some problems with their neighbors (for some functional and/or aesthetic reasons)

After exploring three main themes in the interview, it was intended to get more detailed suggestions from wheelchair users about how a good-designed deployable ramp should be. To this end, some videos of portable ramps in the market with three different types of deployment method (foldable, telescopic and rollable) were demonstrated to the participants. Thereafter, participants' opinions were asked for uncovering the most wanted and desired functional features from a portable ramp. It was understood that all participants had a common view about the most desirable features are:

- Lightness
- Ease of deployment, transportation and installation
- Compactness

In addition, all participants who have seen these portable ramps for the first time, claim that they are going to acquire one because they have found the idea of having a portable and storable ramp very interesting, practical and useful.

According to attendees, rollable ramps are the most desired design with respect to their modularity that offers flexibility to extend the ramp length easily. Besides, they have found telescopic ramps are practical in terms of loading their wheelchair to their personal motorized vehicles such as van or car. On the other hand, jackknife-like foldable ramps were found very bulky, heavy and impractical by the attendees.

Weaknesses of the rival products in the market were also determined during the interview. The most important shortcomings of the rolled ramps are their bulky and heavy structures and high marketing price due to participants' point of view.

3.1.4. Ideate

This step is creating the potential solutions or products and making selections between generated alternatives. It is important that the potential solutions meet users' inclinations and needs.

To create potential product alternatives design engineering tools can be used. One of these tools is creating a morphological chart to generate alternatives. To determine the best solution that meets the users' inclinations and needs, which are elaborately identified in define step. In the following sub-sections, Morphological Chart is adapted to the case study of the thesis.

3.1.4.1 Morphological Chart

Basically, a Morphological Chart is a design tool which helps to find product and/or service ideas and also can serve as a design catalogue during all phases of design process (Pahl et al., 2007). To create a systematic combination, different solutions that satisfy the functions and design criteria are listed in Fig. 3.5 to create a morphological chart.

The morphological chart created for the case study and offers 4^7 possible solutions. However, it is possible to increase the amount of possible solutions by adding more category and alternatives, but it takes much time to evaluate and make a decision. For this reason, it is important to limit the number of alternatives by focusing on the most important design criteria. The chart is guiding during detailed design process. In the light of define step and patent survey, conceptual ideas focus on rollable-portable ramps which are more suitable for users' inclinations in terms of providing lightness, compactness, ease of carrying and installation. It is intended for that these design criteria will be improved during Chapter 4.

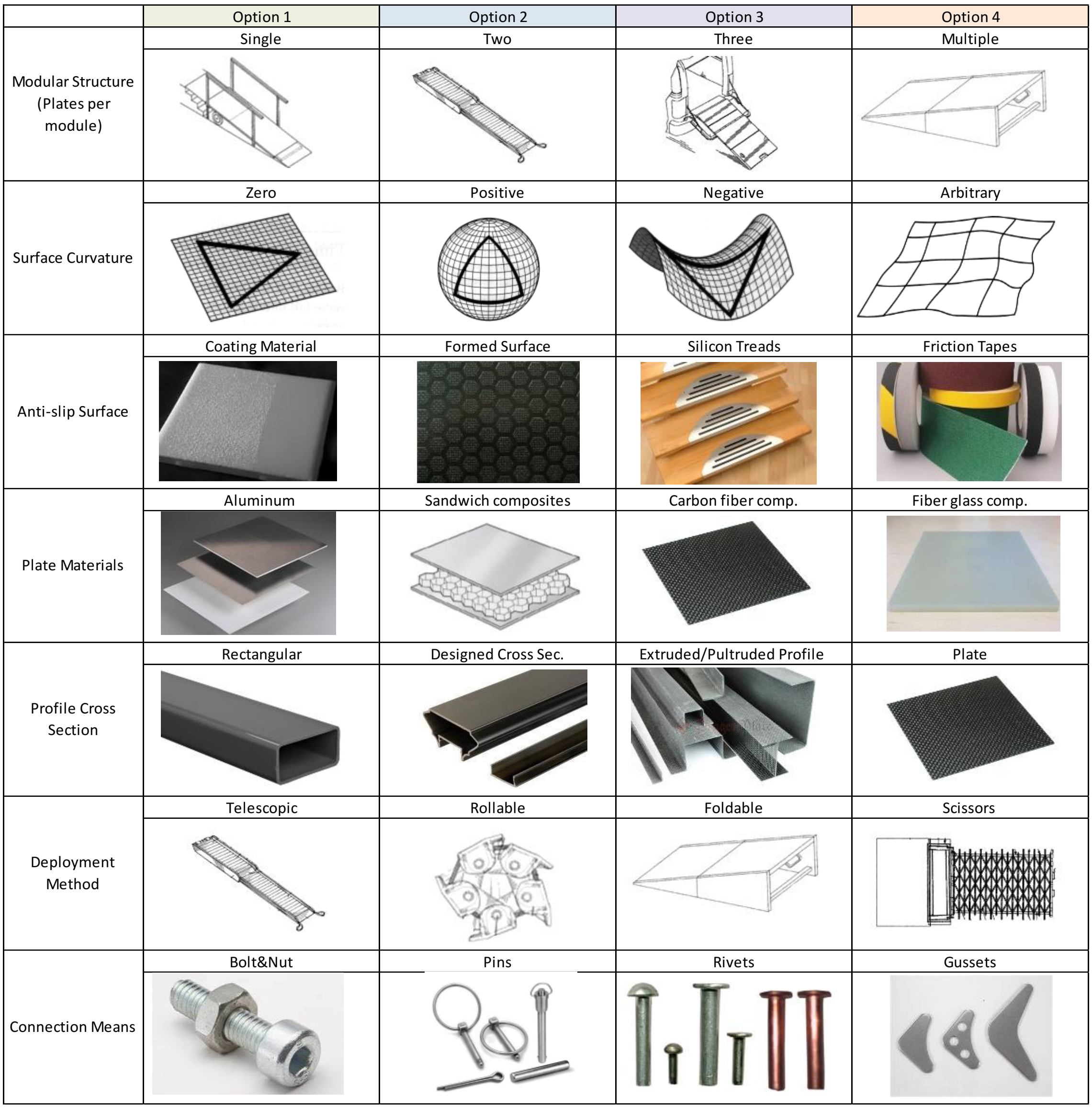

Figure 3.5 Morphological Chart

3.1.5 First Prototype and Test

At the very beginning of prototyping step, first a scaled rollable ramp is modelled (Fig. 3.6) and manufactured (Fig. 3.7) in the direction of users' inclinations. The deployable ramp is designed with links which are connected to each other on the side faces. The links are able to rotate about the pin to form a rolled and unrolled configuration. The ramp structure is sufficiently flexible to be rolled-up for storage conveniently.

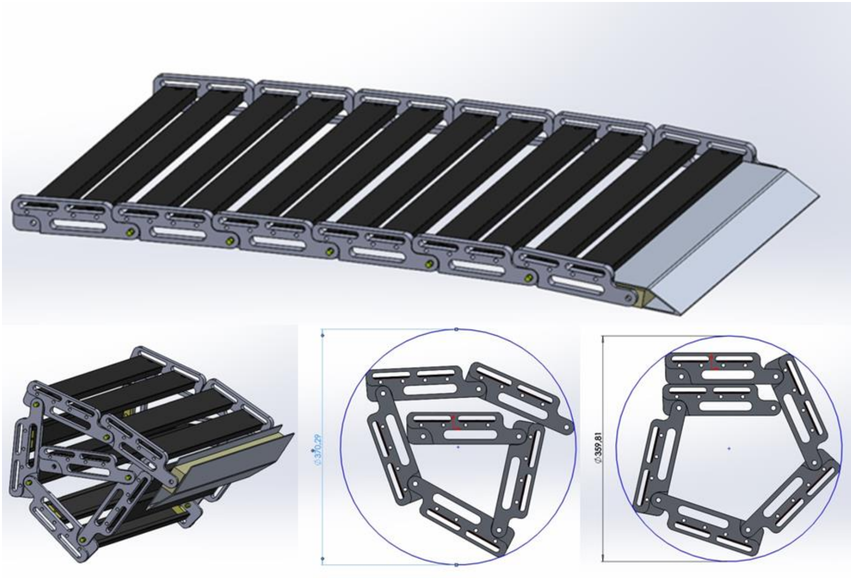

Figure 3.6 CAD model of the first prototype

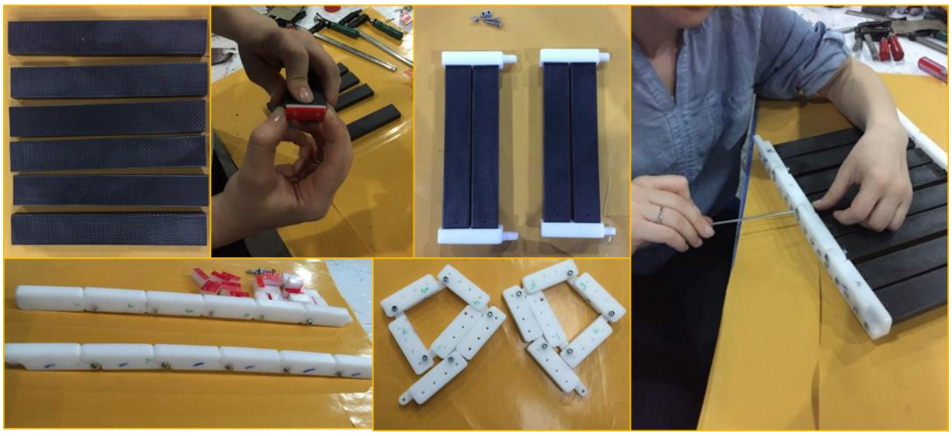

Figure 3.7 Assembling the first prototype

First test of conceptual design is performed only in terms of rolling ability. As can be seen from figure 3.5, 3.6 and 3.7, links can not be rolled effectively and empty space in between rolled links need to be reduced. Figure 3.8 illustrates the conceptual design which should be easily carried by user and compact enough while it is in rolled position for storing effectively. To this end, chapter 4 gives brief information about detailed design of the ramp.

Figure 3.8 First prototype and check

Figure 3.9 Conceptual design

Fig. 3.9 illustrates the conceptual design which should be easily carried by user and compact enough while it is in rolled position for storing effectively

CHAPTER 4

DETAILED DESIGN

This chapter gives brief information about geometric calculations, kinematic analysis, material selection and strength calculations for the design. At the very beginning, different link geometries which can provide deployment are modeled in SolidWorks. Afterwards, kinematic analysis is conducted for observing compactness by using convex hull and smallest enclosing circle algorithm. Material and manufacturing method selections are carried out after deciding on the link geometry and the most effective rotation angle which provides better compactness. Moreover, sandwich composite plates are also tested in terms of flexural behavior of the material. Design iterations are performed by performing strength analysis, kinematic analysis and geometric calculations simultaneously by changing design parameters such as link length, height and thickness.

4.1 Geometric Calculations

Geometric calculations have been conducted for achieving better compactness while the ramp is in rolled position. In accordance with this purpose, several geometric patterns of ramp links have been modeled both in SolidWorks (Figure 4.1) and Excel with the help of convex hull and smallest enclosing circle algorithms to find optimal link lengths and shape.

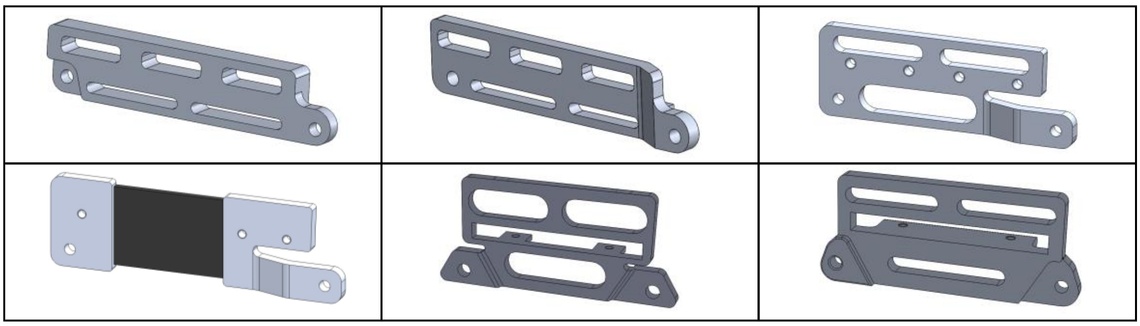

Figure 4.1 Link Alternatives

Before beginning with the kinematic analysis, link alternatives have been 3D printed and evaluated in terms of manufacturability, and ease of assembly (design for assembly).

4.1.1 Kinematic Analysis and Design

At the very beginning of the kinematic analysis, two different type of load-bearing links were designed. 5-to-10 identical links are assembled per meter, where the link length depends on number of links per meter. One of these links has an asymmetrical shape, whereas the second link has a symmetrical shape on the XY-plane shown in Fig 4.2.

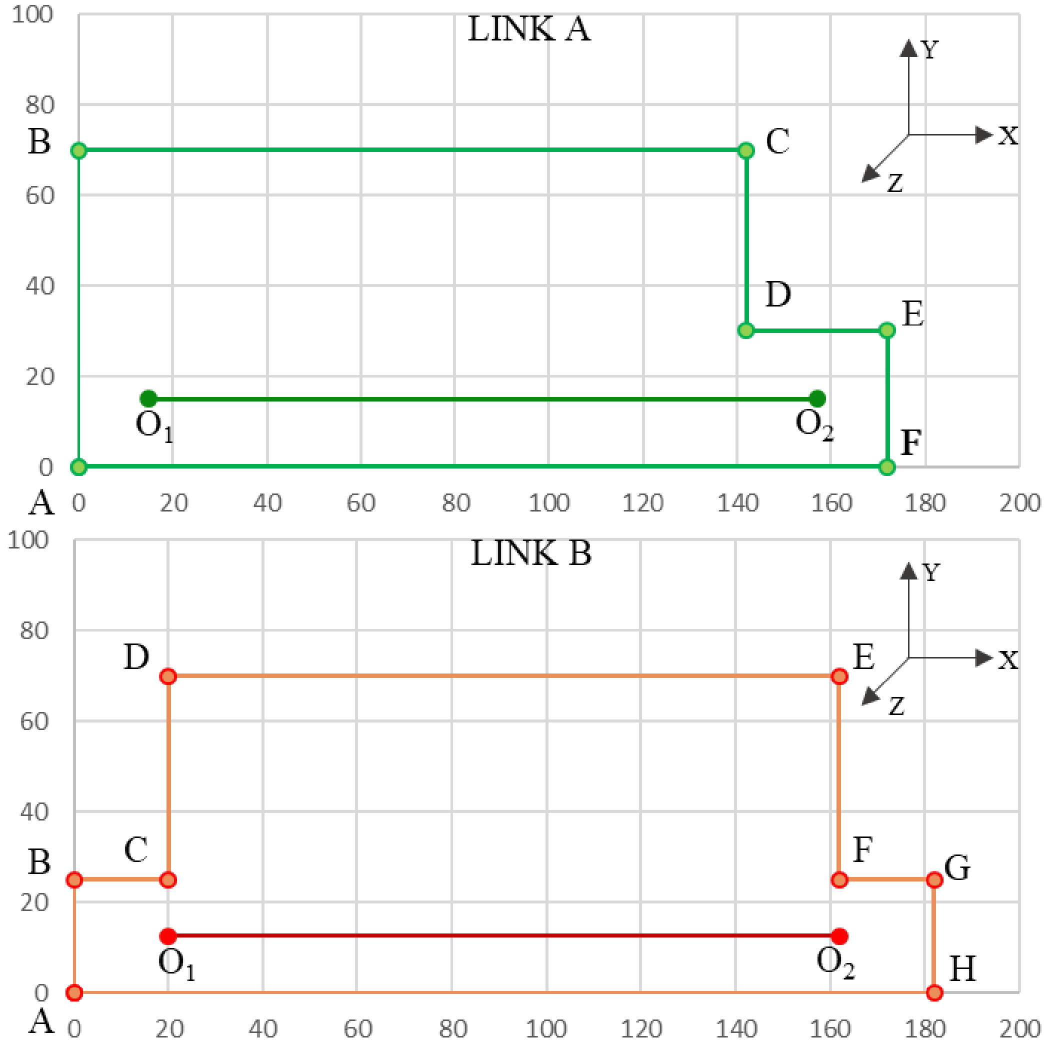

Figure 4.2 A. Asymmetrical and B. Symmetrical Link Patterns

To carry out the kinematic analysis, the link dimensions and relative angular positions of the links with respect to each other need to be known. The vertices of load-bearing links are defined as points named as A, B, C, etc. in the XY-plane of a coordinate system. The first link is considered stationary as illustrated in Table 4.1 and the positions of each of the other sequentially attached link is defined relative to the previous link.

Table 4.1 Link Coordinates

LINK A1			**LINK B1**		
	X	**Y**		**X**	**Y**
A	0	0	**A**	0	0
B	0	AB	**B**	0	AB
C	BC	AB	**C**	BC	AB
D	BC	AB-CD	**D**	BC	AB+CD
E	AF	AB-CD	**E**	BC+DE	AB+CD
F	AF	0	**F**	BC+DE	AB
			G	AH	AB
			H	AH	0

The position of a link with respect to the previous one is defined by a rotation by $\emptyset$ and a translation by x_t, y_t. The coordinate transformation of a point on a link is performed as

$$\begin{bmatrix} \cos\emptyset & -\sin\emptyset & x_t \\ \sin\emptyset & \cos\emptyset & y_t \\ 0 & 0 & 1 \end{bmatrix} \begin{bmatrix} x \\ y \\ 1 \end{bmatrix} = \begin{bmatrix} x\cos\emptyset - y\sin\emptyset + x_t \\ x\sin\emptyset + y\cos\emptyset + y_t \\ 1 \end{bmatrix} \tag{4.1}$$

Let m be the distance between the rotation centers O_i and O_{i+1} of links i and $i+1$. Then coordinates of left bottom corner of each link is computed as

$$A_{i+1,x} = O_{1x} + m + (A_{ix} - O_{1x})\cos\left(\sum_{n=1}^{i}\emptyset_n\right) - \left(A_{iy} - O_{1y}\right)\sin\left(\sum_{n=1}^{i}\emptyset_n\right) \tag{4.2}$$

$$A_{i+1,y} = O_{1y} + (A_{ix} - O_{1x})\sin\left(\sum_{n=1}^{i} \emptyset_n\right) + \left(A_{iy} - O_{1y}\right)\cos\left(\sum_{n=1}^{i} \emptyset_n\right) \tag{4.3}$$

The coordinates of the other points of the links are evaluated similarly. The aim in the kinematic design is to select proper number of links with proper link dimensions and proper folding angles so that a ramp with a specified deployed length will roll into the most compact form. For this purpose, a convex hull algorithm is used.

4.1.2 Convex Hull Algorithm

Imagine that the vertices of the ramp links are nails sticking out of the plane, take a rope, wrap it around the nails until it comes back to the starting point. The area enclosed by the rope is called the convex hull. This algorithm is called *Jarvis' March* or "*gift-wrapping" algorithm* in the literature (Berg et al., 2008). Jarvis' March is one of the simple-minded algorithms for convex hulls. The basic idea is:

- Select a point outside the point cloud and take this as a centre of a circle, then find the closest point of the set to this centre. This point becomes the first vertex of the convex hull.
- Starting from the first vertex, test each of the other points in the set to find the next vertex which creates the smallest right-hand turn. Repeat this step with the new vertex until the first vertex is reached and the polygonal loop is closed (Jarvis, 1973).

Let $S = \{S_1, S_2, \dots, S_n\}$ be the finite set of points in the plane and X_i and Y_i be the Cartesian coordinates of the i^{th} point in the set. Then the algorithm steps are as follows:

Step 1. Pick an origin point outside the set (for example pick $X_{origin} \leq min\{X_i\}$ and $Y_{origin} \leq min\{Y_i\}$) (Fig. 4.3). Set a Cartesian reference frame at this origin.

Step 2. Find S_k such that $\theta_{0k} \leq min\{\theta_{0i}\}$, $i = 1,2, \dots, n$, where θ_{0i} is the angle of the position vector of point S_i with respect to the original reference frame. For equal minimum angles pick the point closest to the origin.

Step 3. Shift origin to S_k and repeat step 2 with consistent angle direction and origin until first convex hull point is re-found (Jarvis, 1973).

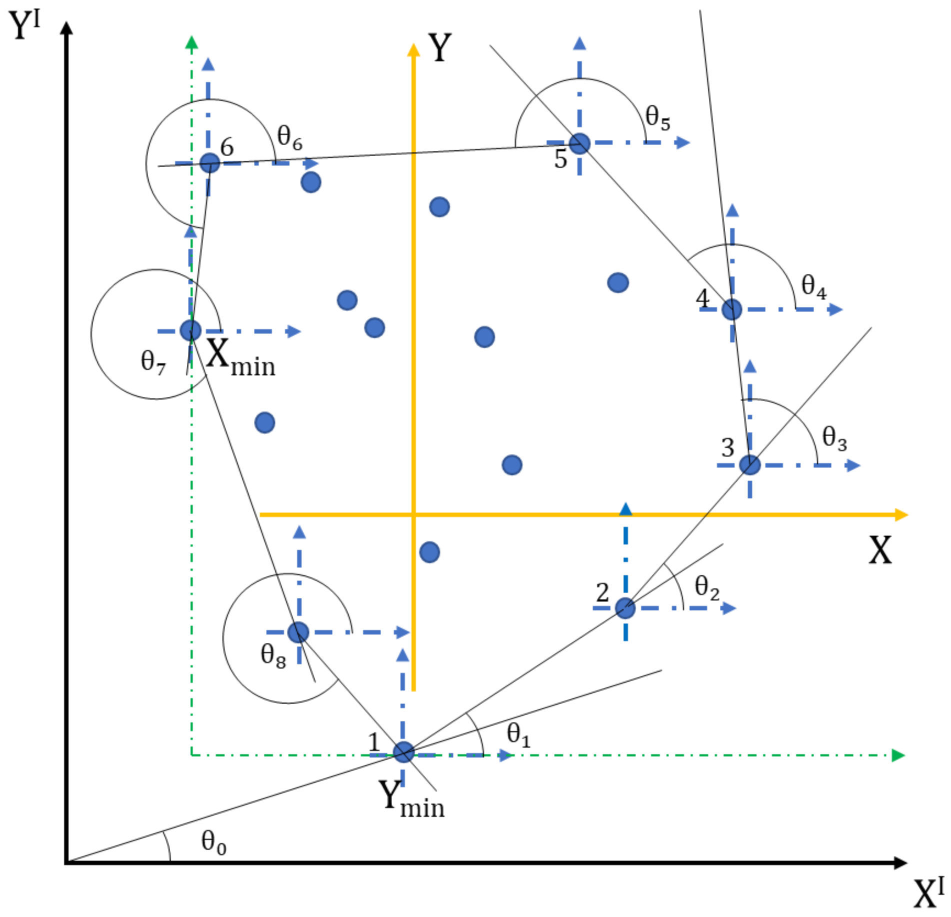

Figure 4.3 Illustration of the convex hull algorithm

The convex hull algorithm has been used to identify the outmost points of the point set and to plot the periphery of the ramp while it is in rolled position. Two different link shapes were modelled in Excel to observe the effects of link geometry on compactness. In the following examples, a seven-link assembly is used for a ramp with 1 m deployed length. As can be seen from Fig 4.4 and 4.5, convex hull gives a foresight about how much space the link chains are occupying when the ramp is in rolled position.

Convex hull of the Link A1 looks less round due to the asymmetrical link shape, however Link B1 is designed to be symmetrical, and its convex hull looks rounder which provides more regular deployment.

To observe compactness of the links in more detail, smallest enclosing circle algorithm can guide.

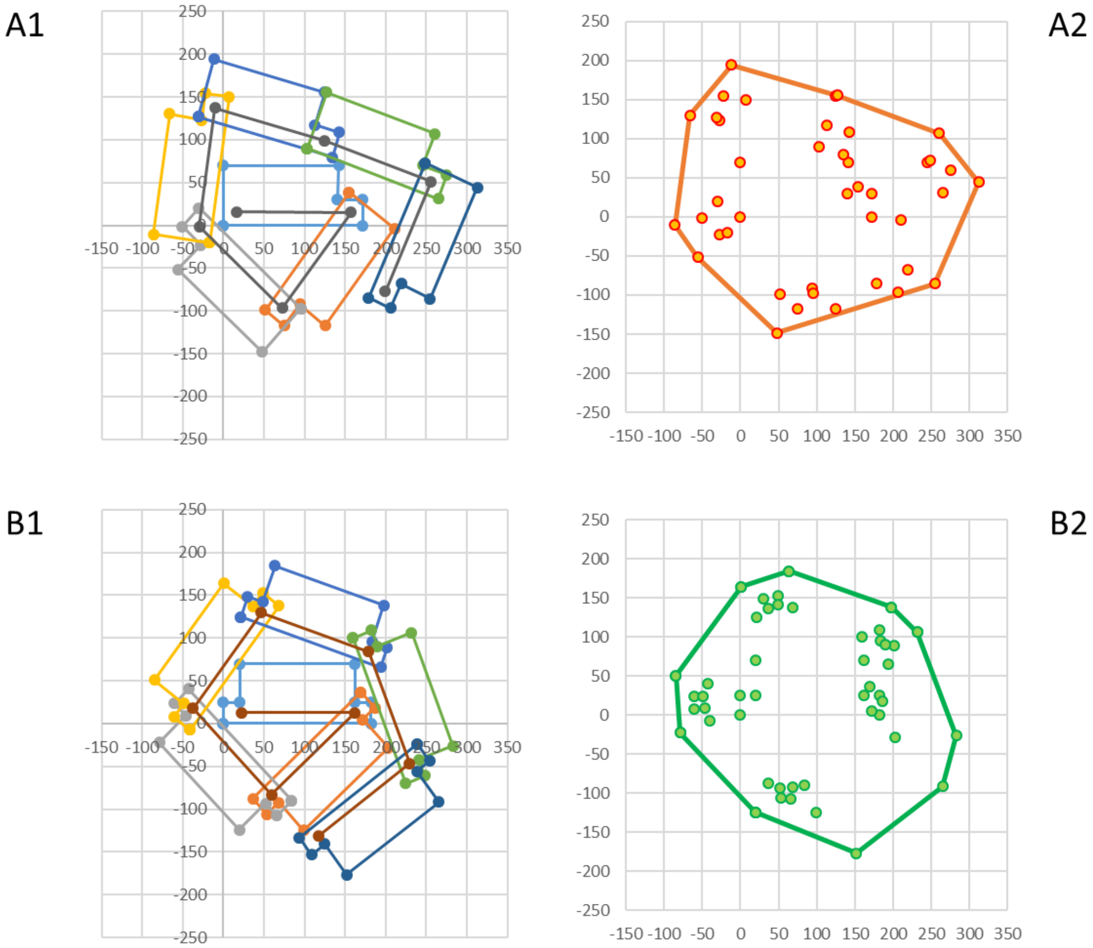

Figure 4.4 Convex Hull of the Links

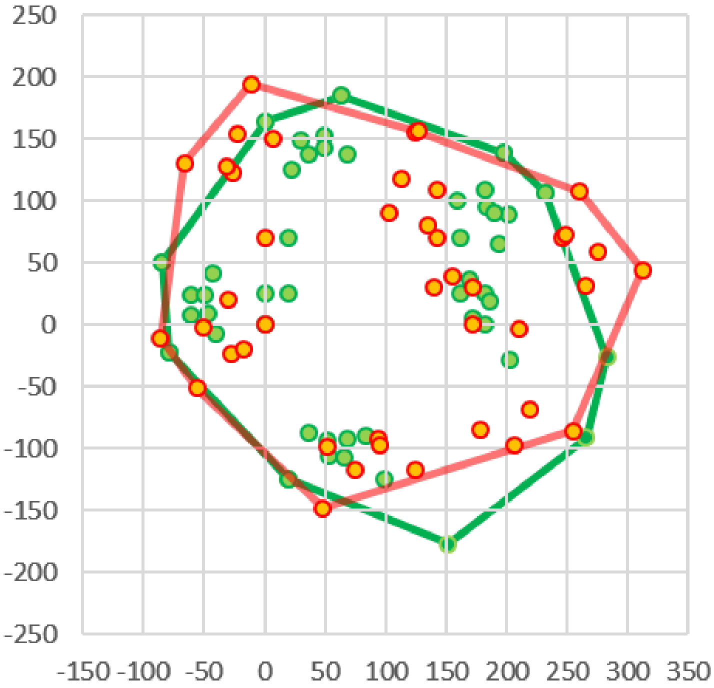

Figure 4.5 Comparison of the Convex Hulls

4.1.3 Smallest Enclosing Circle Algorithm

This algorithm can be simplified by using the convex hull algorithm to eliminate null points which are encircled in the circle. Hereby, the problem transforms into computing the smallest enclosing circle of a convex polygon (Skyum, 1991).

This time $= \{S_1, S_2, \dots, S_n\}$, is the finite set of vertices of a convex hull. Let $p = (x_i, y_i)$, $q = (x_j, y_j)$, $t = (x_k, y_k)$ be the three points in S which defines the smallest enclosing circle. Two of these points, say p and t, may be concurrent, in which case, the circle passes through two points $p = t$ and q which constitute the diameter of the smallest enclosing circle. A circle with center (a, b) and radius r can be expressed as

$$(x - a)^2 + (y - b)^2 = r^2 \tag{4.4}$$

a, b and r can be expressed in terms of the three-point coordinates as

$$\Delta = (x_i - x_j)(y_i - y_k) - (x_i - x_k)(y_i - y_j) \tag{4.5}$$

$$a = \frac{(x_i^2 + y_i^2 - x_j^2 + y_j^2)(y_i - y_k) - (x_i^2 + y_i^2 - x_k^2 + y_k^2)(y_i - y_j)}{2\Delta} \tag{4.6}$$

$$b = \frac{(x_i^2 + y_i^2 - x_k^2 + y_k^2)(y_i - y_j) - (x_i^2 + y_i^2 - x_j^2 + y_j^2)(y_i - y_k)}{2\Delta} \tag{4.7}$$

$$r = \sqrt{(x_i - a^2) + (y_i - b^2)} \tag{4.8}$$

The smallest enclosing circle is found by trying out all possible point combinations in S letting $i = 1\ to\ n$, $j = i + 1\ to\ n$ and $k = j + 1\ to\ n$, where n is the number of convex hull points.

4.1.3.1 The effect of link geometry on compactness

Two different link shapes are compared with each other to observe the effect of link geometry on compactness. In the rolled form, the rotation angle of first link is arbitrarily chosen as 139º and all the other rotation angles are increased until the links interfere with other links. As can be seen in Figure 4.6, symmetrical link shape is more effective in terms of rolling capability.

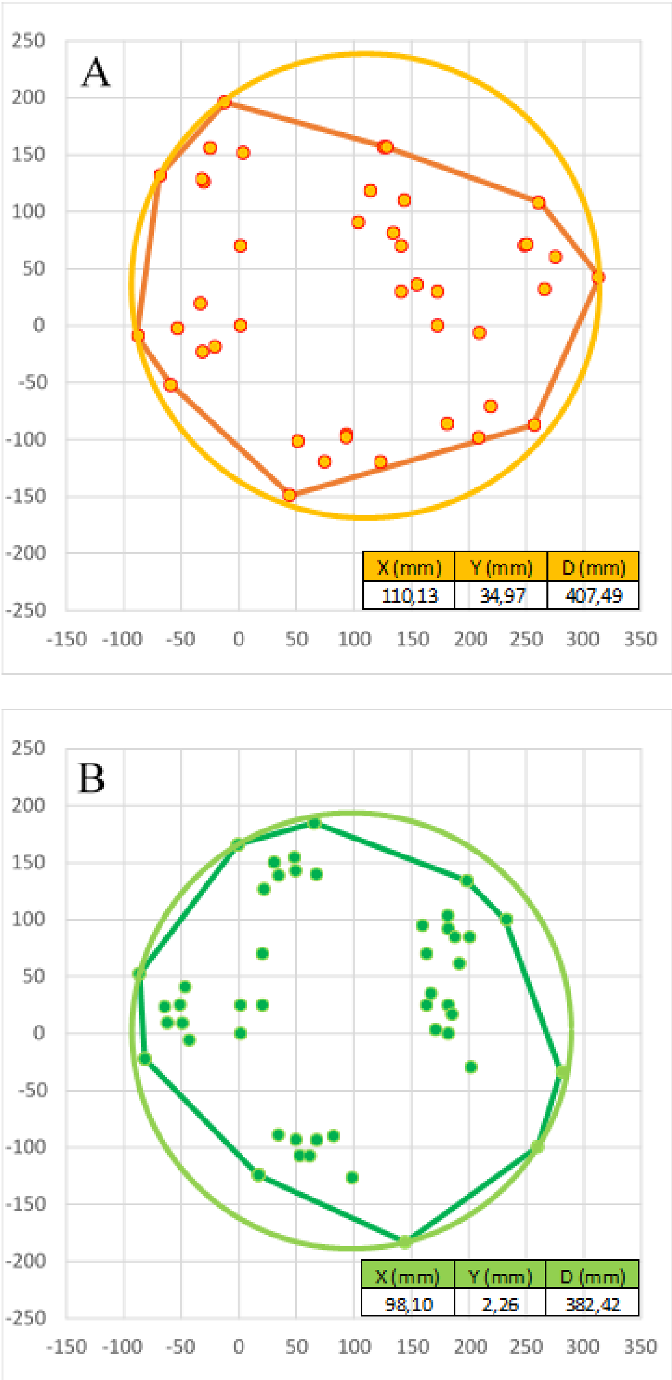

Figure 4.6 Smallest Enclosing Circle of A. Asymmetrical and B. Symmetrical Links

4.1.3.2 The effect of link length on compactness and total weight

This time, 6-to-10 identical symmetrical links are assembled for a 1 m ramp to observe the effect of link length on the compactness and total weight where the link length (DE) depends on number of links (N) per meter while the other parameters remain constant. The rotation angle of first link is (N) chosen as 139º and all the other rotation angles are increased until the links interfere with other links. Total link weight per meter is proportional to the total area of the link while the thickness remains constant. Results for N = 6, 7, 8, 9 and 10 are illustrated in Figs. 4.7-4.8.

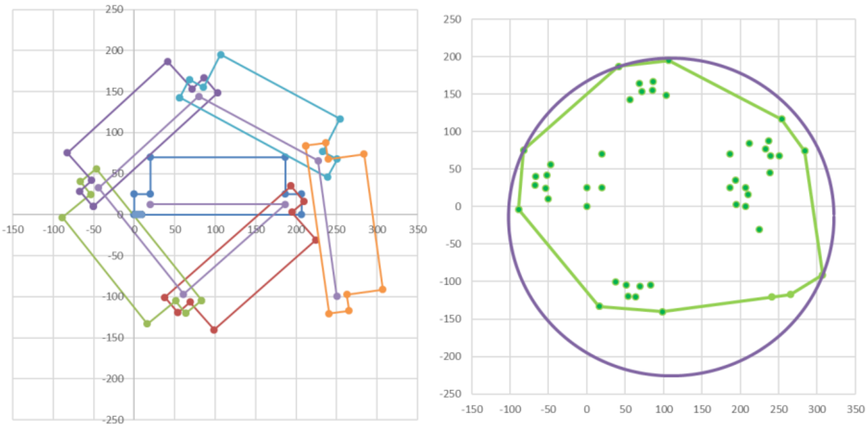

COMBINATION 1		
N	6	
DE	166,67	
ROT. ANGLE	RAD	DEG
φ2	-2,43	-139
φ3	-1,61	-92
φ4	-1,52	-87
φ5	-1,22	-70
φ6	-0,94	-54
MAX RAD	211,95mm	
TOTAL AREA	76000mm²	

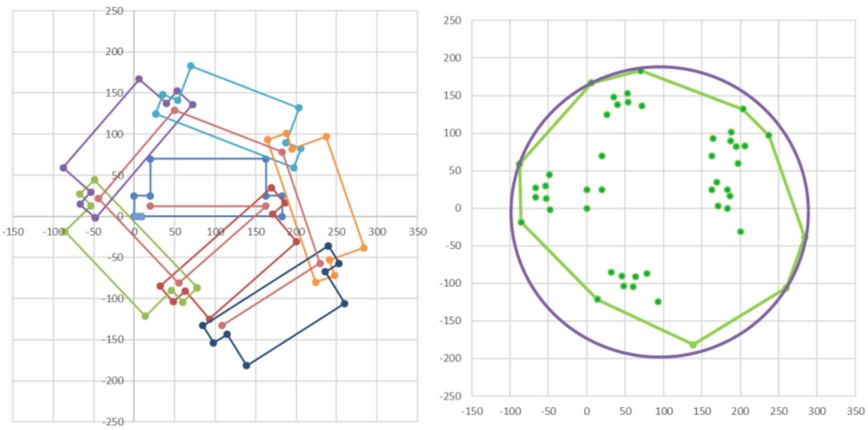

COMBINATION 2		
N	7	
DE	142,86	
ROT. ANGLE	RAD	DEG
φ2	-2,43	-139
φ3	-1,52	-87
φ4	-1,48	-85
φ5	-1,22	-70
φ6	-0,87	-50
φ7	-1,33	-77
MAX RAD	193,40mm	
TOTAL AREA	77000mm²	

Figure 4.7 The effect of link length on compactness and total weight for N = 6 and 7

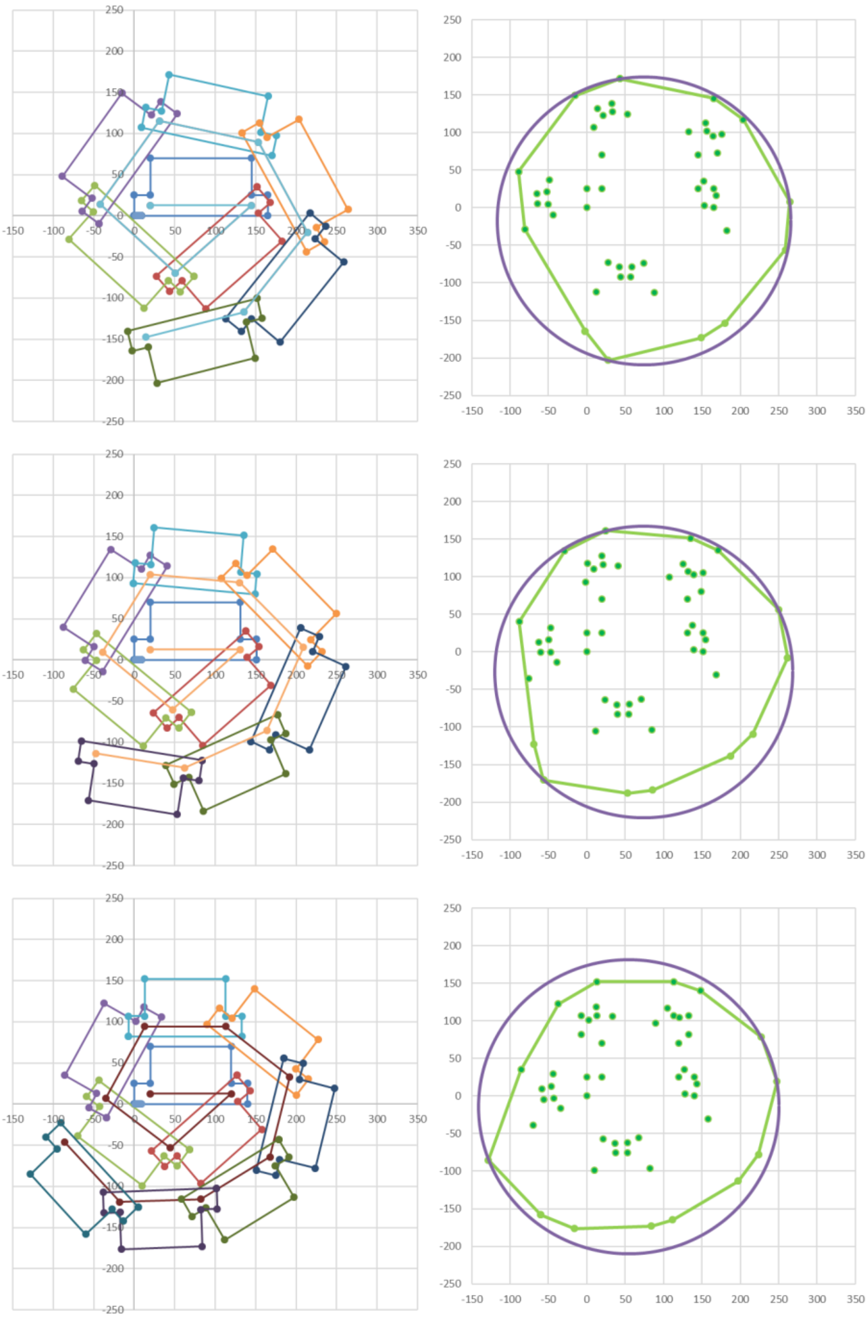

COMBINATION 3		
N	8	
DE	125	
ROT. ANGLE	RAD	DEG
φ2	-2,43	-139
φ3	-1,45	-83
φ4	-1,47	-84
φ5	-1,15	-66
φ6	-0,86	-49
φ7	-1,19	-68
φ8	-0,59	-37
MAX RADIUS	190,90mm	
TOTAL AREA	78000mm²	

COMBINATION 4		
N	9	
DE	111,11	
ROT. ANGLE	RAD	DEG
φ2	-2,43	-139
φ3	-1,40	-80
φ4	-1,45	-83
φ5	-1,10	-63
φ6	-0,70	-40
φ7	-1,20	-69
φ8	-0,73	-42
φ9	-0,58	-33
MAX RADIUS	194,20mm	
TOTAL AREA	79000mm²	

COMBINATION 5		
N	10	
DE	100	
ROT. ANGLE	RAD	DEG
φ2	-2,43	-139
φ3	-1,36	-78
φ4	-1,43	-82
φ5	-1,06	-61
φ6	-0,66	-38
φ7	-1,15	-66
φ8	-0,79	-45
φ9	-0,51	-29
φ10	-0,86	-49
MAX RADIUS	196,00mm	
TOTAL AREA	80000mm²	

Figure 4.8 The effect of link length on compactness and total weight for N = 8, 9 and 10

Although the smallest enclosing circle forms for the N = 8, total link weight is larger than the case with N = 7 and the radii are close to each other. Therefore, considering both compactness and lightness, N is selected as 7.

4.1.3.3 The effect of rotation angle on compactness

Another design parameter that has a significant effect on compactness is rotation angle between first two consecutive links. To determine the optimum rolling ability, compactness is observed by changing first rotation angle from 120º to 145º. Some results are illustrated in Figs. 4.9 and 4.10.

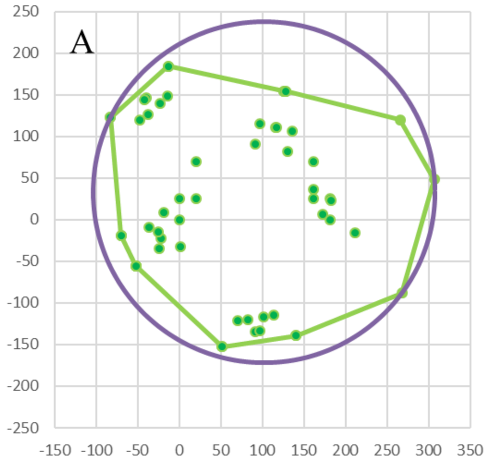

ROTATION ANGLE		
φ2	-2,09	-120,00
φ3	-1,80	-103,00
φ4	-0,73	-42,00
φ5	-1,87	-107,00
φ6	-0,03	-2,00
φ7	-1,61	-92,00
X	Y	R
102,03	32,94	205,26

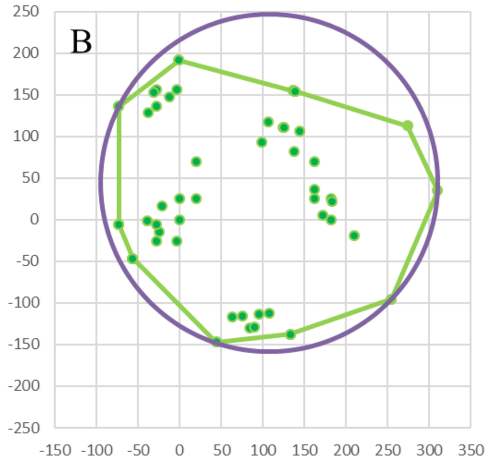

ROTATION ANGLE		
φ2	-2,15	-123,00
φ3	-1,78	-102,00
φ4	-0,79	-45,00
φ5	-1,83	-105,00
φ6	-0,03	-2,00
φ7	-1,68	-96,00
X	Y	R
107,54	43,95	202,79

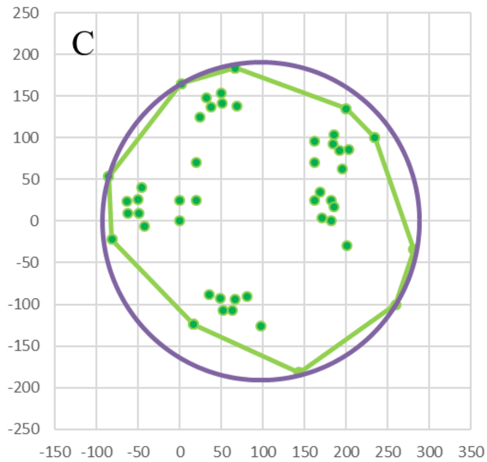

ROTATION ANGLE		
φ2	-2,39	-137,00
φ3	-1,55	-89,00
φ4	-1,43	-82,00
φ5	-1,26	-72,00
φ6	-0,89	-51,00
φ7	-1,29	-74,00
X	Y	R
97,41	0,16	190,73

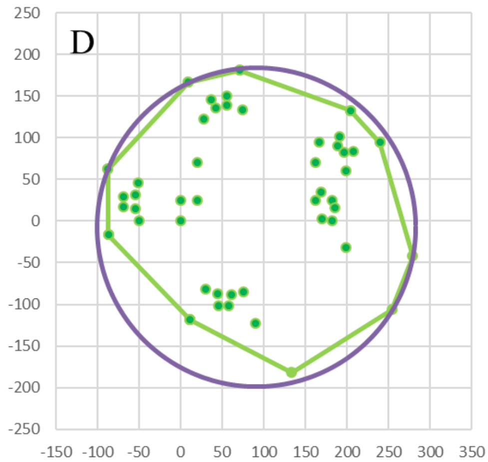

ROTATION ANGLE		
φ2	-2,44	-140,00
φ3	-1,50	-86,00
φ4	-1,52	-87,00
φ5	-1,17	-67,00
φ6	-0,94	-54,00
φ7	-1,29	-74,00
X	Y	R
91,03	-6,79	191,51

Figure 4.9 Effect of the rotation angle on compactness - 120º, 123º, 137º, 140º cases

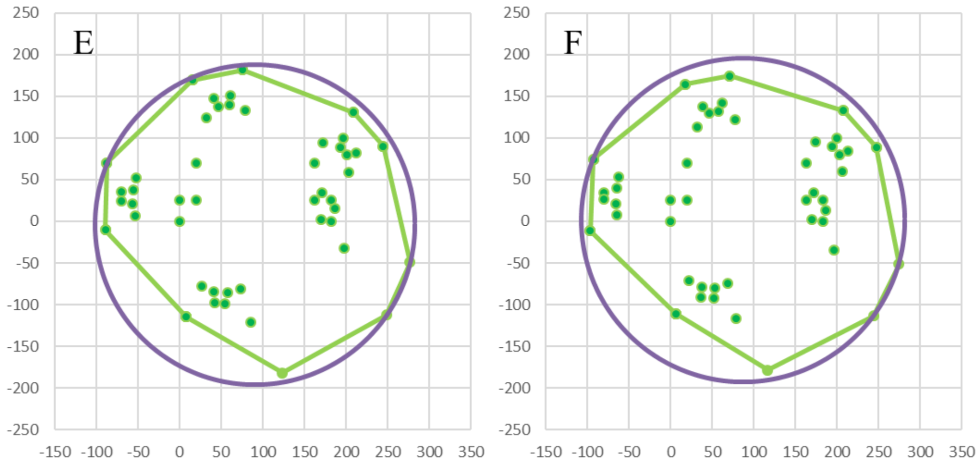

ROTATION ANGLE		
φ2	-2,48	-142,00
φ3	-1,48	-85,00
φ4	-1,55	-89,00
φ5	-1,13	-65,00
φ6	-0,98	-56,00
φ7	-1,29	-74,00
X	Y	R
89,92	-3,29	193,16

ROTATION ANGLE		
φ2	-2,53	-145,00
φ3	-1,38	-79,00
φ4	-1,69	-97,00
φ5	-0,98	-56,00
φ6	-1,08	-62,00
φ7	-1,29	-74,00
X	Y	R
87,19	1,48	194,52

Figure 4.10 Effect of the rotation angle on compactness - 142º, 145º cases

As can be seen from Figs 4.9 and 4.10, maximum compactness is obtained when the angle between first two consecutive links is 137º.

4.2 Manufacturing Method and Material Selection

One of the most important design step is selection of strong and light-weight materials for the ramp. Manufacturing methods and materials must be selected by taking into consideration that the ramp has two main parts which are load-bearing and rotating links and panels. Load-bearing links are designed to form two parallel serial chains and rotate about their pivot points to be able to roll. On the other hand, the panels are designed to be attached in between wo load-bearing links to transfer the wheelchair user throughout the ramp.

4.2.1 Load-Bearing Links

Load-bearing link geometry is modeled to constitute a self-standing assembly while the ramp is in deployed position. The use of materials with low density and high strength-to-weight ratio is an effective way to reduce total weight of a structure. Although, the first thing that comes to mind is using composite materials due to lightness, manufacturing cost is quite high due to complicated link shape.

Aluminum is a conventional lightweight material with density of 2.7 g/cm^3 - approximately one-third of the density of steel. Although pure aluminum doesn't have a high tensile strength, these properties can be increased with alloy elements like silicon, zinc, copper, manganese and magnesium. Thus, it becomes possible to produce different alloys with tailored properties for specific applications. Some of these alloys are used in aircraft, aerospace and automotive industry where the weight is an important design parameter. Moreover, even aluminum alloys have low tensile properties compared with steel, their specific strength (or strength-to-weight ratio) is quite outstanding (Askeland & Phulâe, 2006; Songmene et al., 2011; Rana et al., 2012)

Aluminum alloys can be divided into two main groups: wrought and casting alloys, depending on their fabrication method. Cast alloys tend to be porous due to gas dissolving during casting process. On the other hand, wrought alloys are shaped by plastic deformation. Moreover, their compositions and microstructures are significantly different from casting alloys which make them demonstrate different mechanical properties (Kaufman, 2000; Rana et al., 2012).

According to international alloy designation system for wrought aluminum alloys (Table 4.2), first digit defines alloying class and the remaining numbers define the specific composition of the alloy. The degree of strengthening is given by T or H, depending on whether the alloy is manufactured with heat-treatment (T) or strain hardening (H) and the following numbers indicate the amount of hardening or the type of heat-treatment (Askeland & Phulâe, 2006).

Table 4.2 International alloy designation system for wrought aluminum alloys

1XXX	Commercially pure Al (>99% Al)	Not age-hardenable
2XXX	Al-Cu and Al-Cu-Li	Age-hardenable
3XXX	Al-Mn	Not age-hardenable
4XXX	Al-Si and Al-Mg-Si	Age-hardenable
5XXX	Al-Mg	Not age-hardenable
6XXX	Al-Mg-Si	Age-hardenable
7XXX	Al-Mg-Zn	Age-hardenable
8XXX	Al-Li, Sn, Zr, B, Fe or Cr	Mostly age-hardenable

For material selection two different types of aluminum alloys are compared due to their mechanical properties (Table 4.3) and material cost. Although, 7075-T6 is one of the strongest aluminum alloys in the market and used widely in aerospace industry, its high price, embrittlement, lower corrosion resistance and tougher machinability should not be considered compared to 6061-T6. On the other hand, 6061-T6 is one of the commonly used strongest alloys in 6XXX series and it has lower price compared to 7075-T6. Material selection step is conducted simultaneously with the strength calculation step by comparing the structure's factor of safety.

Table 4.3 Mechanical properties of Al 7075-T6 and 6061-T6

	7075-T6	**6061-T6**
Ultimate Tensile Strength	572 MPa	310 MPa
Tensile Yield Strength	503 MPa	276 MPa
Modulus of Elasticity	71.7 GPa	68.9 GPa
Poisson's Ratio	0.33	0.33
Fatigue Strength	159 MPa	96.5 MPa
Shear Modulus	26.9 GPa	26 GPa
Shear Strength	331 MPa	207 MPa

The manufacturing method selection can be done properly according to design parameters and selected material characteristics. The most effective manufacturing method for building a prototype with aluminum is machining due to material characteristics and budged constraint.

4.2.2 Load-Bearing Panels

The conceptual shape of load-bearing panels are relatively more regular than load-bearing links so composite materials can be used. Composite materials are formed from two or more materials to produce properties which are not found in any single conventional material. Although, both raw materials and manufacturing methods of composite materials are high priced, it is possible to reduce the total cost of composite panels by using core materials like foam, kraft and/or honeycomb structures. These types of materials (Fig 4.11) which have thin layers as a facing material joined to a lightweight core material are called sandwich composites (Askeland & Phulâe, 2006).

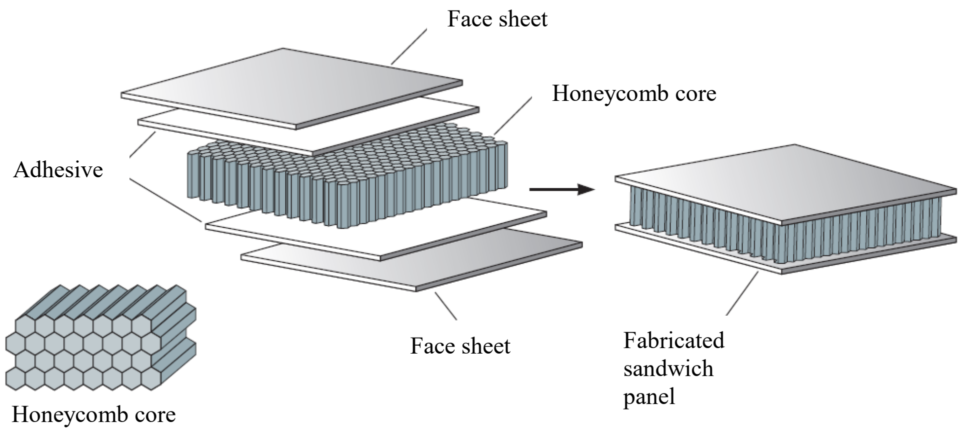

Figure 4.11 Sandwich composite structure (Source: Askeland & Phulâe, 2006)

Sandwich panels typically consist of two thin face sheets which are adhesively bonded to a lightweight thicker core (Askeland & Phulâe, 2006; Carlsson & Kardomateas, 2011). Determination of mechanical properties of a sandwich composite structure's face sheets and core materials is crucially important for analysis and design. It is possible to find mechanical properties of conventional materials especially metals, in textbooks on materials science and strength of materials (Beer et al., 2001; Askeland & Phulâe, 2006; Ashby, 2005). However, composite materials contain large variety of fibers, matrix materials (epoxy, polyester, etc.) and different fiber orientations make mechanical test a necessity to determine the mechanical properties of them (Carlsson & Kardomateas, 2011). Ashby's materials property charts (Fig. 4.12) can guide to select face and core materials (Ashby, 2005). Face sheets are generally made of composite laminates and light-weight alloys with high modulus, while cores with lower density are formed of thicker metallic and non-metallic honeycombs, foams, balsa wood or trusses (Daniel & Abot, 2000).

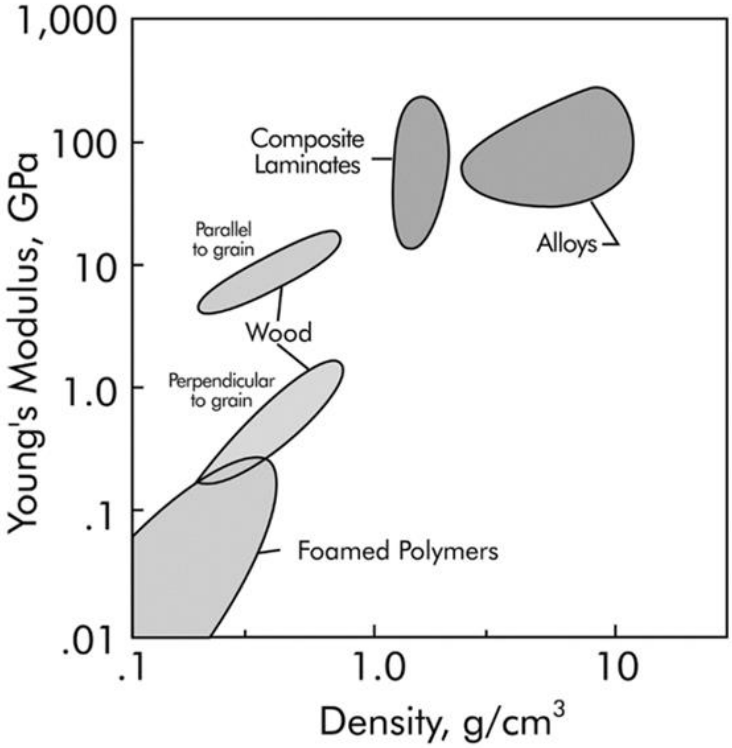

Figure 4.12 Modulus-density chart for various classes of materials
(Source: Ashby, 2005)

Using the chart in Fig. 4.12, sandwich beams are fabricated by bonding twill-woven 245 g/m^2 carbon fiber fabric/epoxy resin face sheets to polypropylene, aluminum, kraft honeycomb and airex foam cores with an epoxy adhesive (Fig. 4.13).

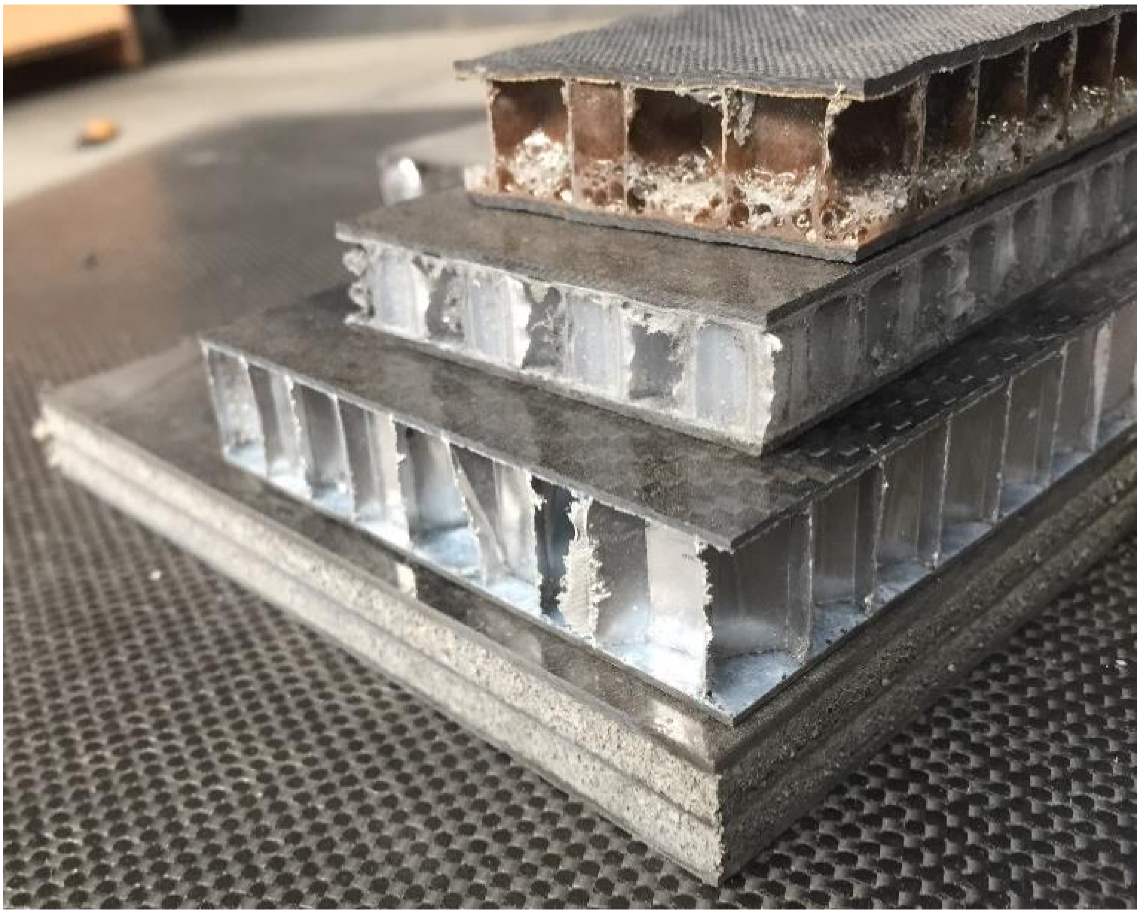

Figure 4.13 Sandwich composite panels

After producing the samples, it is decided that panels with PP and Al honeycomb core should be subjected to flexural test. Panels with Kraft honeycomb and Airex foam core do not meet the expectation in terms of lightness and also, it is hard to find these cores with various thickness in the market.

Sandwich composite panel length (ramp width) is selected as 800 mm according to standard adult wheelchair's measurement. Although, there are some special designed wheelchairs with the width of 760 mm in the market, standard wheelchair width is in range between 600-650 mm.

There is no known standard for portable ramps. However, there is a standard for fixed ramps called "TSE 9111- The requirements of accessibility in buildings for people with disabilities and mobility constraints". The measurements mentioned in this standard are highly extreme for a portable ramp due to users' expectation about easy transportation. However, the ramp width can be changed easily by changing the panel length according to requirements which are explained in TSE 9111.

4.2.2.1 Flexural Testing Procedure

Flexure tests on flat sandwich construction may be conducted to determine the sandwich flexural stiffness, the core shear strength and shear modulus, or the facing's compressive and tensile strengths. Tests to evaluate the shear strength of the core may also be used to evaluate core-to-facing bonds. This test method provides a standard method of obtaining the sandwich panel flexural strengths and stiffness.

Sandwich beams are fabricated with proper measurements, and loaded with a loading speed 2 mm/sec, under three-point bending (Fig. 4.14) in a Shimadzu AG-IC universal testing machine according to ASTM C 393 Standard Test Method for Flexural Properties of Sandwich Constructions. The data sets relating the loads and the mid-span deflection of the panel specimen are automatically detected and directly recorded with a computer in real time while the stroke of the actuator advances.

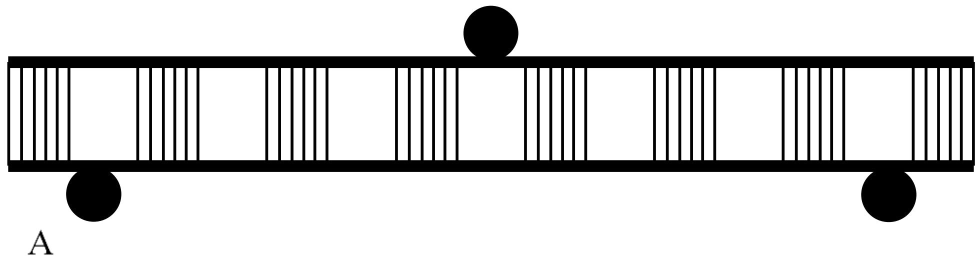

Figure 4.14 Schematic view of the three-point bending test set-ups

Test specimens are prepared according to ASTM C393 with 200 mm length and 75 mm width and span length is selected as 150 mm. First test (Fig. 4.15) is conducted with 10 mm-thick PP honeycomb (0,08 g/cm^3) and 10 mm-thick Al. honeycomb core material with 0,034 g/cm^3 density and 4 layer of twill woven carbon fiber fabric face sheets to observe the effect of different core materials on core ultimate shear and panel bending strength and stiffness (D).

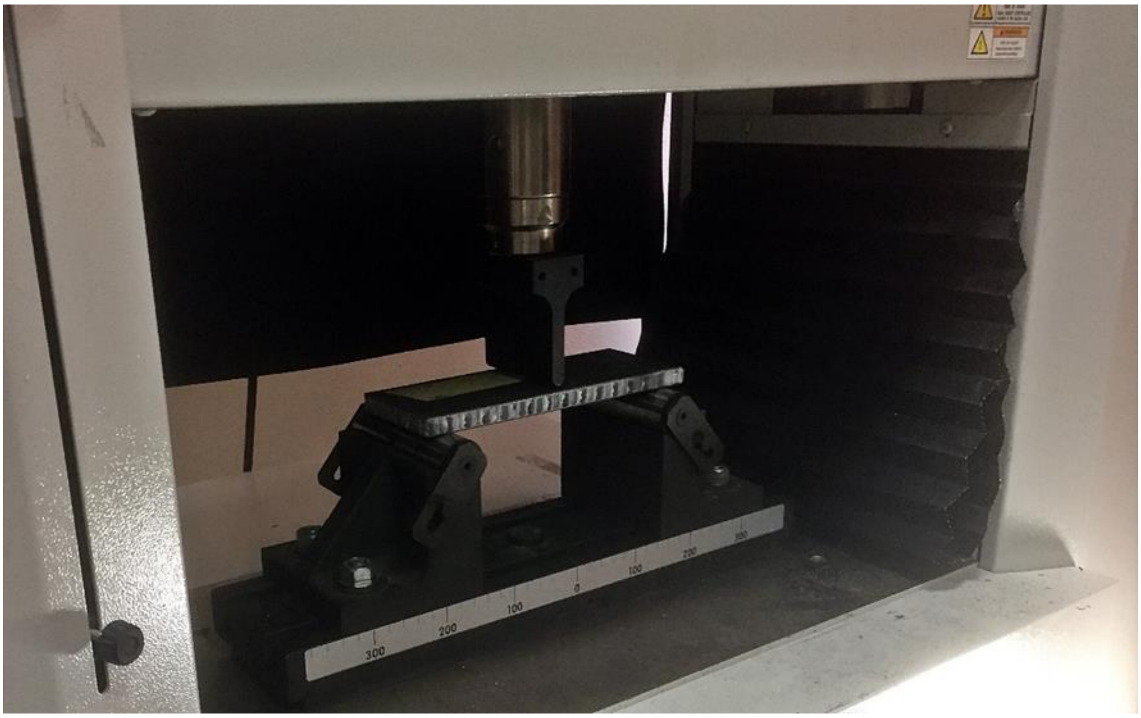

Figure 4.15 Three-point bending test

First group of flexural test results (Table 4.4) show the effects of different core materials on core ultimate shear, bending ultimate shear strength and panel bending stiffness.

Table 4.4 Three-point bending test results

Core material	Face Thickness (mm)	Panel Thickness (mm)	Core Ultimate Shear Strength (Mpa)	Bending Ultimate Strength (Mpa)	Panel Bending Stiffness (D) ($N \cdot mm^2$)
Al Honeycomb	1,26	12,52	0,505	37,5	31756226
PP Honeycomb	1,425	12,85	0,678	20,426	18242777

The linear elastic behavior for green specimen of Al honeycomb cored sandwich panel is apparent in Fig. 4.16.A until the load approaches to about 1250 N, however standard deviation is relatively high and results can be considered inconsistent compared to Fig. 4.16.B. Although, bending ultimate strength and panel bending stiffness of Al honeycomb cored sandwich are higher than PP Honeycomb cored sandwich panel, core ultimate shear strength is lower. The reason of these inconsistencies for Al honeycomb cored sandwich panel may be weak bonding surface area between face and core material that causes core-skin seperation. The possibility of seperation between Al honeycomb core and face material may be reduced by wrapping panel with pre-preg CF face material which is basically pre-impregnated CF fabric where the epoxy is already present in the material.

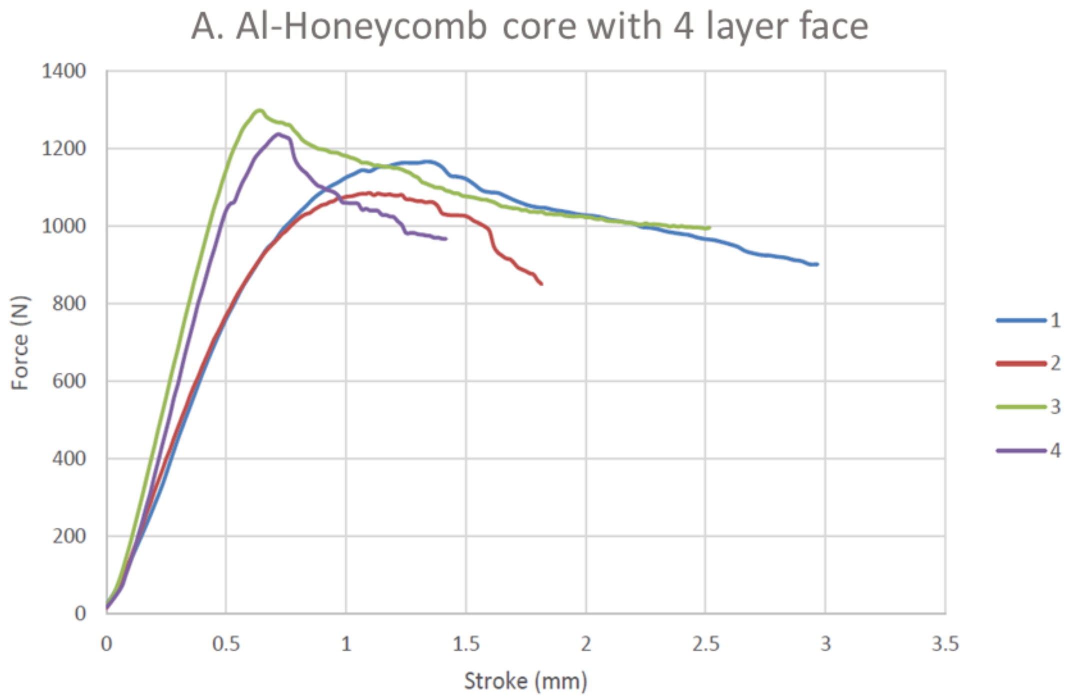

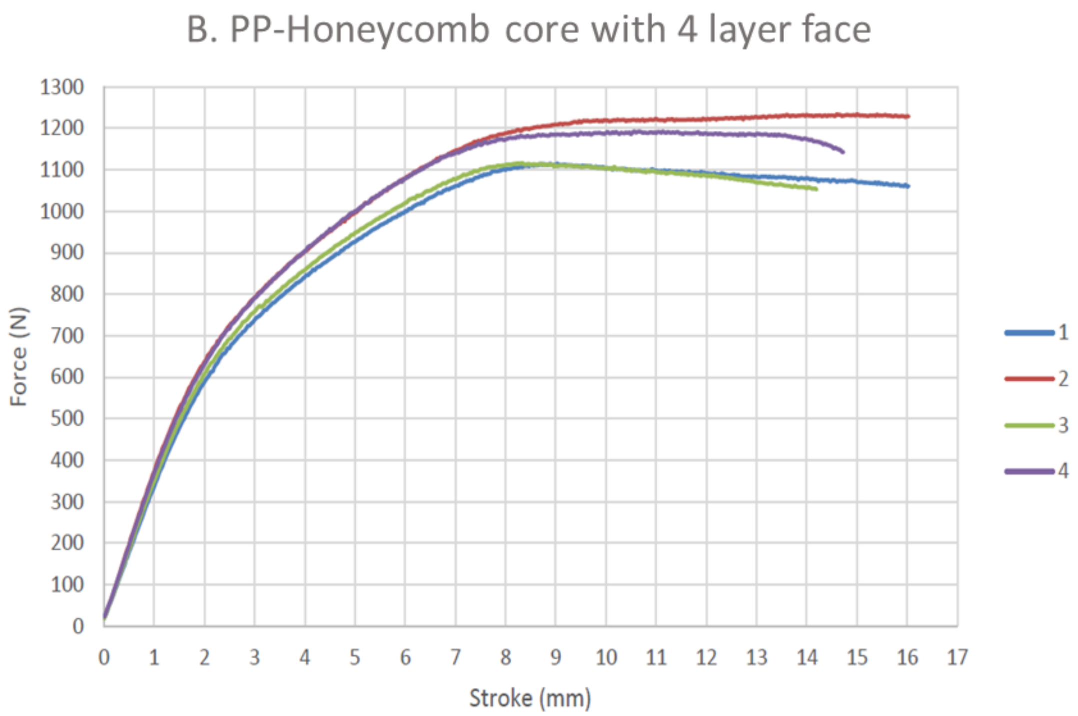

Figure 4.16 Force-Stroke diagram of A. Al and B. PP honeycomb core sandwich panels

Second group of flexural test is conducted with the Al honeycomb sandwich beams which are fabricated according to ramp design measurements, and loaded under four-point bending (Figs. 4.17 and 4.18) in a Shimadzu AG-IC universal testing machine according to ASTM C 393 Standard Test Method for Flexural Properties of Sandwich Constructions. Two different test specimens are tested. Al honeycomb core with 10 mm and 15 mm-thick cored 740 mm span length, 125 mm width sandwich panel are tested with 220 mm load span length (Table 4.5).

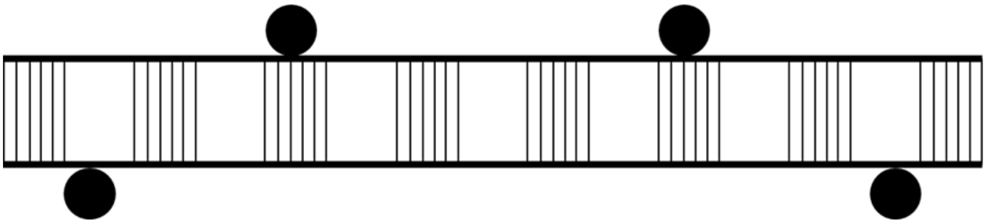

Figure 4.17 Schematic view of the four-point bending test set-ups

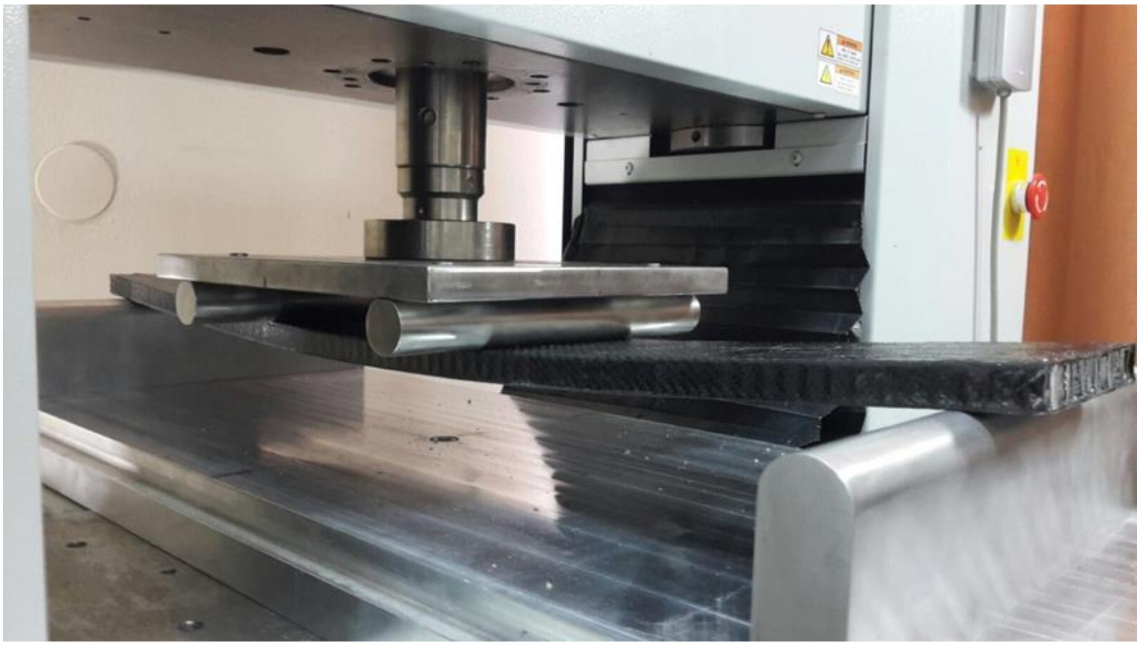

Figure 4.18 Four-point bending test

Table 4.5 Sandwich panel test specimens with Al honeycomb core

No	Core Thichkness (mm)	Face Thickness (mm)	Panel Thickness (mm)	Width (mm)	Panel Length (mm)	Support Length (mm)	Loading Span Length (mm)
1	10	1,425	12,85	125	800	740	220
2	15	1,475	17,95	125	800	740	220

Fig. 4.19 shows the new prepreg coated sandwich panel test results which exhibit a different behavior than a classical sandwich panel (Fig 4.16.A). Face fracture occurs before core yields (Fig. 4.20). For design, 10 mm-thick cored sandwich panel is selected in terms of lightness and high bending ultimate strength. Factor of safety calculations, shear, bending moment and deflection diagrams are illustrated in Section 4.3.5.

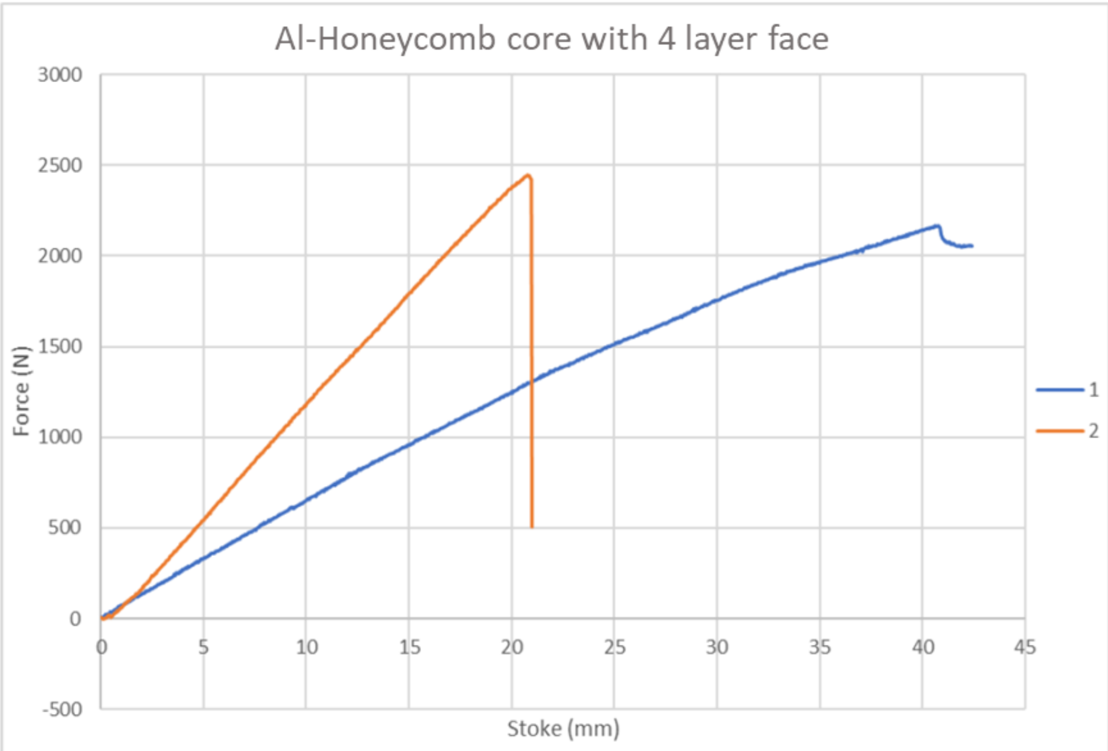

Figure 4.19 Force-Stroke diagram of Al honeycomb core sandwich panels

Figure 4.20 Sandwich beam face fracture

Table 4.6 Four-point bending test results

No	Core Ultimate Shear Strength (MPa)	Bending Ultimate Strength (MPa)	Panel Bending Stiffness (D) ($N \cdot mm^2$)
1	0,763	118,307	421603798
2	0,62	84,598	605753241

4.3 Strength Calculations

Strength calculations are conducted by selecting a simply supported beam with certain link length, height and thickness. The beam model for the evaluations is constructed assuming a self-standing form of the ramp in deployed state. First, the free-body diagram of a standard wheelchair is illustrated in the following subsection.

4.3.1. Free-Body Diagram of a Wheelchair

Even though the total weight capacity of a standard wheelchair and product itself is lower than 200 kgf, there are some heavy-duty type products total weight more than 250 kgf (Fig. 4.21).

Heavy Duty Products			
Weight Capacity (kgf)	100	204	183
Product Weight (kgf)	115	55	94
Total Weight (kgf)	215	259	277
Average (kgf)	250,3		
Total Width (mm)	599-650	630	635
Average (mm)	628,5		

Figure 4.21 Heavy duty products in the market
(Source: 1800Wheelchair.com, n.d.)

The ramp's load bearing capacity is expected to be 2942 N (300 kgf) per 2 meters to prevent the possibility of user error in terms of exceeding load capacity. The aim of this selection is to take extra safety precaution besides the factor of safety during structural design.

The center of gravity (CG) of a wheelchair is the average location of the total weight of both user and the wheelchair (Fig 4.22). The reaction forces at the wheels due to the wheelchair and user weight ($F_{person} + F_{wheelchair} = 2942\ N$) can be computed from force and moment equilibrium equations:

$$\sum F = 2F_{wheel} + 2F_{caster} - \left(F_{person} + 2F_{wheelchair}\right) = 0 \qquad (4.9)$$

$$\sum M_{caster} = \left(F_{person} + 2F_{wheelchair}\right)L_{caster} - 2F_{wheel}\left(L_{caster} + L_{wheel}\right) = 0 \quad (4.10)$$

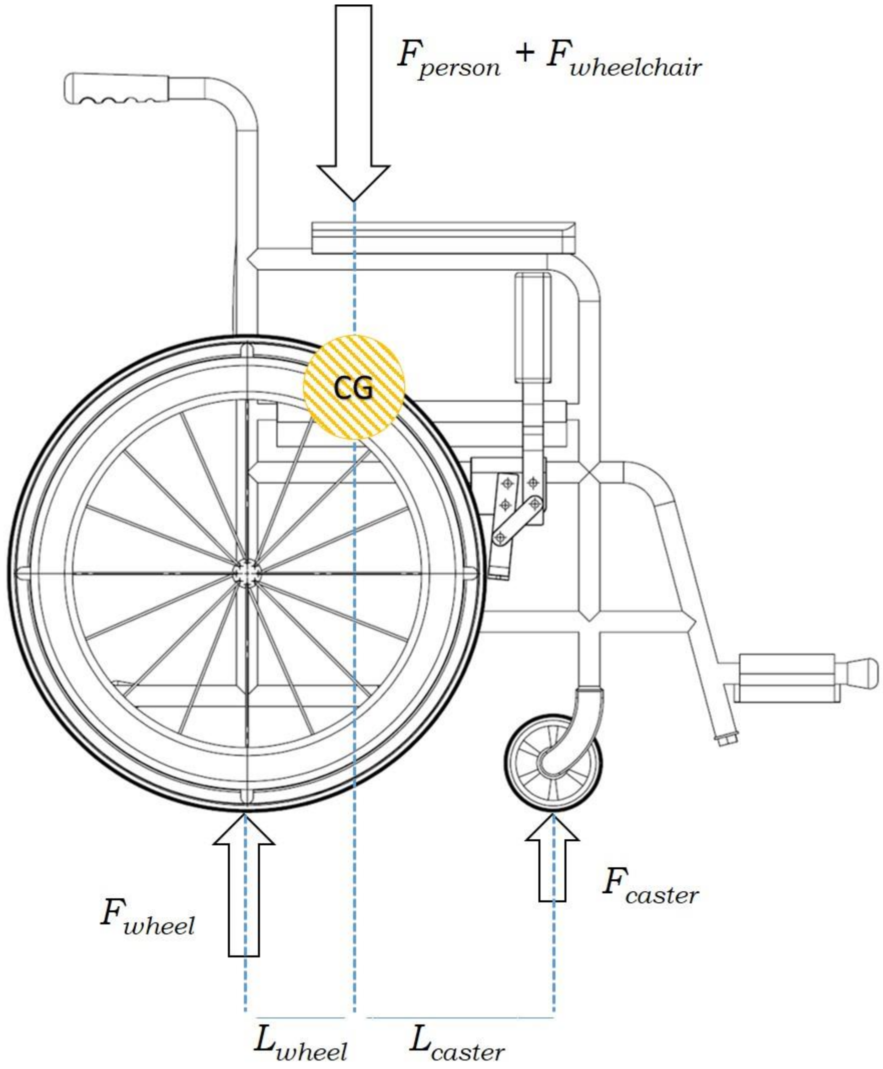

Figure 4.22 Free-Body Diagram of a Wheelchair
(Source: GrabCAD Library, 2016; Winter and Hotchkiss, 2006)

$L_{caster} = 406\ mm$ and $L_{wheel} = 102\ mm$, so

$$F_{wheel} = \frac{(F_{person}+F_{wheelchair})(L_{caster})}{2(L_{caster}+L_{wheel})} = 1175\ N \tag{4.11}$$

$$F_{caster} = \frac{(F_{person}+F_{wheelchair})-2(F_{wheel})}{2} = 296\ N \tag{4.12}$$

4.3.2 Deflection of Beams by Integrating Transverse Loading

A prismatic beam subjected to pure bending is bent into an arc. Within the elastic range, the curvature of neutral surface may be expressed as

$$\frac{1}{\rho} = \frac{M(x)}{EI} \tag{4.13}$$

where M is bending moment, E is the modulus of elasticity, I is the area moment of inertia of the cross section about its neutral axis and x is the distance of the section from the left end of the beam. For a curve $y(x)$ the curvature can be expressed as

$$\frac{1}{\rho} = \frac{\frac{d^2y}{dx^2}}{\left[1+\left(\frac{dy}{dx}\right)^2\right]^{3/2}} \tag{4.14}$$

But, in the case of an elastic curve of a beam, the slope dy/dx is very small, and its square is negligible compared to unity. Therefore, a good approximation to Eq. (4.14) is

$$\frac{1}{\rho} = \frac{d^2y}{dx^2} \tag{4.15}$$

Substituting Eq. (4.15) into Eq. (4.13)

$$\frac{d^2y}{dx^2} = \frac{M(x)}{EI} \tag{4.16}$$

Eq. (4.17) is the governing differential equation for the elastic curve and it is a second-order ordinary differential equation.

The product EI is known as the flexural rigidity. In case of a prismatic beam the flexural rigidity is constant. Integrating Eq. (4.16)

$$\mathrm{EI}\frac{dy}{dx} = \int_0^x M(x)\,dx + C_1 \tag{4.17}$$

where C_1 is an integration constant. Denoting the slope at any given point to the elastic curve by angle $\theta(x)$ and noting that this angle is very small

$$\frac{dy}{dx} = \tan\theta \simeq \theta(x) \tag{4.18}$$

Thus an alternative form of Eq. (4.17) is

$$EI\,\theta(x) = \int_0^x M(x)\,dx + C_1 \tag{4.19}$$

Integrating Eq. (4.17)

$$EI\,y = \int_0^x \left[\int_0^x M(x)\,dx\right] dx + C_1 x + C_2 \tag{4.20}$$

The constants C_1 and C_2 are determined from the boundary conditions or, more precisely, from the conditions imposed on the beam by its supports (Beer et al., 2012).

4.3.3 Use of Singularity Functions to Determine the Maximum Deflection of the Beam

A simply supported beam is modelled according to transverse loading conditions of the free-body diagram of a wheelchair to find numerical and analytical solution with the help of singularity function. The reason of this calculation is determining where the maximum deflection occurs throughout the ramp, the factor of safety and afterwards, conducting structural optimization.

In the case of a beam loaded with a uniformly distributed load w the shear force and bending moment can be represented by continuous analytical functions. However, in the case of a simply supported beam as in Figure 4.23, the loads applied at B and C represents a singularity in the beam loading. This singularity results in discontinuities in the shear force V and bending moment M and requires use of different analytical functions to represent V and M in different portions of the beam. The use of singularity functions makes it possible to represent the shear force, the bending moment or the deflection in a beam by a single expression, valid at any point of the beam.

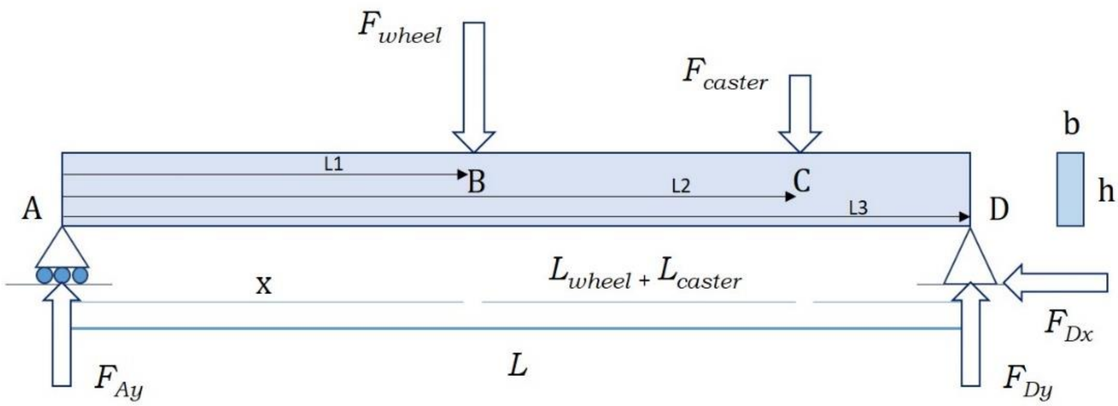

Figure 4.23 Determining the maximum deflection of the simply supported beam

Singularity function of x is denoted by $\langle x - x_0 \rangle^n$, where *n* is any integer (positive or negative) including zero, and x_0 is a constant equal to the value of x at the beginning of a specific interval along the beam. Singularity function for $n \geq 0$ is partially defined as

$$\langle x - x_0 \rangle^n = \begin{cases} (x - x_0)^n, & for\ x \geq x_0 \\ \quad 0 \quad , & for\ x < x_0 \end{cases} \tag{4.21}$$

Integral and derivative of singularity functions are required for beam deflection problems. For *n* > 0

$$\int \langle x - x_0 \rangle^n \, dx = \frac{1}{n+1} \langle x - x_0 \rangle^{n+1} + C \tag{4.22}$$

$$\frac{d}{dx} \langle x - x_0 \rangle^n = n \langle x - x_0 \rangle^{n-1} \tag{4.23}$$

For the beam in Figure 4.23, the shear force and bending moment should be represented for the three intervals: $0 \leq x \leq L_1$, $L_1 \leq x \leq L_2$ and $L_2 \leq x \leq L$. For the three intervals, the shear force and the bending moment can be represented using singularity functions as

$$V(x) = F_{Ay} - F_{wheel}\langle x - L_1\rangle^0 - F_{caster}\langle x - L_2\rangle^0 \tag{4.24}$$

$$M(x) = F_{Ay}x - F_{wheel}\langle x - L_1\rangle^1 - F_{caster}\langle x - L_2\rangle^1 \tag{4.25}$$

Substituting for $M(x)$ from Eq. 4.27 into Eq. 4.16:

$$EI\frac{d^2y}{dx^2} = F_{Ay}x - F_{wheel}\langle x - L_1\rangle^1 - F_{caster}\langle x - L_2\rangle^1 \tag{4.30}$$

Integrating Eq. (4.30):

$$EI\,\theta = EI\,\frac{dy}{dx} = \frac{F_{Ay}}{2}x^2 - \frac{F_{wheel}}{2}\langle x - L_1\rangle^2 - \frac{F_{caster}}{2}\langle x - L_2\rangle^2 + C_1 \tag{4.31}$$

$$EI\,y = \frac{F_{Ay}}{6}x^3 - \frac{F_{wheel}}{6}\langle x - L_1\rangle^3 - \frac{F_{caster}}{6}\langle x - L_2\rangle^3 + C_1x + C_2 \tag{4.32}$$

The constants C_1 and C_2 can be determined from the boundary conditions: $y = 0$ at $x = 0$ and $x = L$:

$$C_1 = \frac{F_{wheel}(L-L_1)^3 + F_{caster}(L-L_2)^3 - F_{Ay}L^3}{6L} \text{ and } C_2 = 0 \tag{4.33}$$

The first step is determining the position of the maximum deflection, by using singularity function, which depends on design parameters (Table 4.7) and the free body diagram of the wheelchair (Fig. 4.21). The formulations are implemented in Excel to find the position of wheelchair which causes the maximum deflection by increasing x value gradually (Table 4.7). The results of analytical integration (Eqs. (4.31) and (4.32)) are crosschecked with numerical integration using finite differences.

Shear force, bending moment and deflection diagrams of the simply supported beam representing one side of the ramp are illustrated in Figs. 4.24, 4.25 and 4.26.

Table 4.7 Design Parameters

PARAMETERS	
L (mm)	2000
F_{wheel} (N)	1175
F_{caster} (N)	296
X (mm)	910
BC (mm)	508
E (N/mm^2)	68900 - 71700
b (mm)	10
h (mm)	70
I (mm^4)	285833,3333
EI ($N \cdot mm^2$)	19693916667

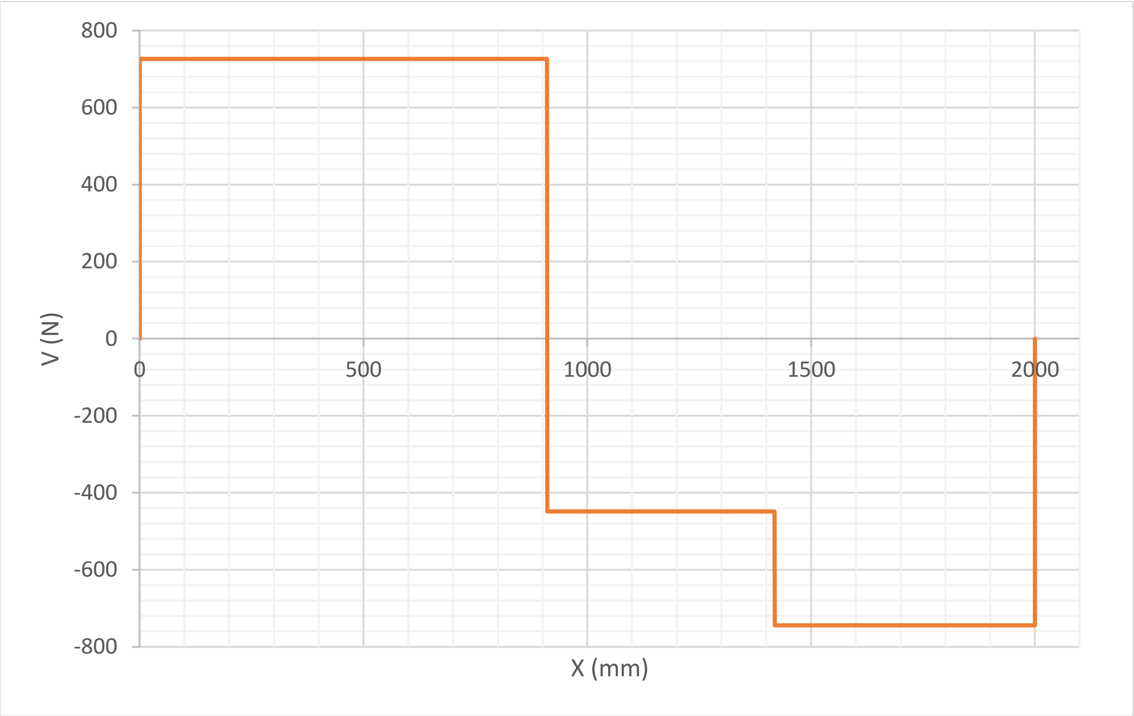

Figure 4.24 Shear force diagram

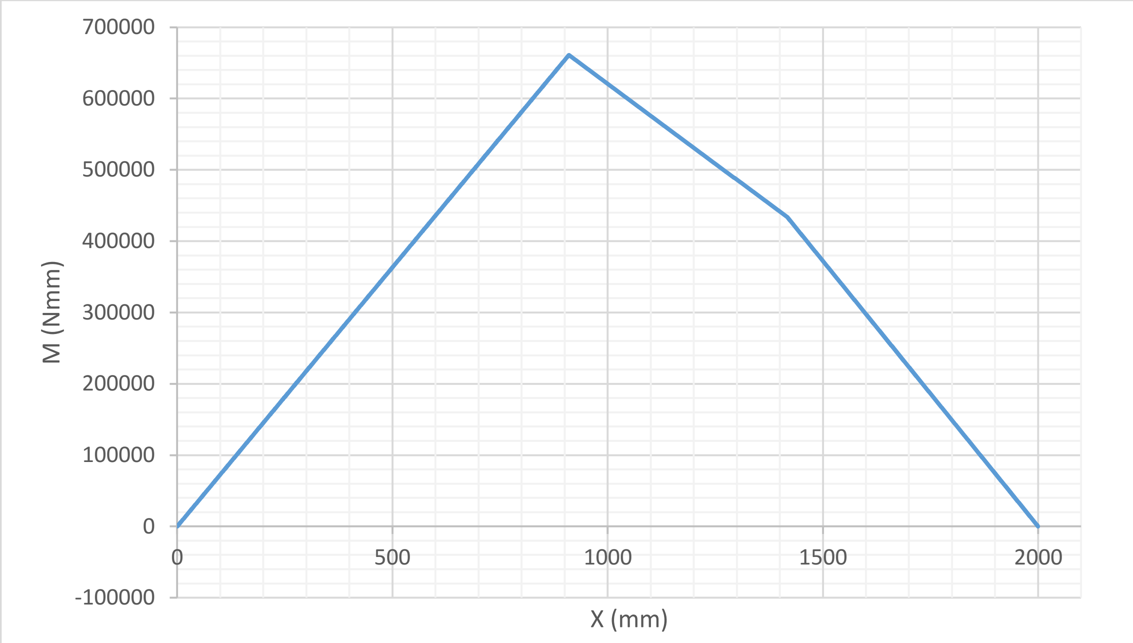

Figure 4.25 Moment diagram

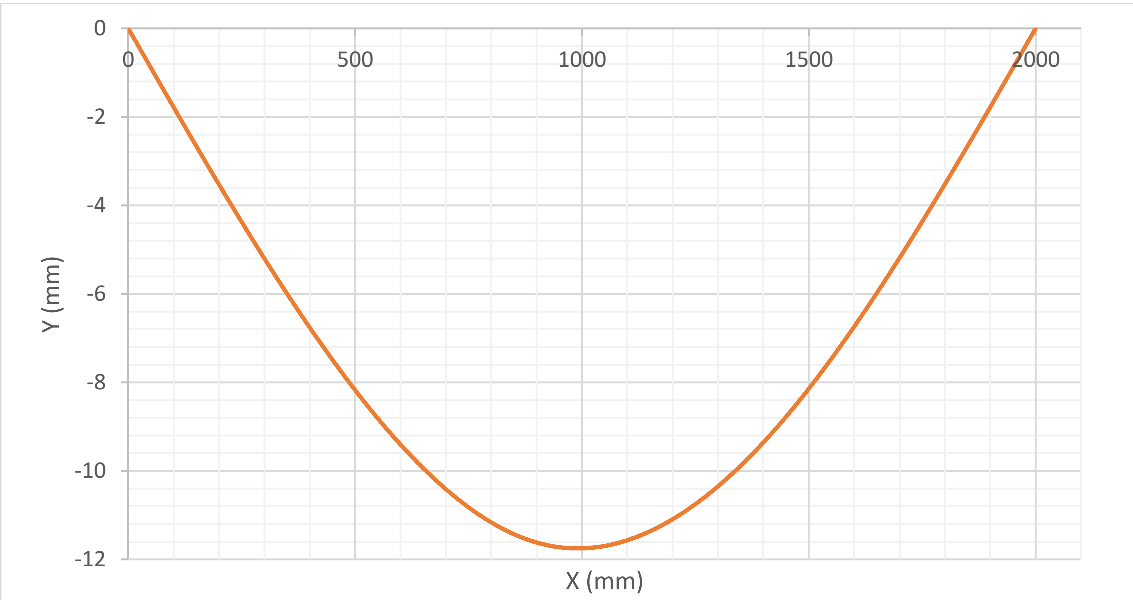

Figure 4.26 Deflection diagram

According to numerical analysis, maximum deflection occurs at 991 mm where the back wheel is at 910 mm. Finite element analysis (Figs. 4.27 and 4.28) is also conducted using Solidworks to verify this result which is used during structural optimization and the results are compared in Table 4.8.

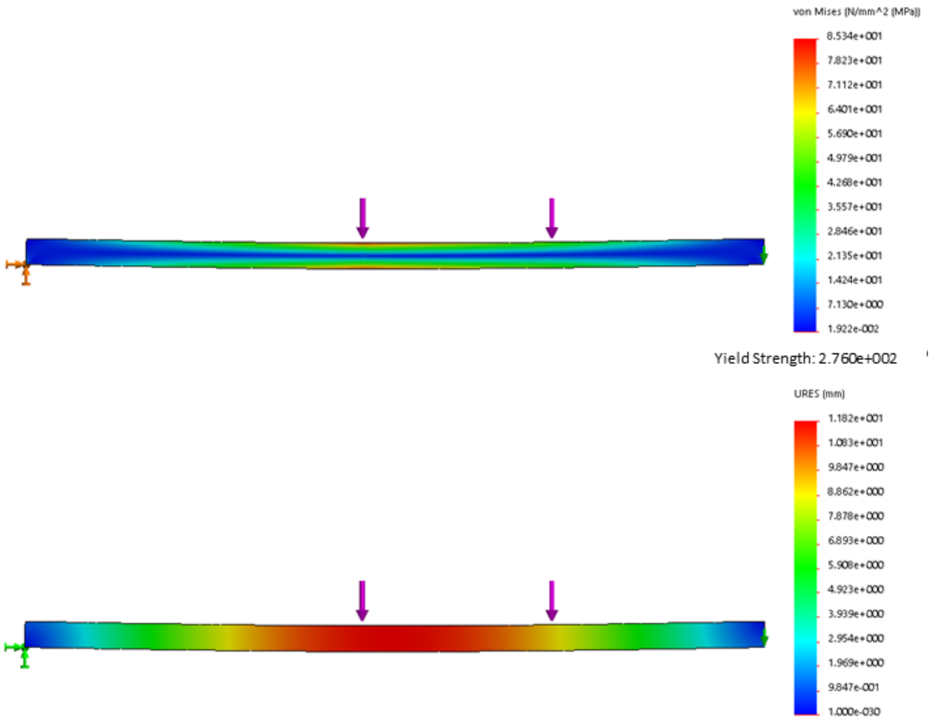

Figure 4.27 Stress and deflection analysis for Al 6061-T6

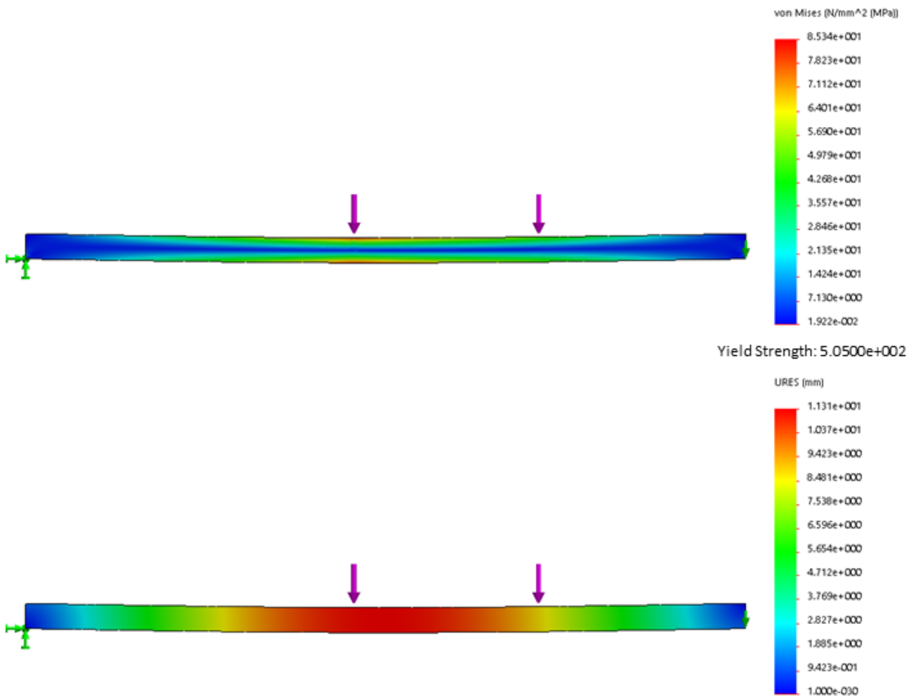

Figure 4.28 Stress and deflection analysis for Al 7075-T6

Table 4.8 Deflection and factor of safety (FOS) analysis

Al 6061 - T6			
Method	**Max Deflection (mm)**	**Max Stress (Mpa)**	**FOS**
Numerical	-11,77	80,95	3,41
Analytical			
Finite Element	-11,82	85,34	3,23
Al 7075 - T6			
Method	**Max Deflection (mm)**	**Max Stress (Mpa)**	**FOS**
Numerical	-11,31	80,95	6,21
Analytical			
Finite Element	-11,31	85,34	5,92

The maximum deflection is -11,82 mm for Al 6061-T6 and -11,31 mm for Al 7075 T6 while the factor of safety (FOS) is 3,32 and 5,91 respectively according to finite element analysis (Figs. 4.27, 4.28 and Table 4.8). The expected FOS is 2, thus the general structural measurements (thickness, height) are quite enough to redesign links for structural optimization to reduce weight. Moreover, maximum deflection values can be decreased and made nonnegative by designing an arch-like curved structure instead of a flat beam.

4.3.4 Structural Optimization

For structural optimization, only one side of the ramp is subjected to analysis for simplifying the finite element analysis. Curved link chains are generated by creating 0º, 0,5º and 1º slope angle at the sides of the links that creates a curved structure to prevent negative deflection (Fig. 4.31). Also, the sharp edges are rounded for decreasing the possible stress concentrations and preventing physical injuries. This small modification makes a slight difference for the compact rolled form of the ramp (Figs. 4.29 and 4.30) As can be seen from Table 4.9, kinematic and CAD models' diameters are slightly different. And the most compact configuration for CAD model forms while the first rotation angle is 142 º.

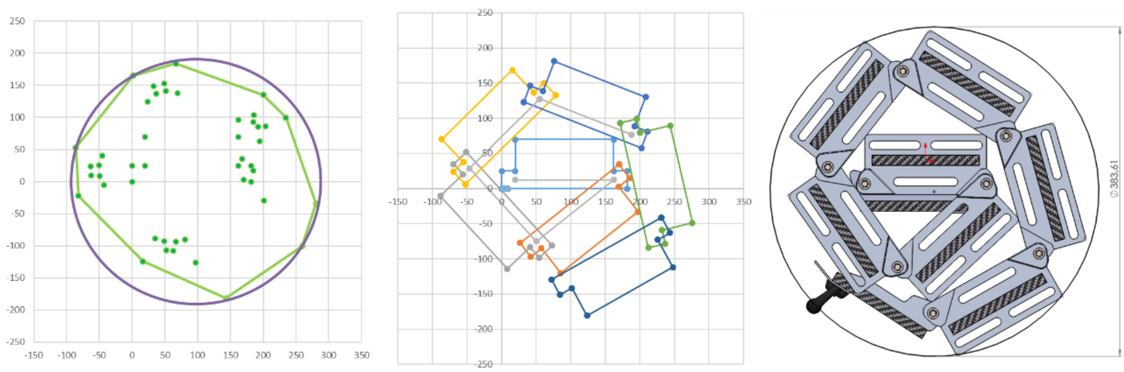

Figure 4.29 Effect of 137 ° rotation angle on compactness

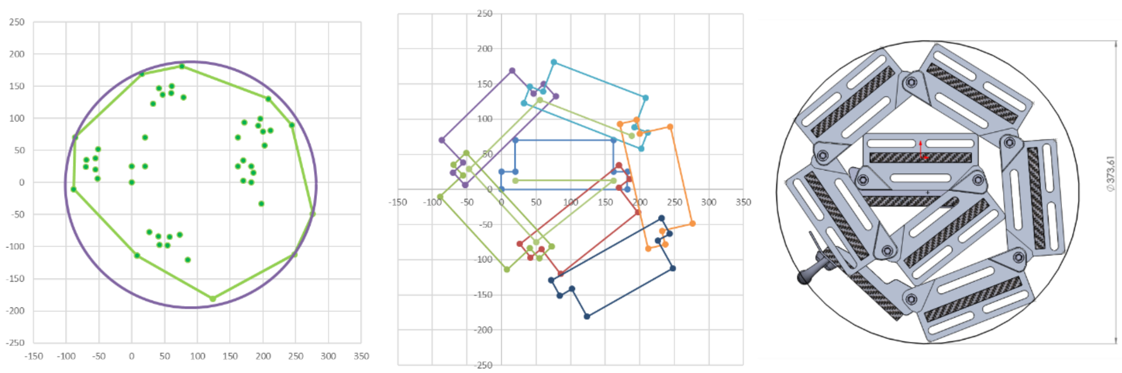

Figure 4.30 Effect of 142 ° rotation angle on compactness

Table 4.9 Comparing effect of the link with sharp edge and rounded edge

First rotation angle (deg)	Diameter (mm)	
	Kinematic Model	CAD Model
137 °	381,46	383,61
142 °	382,9	373,61

First, the curved link chains are represented as simply supported curved beams. Structural optimization is performed by removing redundant material from where the stress occurs less due to loading conditions. The simulation is performed based on the boundary conditions which represents the extreme loading conditions. To this end, link chain is positioned parallel to the ground and loaded according to defined conditions in Section 4.3.3. Results are presented in Figs. 4.32, 4.33, 4.34, 4.35, 4.36 and 4.37.

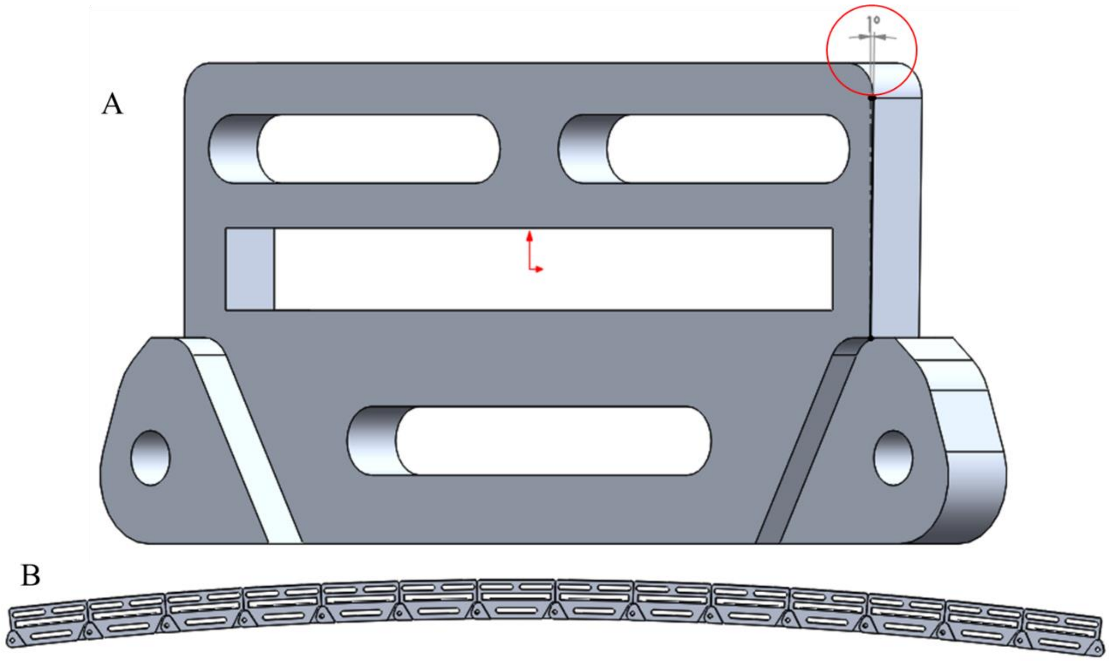

Figure 4.31 Side slope angle effect on B. Curved chain

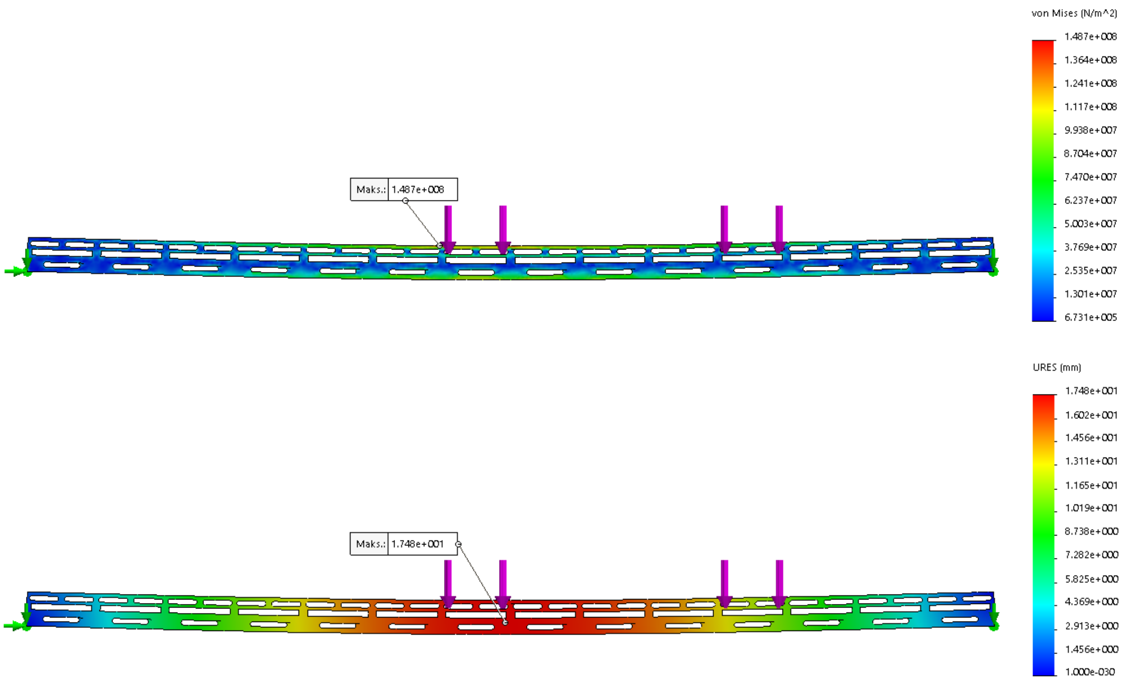

Figure 4.32 Stress and deflection analysis for Al 6061-T6, 0º slope

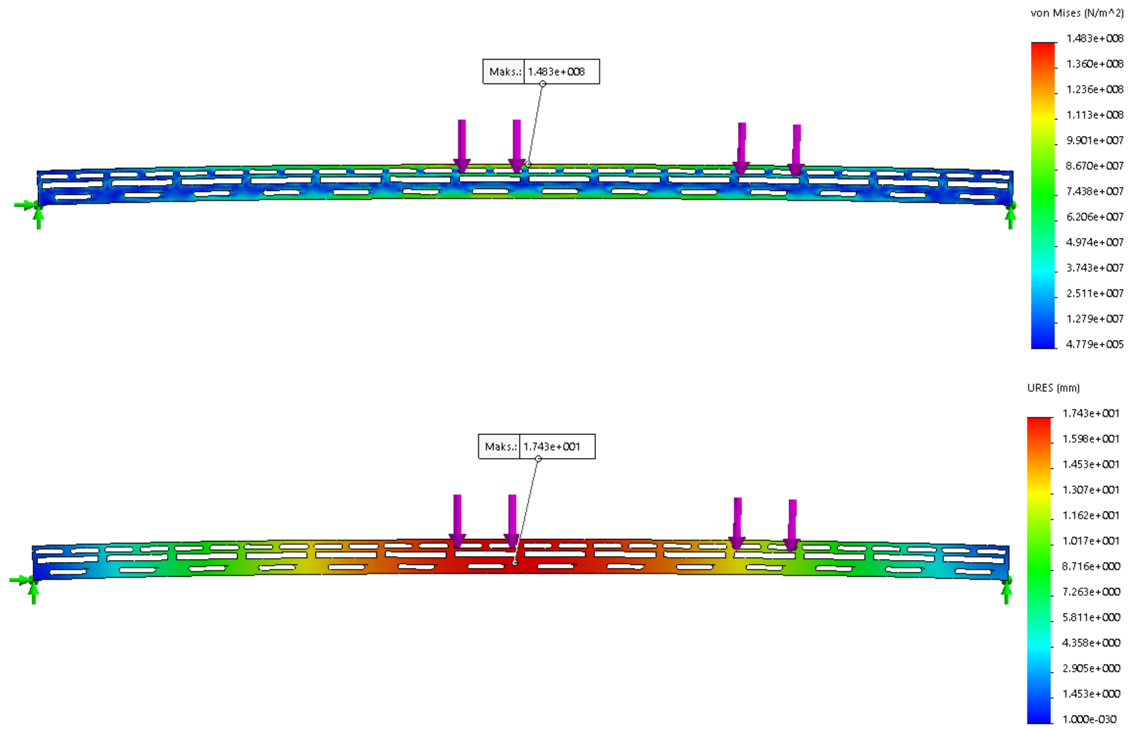

Figure 4.33 Stress and deflection analysis for Al 6061-T6, 0,5º slope

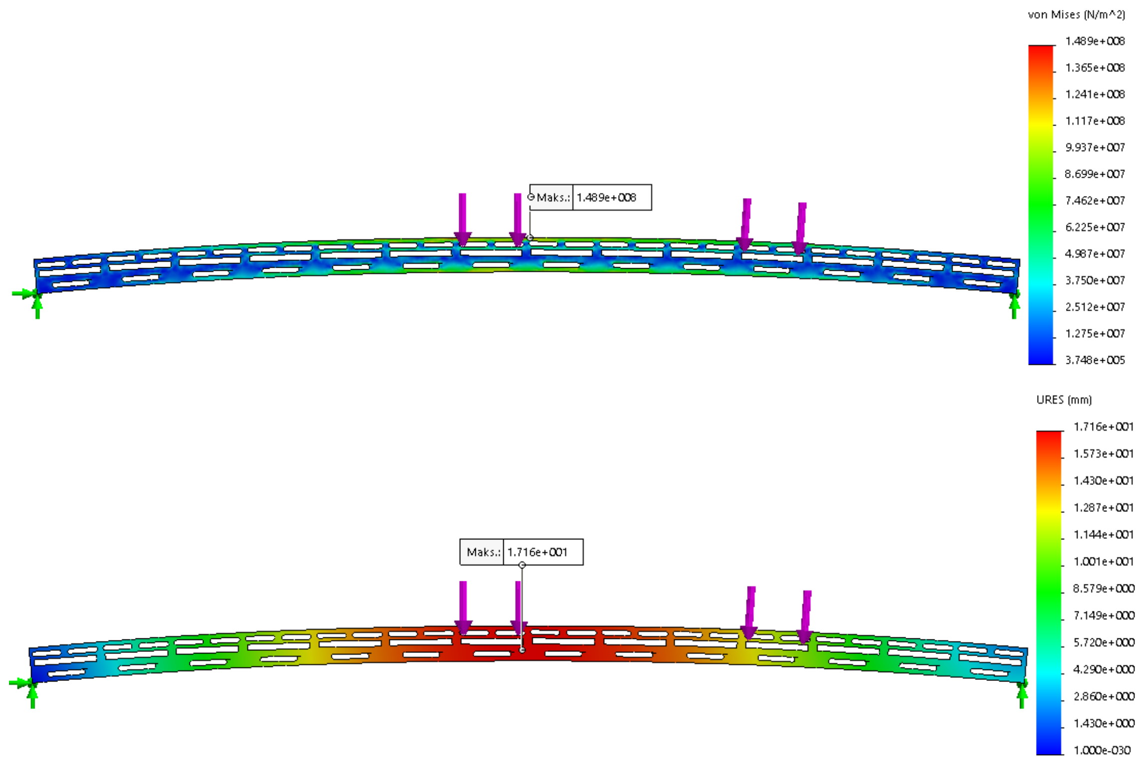

Figure 4.34 Stress and deflection analysis for Al 6061-T6, 1º slope

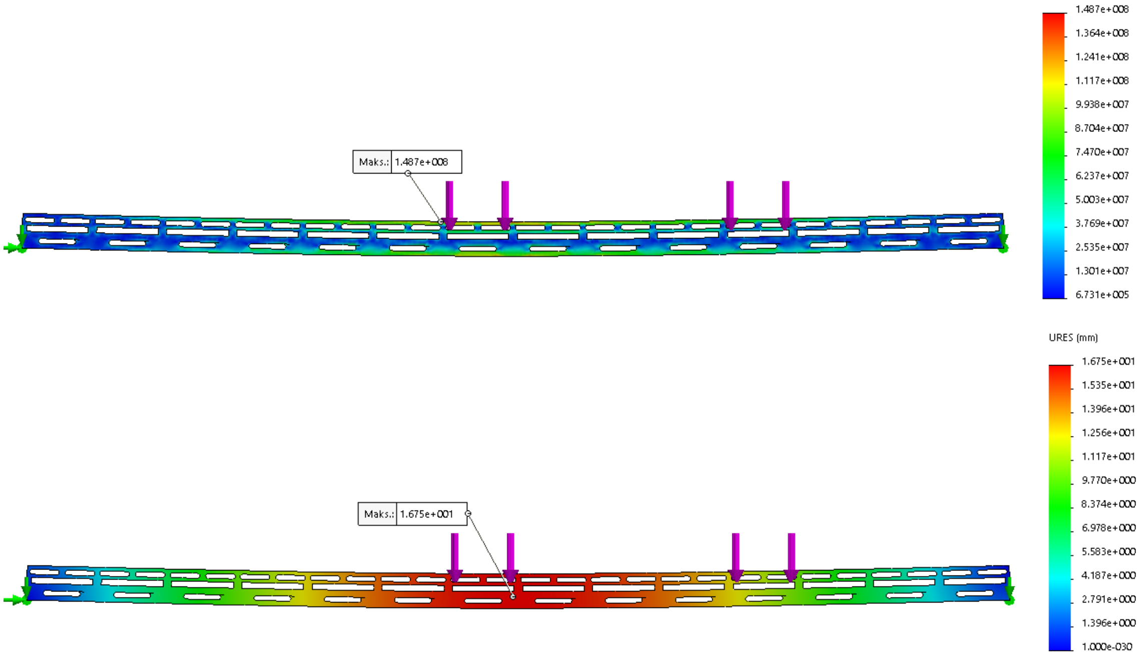

Figure 4.35 Stress and deflection analysis for Al 7075-T6, 0º slope

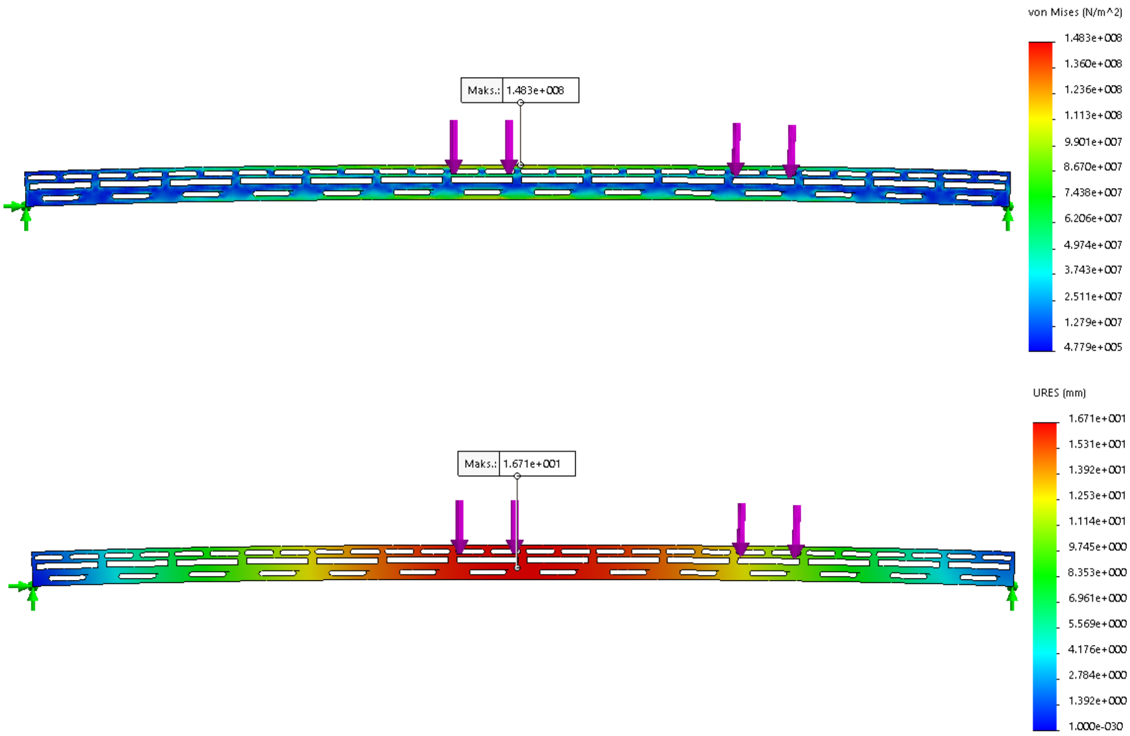

Figure 4.36 Stress and deflection analysis for Al 7075-T6, 0,5º slope angle

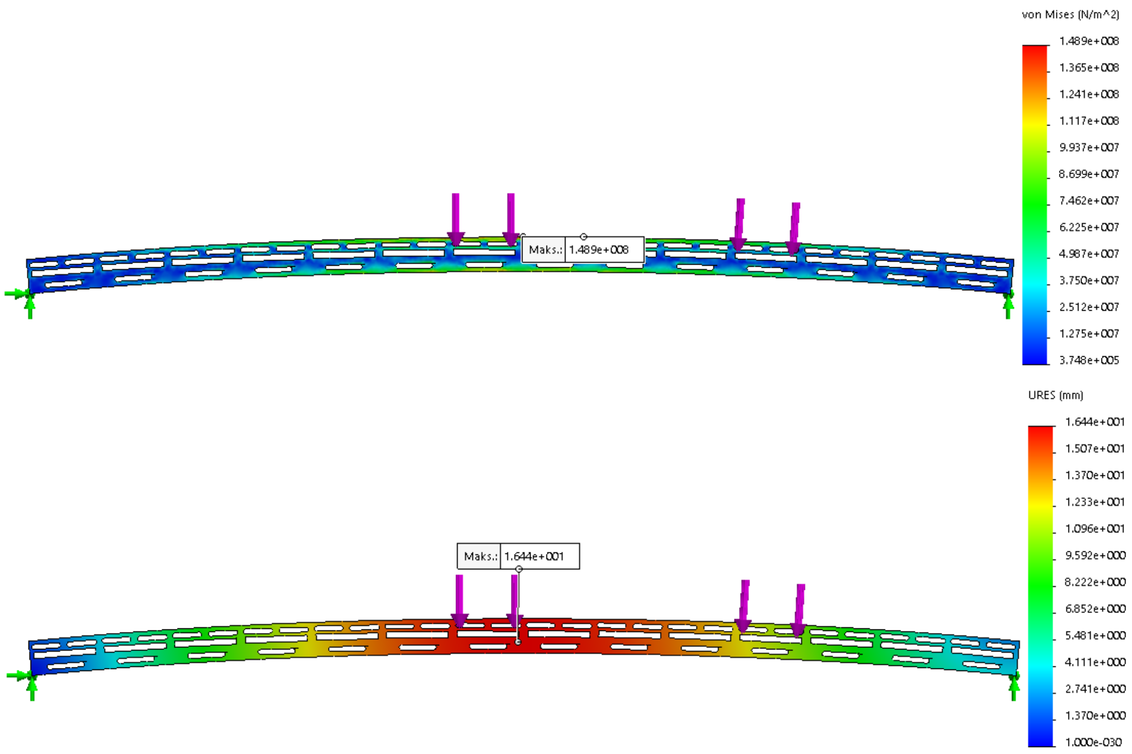

Figure 4.37 Stress and deflection analysis for Al 7075-T6, 1º slope angle

Redundant material pattern, where the blanks are introduced, is determined due to assembly areas where the composite panels, hand rails and telescopic legs may be assembled. Stress distribution is observed whether redundant materials cause to exceed yield point or not. Numerical results are summarized in Table 4.10.

Table 4.10 Deflection and Factor of Safety (FOS) Analysis of flat and curved beams

6061-T6			
Slope Angle (deg)	**Max. Deflection (mm)**	**Max. Stress (Mpa)**	**FOS**
0	17,4	148,7	1,86
0,5	17,4	148,3	1,86
1	17,1	148,9	1,85
7075-T6			
Slope Angle (deg)	**Max. Deflection (mm)**	**Max. Stress (Mpa)**	**FOS**
0	16,7	148,7	3,40
0,5	16,7	148,3	3,41
1	16,4	148,9	3,39

Table 4.10 shows that the small curvature for the single-piece beam has no significant effect on deflection and FOS. This is because the radius of curvature is large enough to be neglected and Eq. 4.32 is valid. A curved beam can be treated as a flat beam if the radius of curvature is greater than 10 times the depth of the beam's cross section (Roark et al., 2012).

However, the curved assembly load-bearing members may not behave the same as the single-piece beam in real case. Therefore, assembly analyses are performed for 0º and 1º slope angles for Al 7075-T6 by selecting no penetration contact type and using soft springs to stabilize the model for simulating the real loading conditions (Figs. 4.38 and 4.39; Table 4.11).

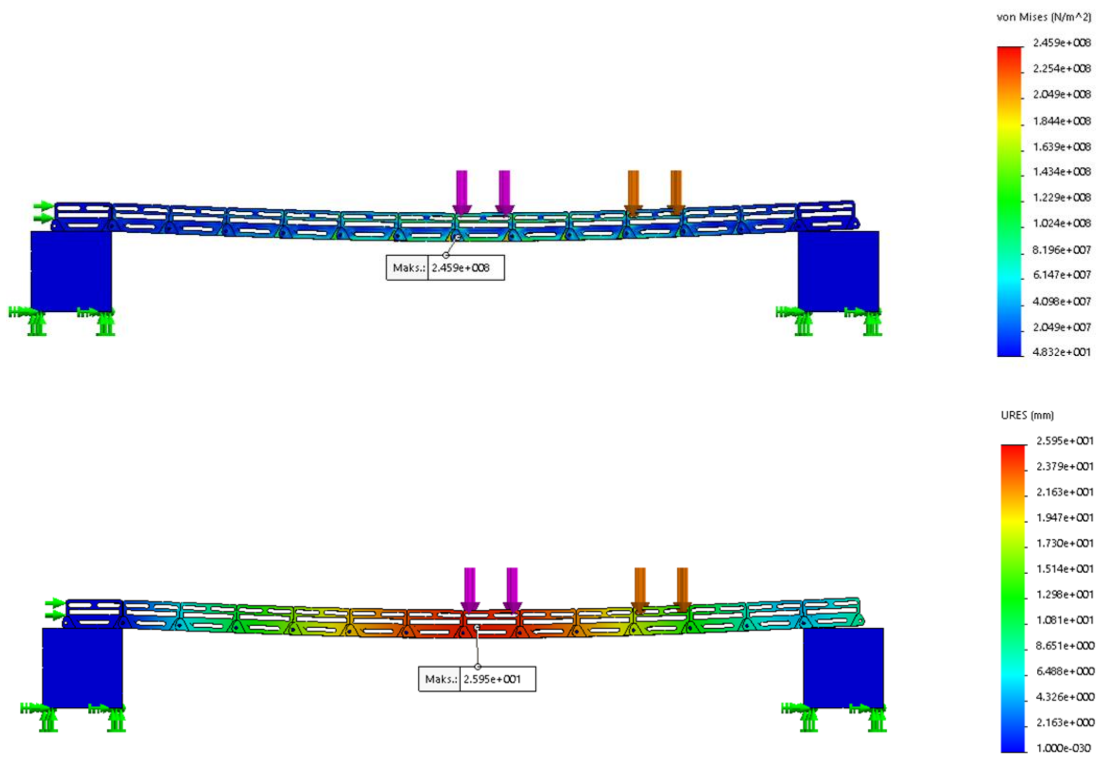

Figure 4.38 Stress and deflection analysis of link chain for Al 7075-T6, 0º slope angle

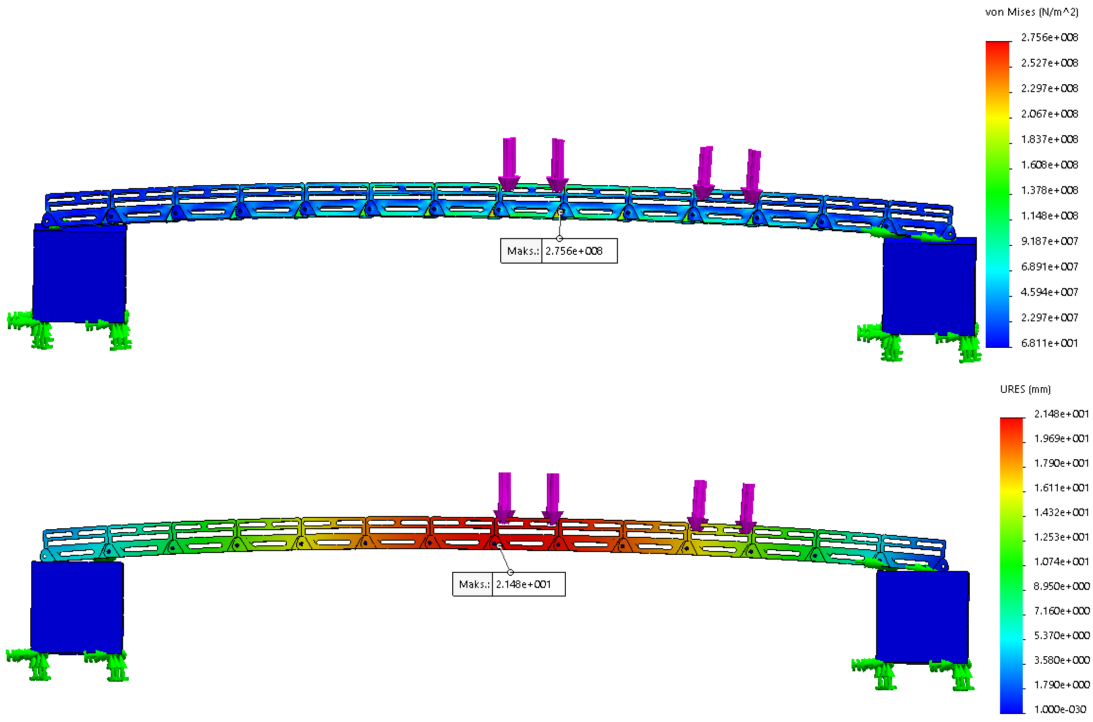

Figure 4.39 Stress and deflection analysis of link chain for Al 7075-T6, 1° slope angle

Table 4.11 Deflection and FOS Analysis of flat and curved link chains

Al 7075-T6			
Slope Angle (deg)	**Max. Deflection (mm)**	**Max. Stress (Mpa)**	**FOS**
0	25,95	245,9	2,05
1	21,48	242,9	2,08

According to the finite element analysis results, curved structures create horizontal reaction forces unlike a flat beam, thus it is expected that the load bearing capacity increases and deflection decreases. Even though the structure is slightly curved, this result can be observed in Table 4.11. Curved design is also used to prevent negative deflections under the level of the supports.

4.3.5 Deflection of a Simply-Supported Sandwich Beam with Antiplane Core and Thin Faces

The stresses and deflections in a sandwich beam as shown in Fig. 4.40 may be approximately found using the theory of bending presented in Section 4.3.2. An antiplane core is an idealized core in which the modulus of elasticity in planes parallel with the faces is zero but the shear modulus in planes perpendicular to the faces is finite. A honeycomb core can be considered an antiplane core and by this definition $E_c = 0$ and the antiplane core makes no contribution to the bending stiffness of the beam (Allen, 1969).

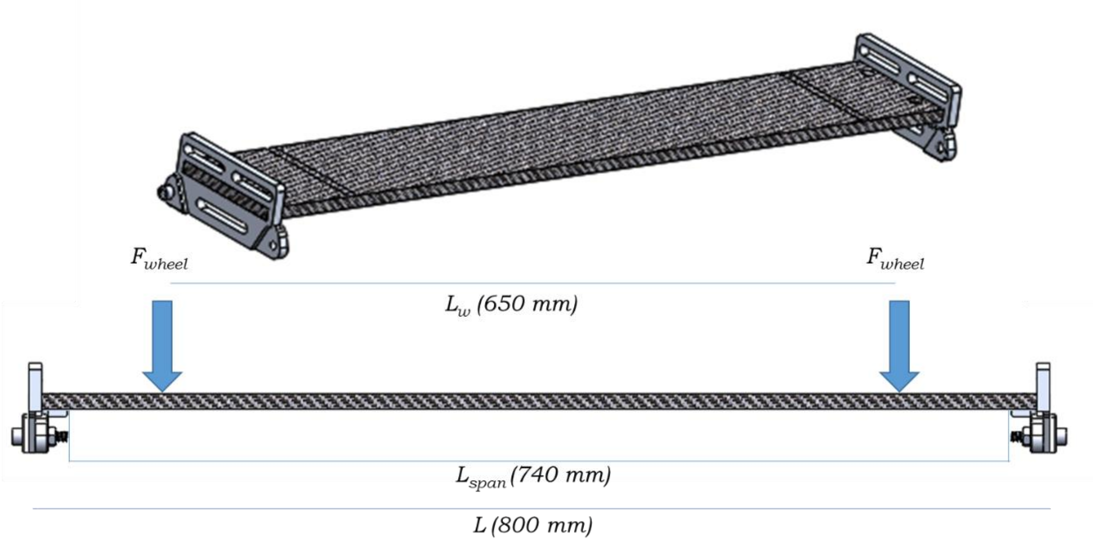

Figure 4.40 Sandwich composite panel loading conditions

The sandwich beam illustrated in Fig. 4.41 consists of two thin faces each of thickness t, separated by a thick core, of low density material of thickness c. The overall thickness of the beam is d and the width is b. All three layers are firmly bonded together and the face material is much stiffer than the core material. It is assumed that the face and core materials are both isotropic. As known, EI is the flexural rigidity (bending stiffness) for an ordinary beam with modulus of elasticity E and area moment of inertia I. It is convenient to denote the flexural rigidity by D. The sandwich beam in Fig. 4.38 is a composite beam, so its flexural rigidity is the sum of the flexural rigidities of the two separate parts, faces and core, measured about the neutral axis of the entire cross-section (Allen, 1969). However, the flexural rigidity of the core material generally provides no stiffness ($E_f \gg E_c$ where E_f and E_c are the moduli of elasticity of the faces and core respectively). Thus, the influence of flexural rigidity of the core can be neglected (Phang & Kraus, 1972).

$$D = E_f \frac{(d^3 - c^3)b}{12} \text{ (N·mm}^2\text{)} \tag{4.34}$$

Panel shear rigidity:

$$U = \frac{G(d+\mathrm{c})^2 b}{4\mathrm{c}} \text{ (N)} \tag{4.35}$$

where G is core shear modulus in MPa. The stresses in the faces and core may be determined using bending theory adapted to the composite nature of the cross-section.

$$\sigma_f = \frac{My}{D} E_f \qquad \left(\frac{c}{2} \leq y \leq \frac{d}{2}; \quad -\frac{d}{2} \leq y \leq -\frac{c}{2}\right) \tag{4.36}$$

$$\sigma_c = \frac{My}{D} E_c \qquad \left(-\frac{c}{2} \leq y \leq \frac{c}{2}\right) \tag{4.37}$$

As expected the maximum face and core stresses are obtained while $y = \pm d/2$ and $y = \pm c/2$ respectively. The assumptions of the theory of bending lead to Eq. (4.36) for the shear stress, τ, in a homogeneous beam at a depth *y*, below the centroid of the cross-section:

$$\tau = \frac{P}{(d+c)b} \tag{4.38}$$

where P is the shear force at the section under consideration. Sandwich panel deflection for four-point load, one-quarter span according to ASTM C-393 is as follows:

$$\Delta = \Delta_1 + \Delta_2 = \frac{11PL^3}{768D} + \frac{PL}{8U} \tag{4.39}$$

For a simply supported beam, shear deflection (Δ_2) is usually ignored because it has a very small effect on entire deflection compared to bending deflection (Δ_1). The central shear deflection of a sandwich composite beam can be calculated as $\frac{PL}{8U}$ where the bending moment at the center is $\frac{PL}{8}$ and U is the panel shear rigidity.

The loading conditions on the sandwich panel are illustrated in Fig. 4.41 and the necessary numerical data are given in Table 4.12.

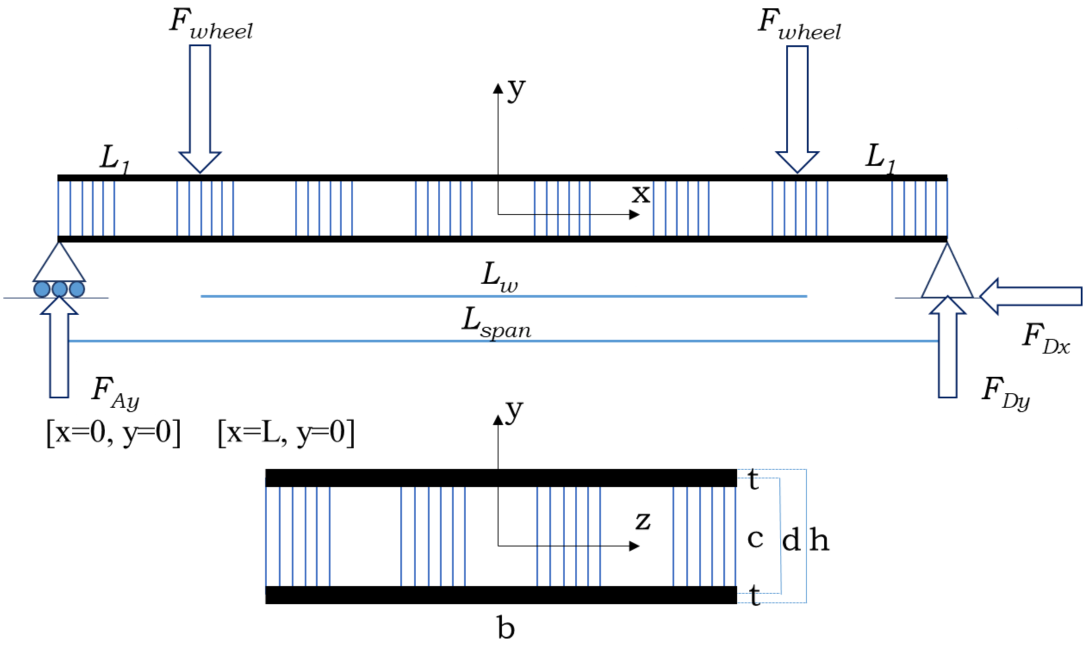

Figure 4.41 Determining the maximum deflection of the simply supported sandwich beam

Table 4.12 Design parameters for sandwich composite beam with 10 mm-thick Al honeycomb core

L_{span} (mm)	740
L_w (mm)	650
F_{wheel} (N)	1175
b (mm)	125
c (mm)	10
t (mm)	1,43
d (mm)	12,85

Force equilibrium for the sandwich panel results in $F_{Ay} = F_{Dy} = F_{wheel} = P$. Similar to Eq. 4.32, the deflection curve of the sandwich panel can be expressed as

$$Dy = \frac{P}{6}\left[(x^2 - L^2)x - \langle x - L_1\rangle^3 - \langle x - (L - L_1)\rangle^3 + \frac{(L-L_1)^3 + {L_1}^3}{L}x\right] \qquad (4.40)$$

Due to the symmetrical loading conditions on the panel, the maximum deflection occurs at the middle $x = L/2$ where the deflection is given by

$$Dy = \frac{P}{6}\left[(x^2 - L^2)x - (x - L_1)^3 + \frac{(L-L_1)^3 + {L_1}^3}{L}x\right] = \frac{PL_1}{6}\left(3x^2 - 3Lx + {L_1}^2\right) (4.41)$$

The shear force, bending moment and deflection diagrams are presented in Figs. 4.42, 4.43 and 4.44. The numerical data are summarized in Table 4.13.

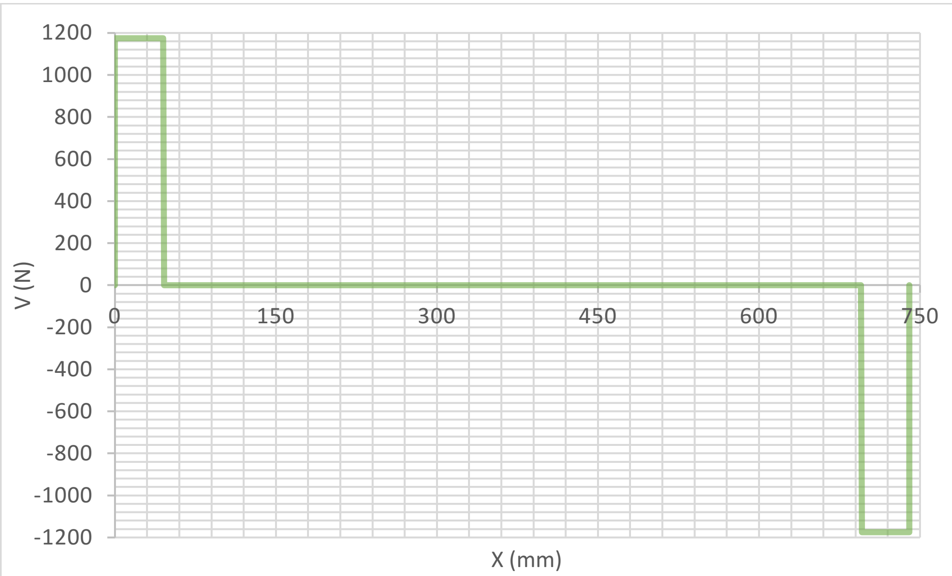

Figure 4.42 Shear Force Diagram of composite panel

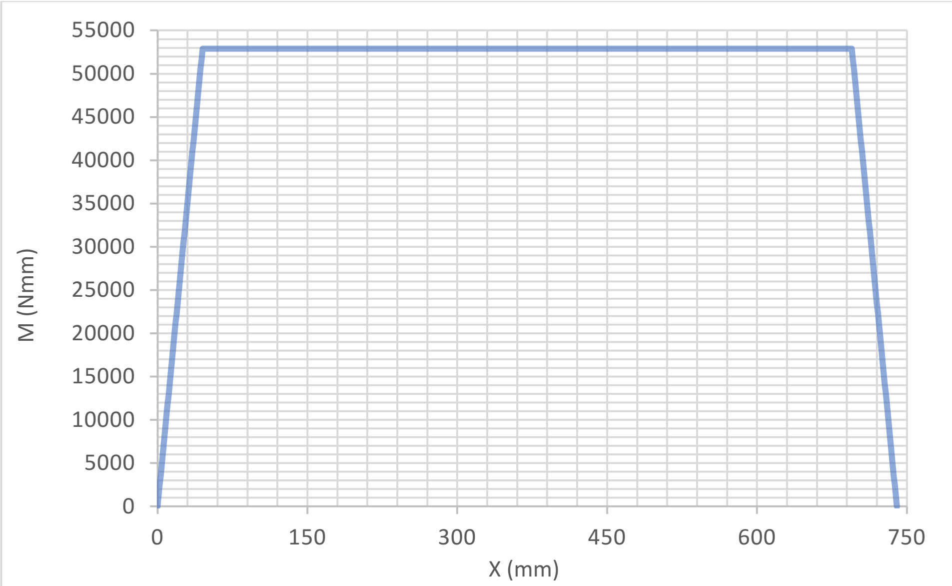

Figure 4.43 Bending Moment Diagram of composite panel

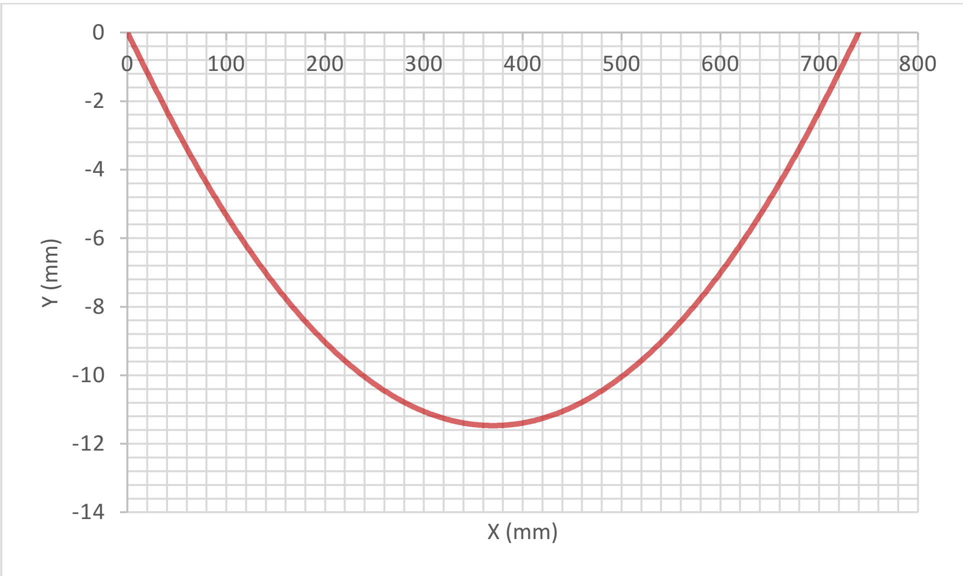

Figure 4.44 Deflection diagram of composite panel

Table 4.13 Loading conditions, material properties and deflection values for the composite panel

P (N)	1175
U (N)	275745,95
D (N·mm^2)	314020502
Bending Ultimate Strength (MPa)	118,307
Core Ultimate Shear Strength (MPa)	0,76
Face Bending Stress (MPa)	13,00
FOS for bending stress	9,1
Core Shear Stress (MPa)	0,41
FOS for Shear Stress (MPa)	1,85
y_{max} (mm)	-11,46

Factor of safety according to face bending stress is 9,1. However, sandwich beam's FOS should be determined according to core ultimate shear stress, because core gets damaged before face fracture occurs due to real loading conditions. FOS for shear stress is 1,85. However, FOS can be increased by increasing core thickness, face thickness and/or panel width or by using smaller cell sized Al honeycomb. limitations can be listed as:

- Core material cell size and thickness can be customized if there is a wholesale demand.
- Face thickness can be increased. This is an expensive solution and causes increasing total weight.
- Panel width is restricted by link length.

CHAPTER 5

PROTOTYPE AND TEST

Final prototype is manufactured step-by-step. Design verification of the prototype is conducted by testing the ramp under overloading conditions. Moreover, the field tests are also performed with 7 wheelchair users who have been using wheelchair at least for 1 year in order to ask their opinions and suggestions about prototype.

5.1 First full-scaled prototype

Ramp links are 3D printed with PLA filament to prevent possible design errors in terms of rolling and assembling ability (Fig. 5.1). Geometric tolerances are found to be fairly good for centering and assembling the connection axes providing rolling ability.

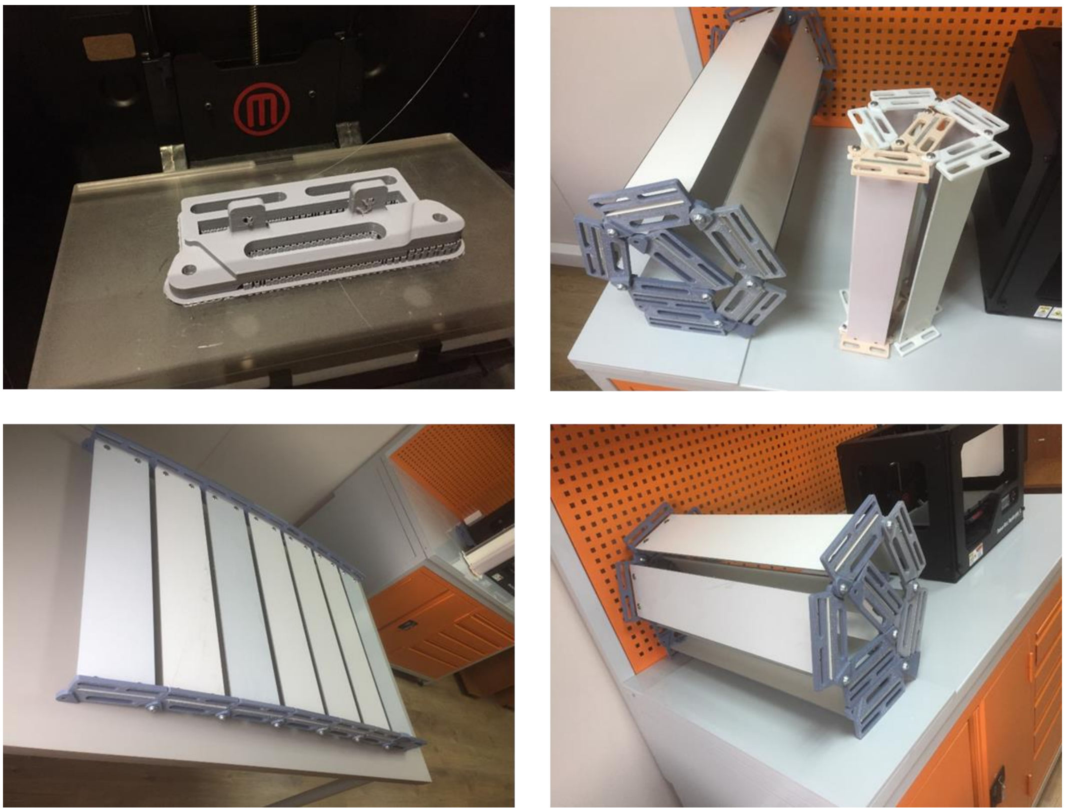

Figure 5.1 First full-scaled prototype

5.2 Final design and prototype

Final assembly is modeled in SolidWorks after geometric and strength calculations are completed. Handrails and telescopic legs may be assembled in case of requirement where the redundant materials are removed (Figs. 5.2 and 5.3; Table 5.1). Ramp length can be extended by adding modules. The whole structure should be supported by telescopic legs at every 14 module.

Figure 5.2 Final assembly illustration

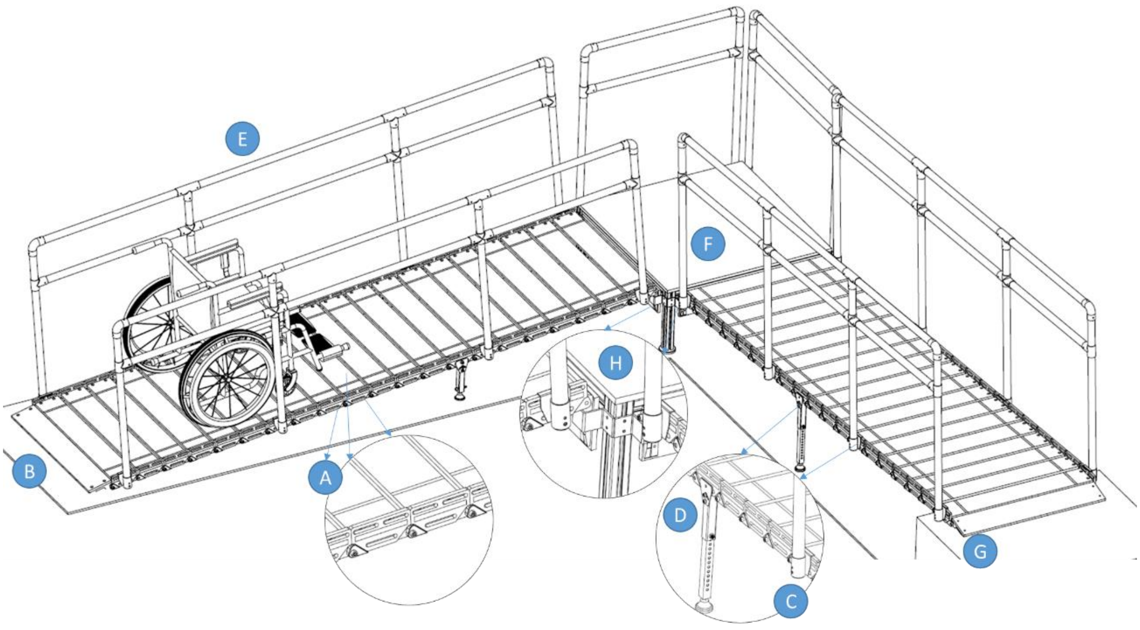

Figure 5.3 Assembling and positioning

Table 5.1 Components of the ramp assembly

A	Approach Plate
B	Approach Plate
C	Handrail's Mounting Bracket
D	Telescopic Legs
E	Handrails
F	Rotation Platform
G	Positioning of the First Module on a Flat Surface
H	Ramp Mounting Bracket

5.3 Manufacturing

Ramp manufacturing process is illustrated in Figure 5.4. First, ramp links and composite panels are manufactured. Then modules are formed by assembling 2 consecutive links with a composite panel. Then modules are assembled together to create a rollable ramp chain. Finally approach plates are assembled to each ends of the ramp to avoid elevation difference between ground and the ramp.

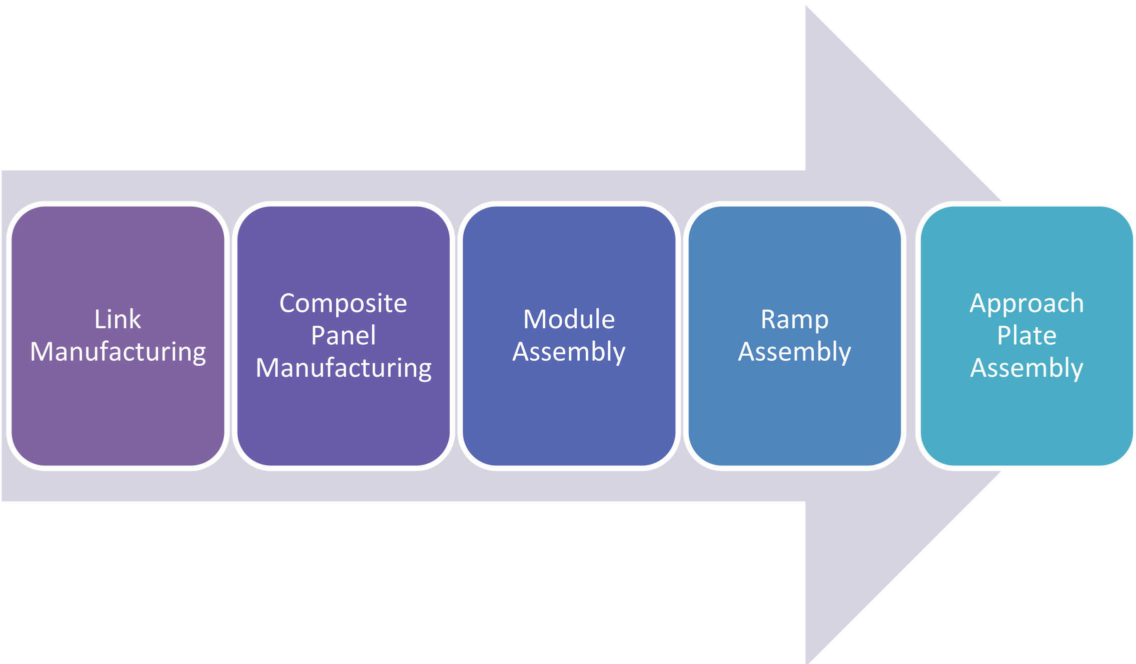

Figure 5.4 Manufacturing Steps

5.3.1 Link Manufacturing

Ramp links are manufactured with a CNC milling machine. Then, burrs are removed with various hand tools such as riffler, dremel and sandpapers. Geometric tolerances are controlled by assembling the links through their connection holes, before assembling the module.

Figure 5.5 Link manufacturing with CNC milling machine

5.3.2 Composite Panel Manufacturing

Sandwich composite panel manufacturing process starts with manufacturing carbon fiber face sheets with vacuum infusion technique (Fig. 5.6). Then, two face sheets are bonded with a 10 mm-thick aluminum honeycomb core with an epoxy adhesive and cured under vacuum pressure (Fig. 5.7). To prevent core-face separation, sandwich panels are cut with a CNC router machine according to design measurements and covered with one layer of prepreg and cured again with vacuum pressure (Fig. 5.8).

Figure 5.6 Face sheets manufacturing through vacuum infusion technique

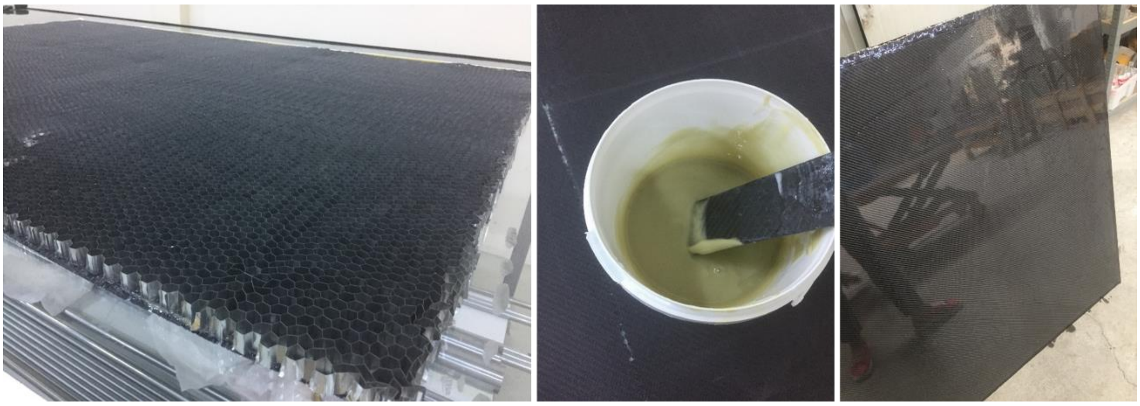

Figure 5.7 Bonding face sheets with aluminum honeycomb core

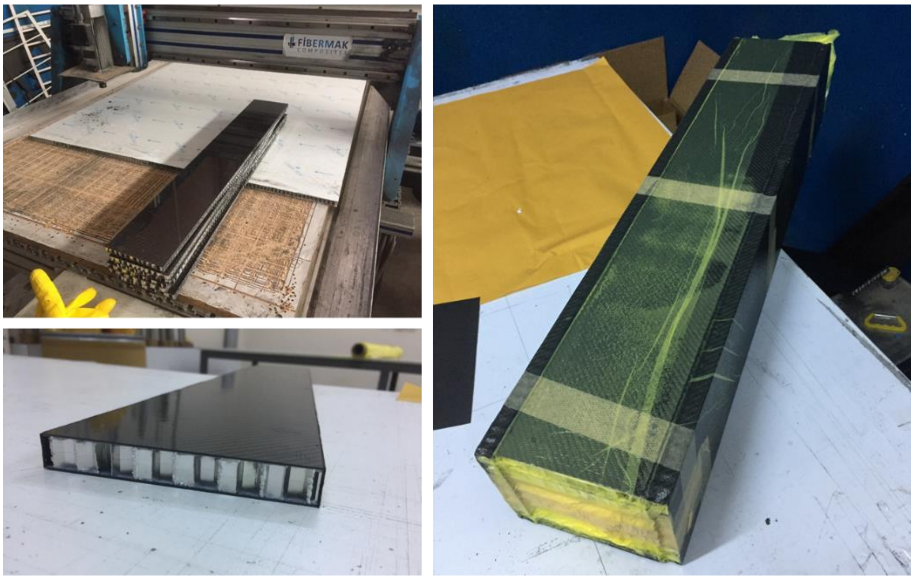

Figure 5.8 Covering sandwich panel with a layer of prepreg

5.3.3 Module Assembly

Modules are formed by assembling 2 aluminum links with a composite panel. First, composite panel is bonded to a link with an epoxy adhesive to prevent clearance between assembling gap on the link and composite panel. Then rivets are used for securing the connection (Fig. 5.9).

Figure 5.9 Module assembly

5.3.4 Ramp Assembly

Modules are assembled together to create the rollable ramp chain. Each module in assembly is able to rotate about their connection axes (Figs. 5.10 and 5.11).

Figure 5.10 Ramp assembly

Figure 5.11 1 m ramp in rolled position

5.3.5 Approach Plate Assembly

Approach plates are designed in order to make elevation difference between ground and ramp zero. The approach links are manufactured with a CNC milling machine, while the approach plate material is the same material as the load-bearing panels. Approach plates are bonded to approach links. Then the plates are assembled to each ends of the ramp. To avoid the slight elevation difference between the ground and approach plates, an aluminum sheet is bended and bonded at the end of the plate. Also a handle is assembled to the approach plates for easy carrying (Fig. 5.12).

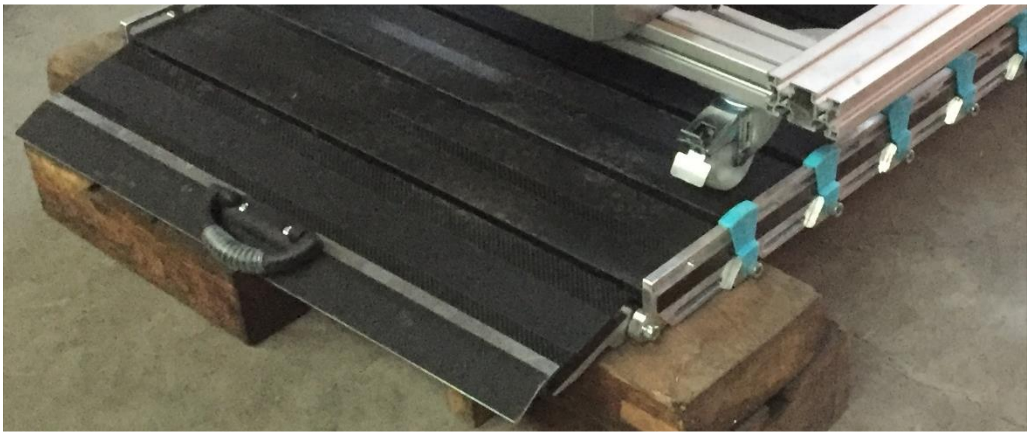

Figure 5.12 Approach plate

5.4 Field Test

Design verification of prototype is conducted by testing the ramp structure under the predetermined loading conditions. Firstly, ramp is loaded with 543 kg (Fig. 5.13), which is nearly two times greater than ramp's determined loading capacity (300 kg / 2m). Then, the field test is performed with 7 wheelchair users who have been used wheelchair at least for 1 year (Fig. 5.14).

Figure 5.13 Field test under overload

Figure 5.14 Field test with wheelchair users

Users' opinions and suggestions about prototype are taken during field test in terms of ramp width, load-bearing capacity, anti-slip surface sufficiency and efficiency. All of the participants indicated that anti-slip surface of the ramp is much more effective than any other fixed public ramps. Four of the participants found the ramp quite wide due to their narrower wheelchairs, and suggested that a narrower ramp may be more effective. All of the participants found the design practical to use in their daily life and claimed that they may purchase one. Two of the participants had their family members during field test and their opinions are also taken. Family members gave feedback about the general design, ease of use, weight and ease of storage and possible place of use. All feedbacks are positive in terms of satisfying users' expectations. One of the family members suggested that the ramp may not only be used for outdoor but also can be used for indoor such as shower stall.

CHAPTER 6

CONCLUSION

In this study, the design of a temporary ramp for wheelchair users is presented. The designed rollable ramp consists of serial chain members which are able to rotate about the connection axes. Geometrical calculations are conducted for achieving a better compactness while the ramp is in rolled form. In accordance with this purpose, several geometric patterns of ramp links are modeled both in SolidWorks and Excel with the help of convex hull and smallest enclosing circle algorithms to find optimal link length and shapes. Strength calculations are conducted for a simply supported beam model for determining height and thickness of the links. Then, blanks are designed in SolidWorks to make the link structure lighter.

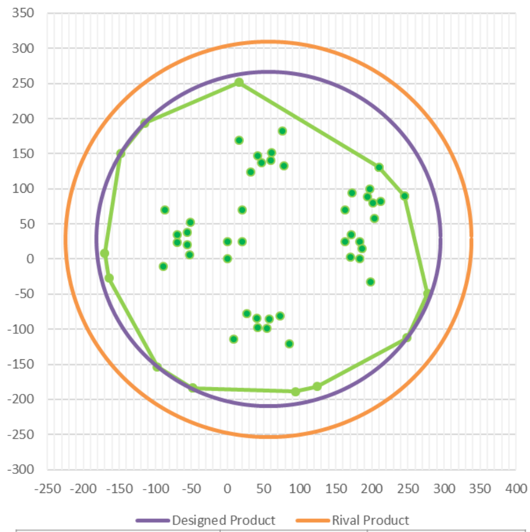

	Rival Product	Designed Product
Diameter (mm) for 1,5 m	563	476,24
Weight per meter (kg)	7,78	6,31

Figure 6.1 Comparison of the rival and designed product

The designed ramp is 15,4% more compact and has 18,87% less weight compared to the best rival product available in the market (Fig. 6.1). At the end of the study field test is performed to get users' opinions and suggestions about the new design.

REFERENCES

1800Wheelchair.com (n.d.). Heavy Duty Power Wheelchairs. Retrieved June 05, 2017, from http://www.1800wheelchair.com/category/heavy-duty-power-chairs/

Ambrose, G., & Harris, P. (2010). Design thinking. Lausanne: AVA Academia.

Anderson, K. (1978). A reevaluation of an efficient algorithm for determining the convex hull of a finite planar set. Information Processing Letters, 7(1), 53-55.

Ashby, M. F. (2005). Materials selection in mechanical design. Amsterdam; Boston: Butterworth-Heinemann, 2005.

Askeland, D. R., & Phulâe, P. P. (2006). The science and engineering of materials. Southbank, Victoria, Australia: Thomson, c2006, 402-411.

Aulicino, K. (2006). Roll Up Ramp System. U.S. Patent No. 20,060,214,456 A1. Washington, DC: U.S. Patent and Trademark Office.

Beer, F. P., Johnston, E. R., & DeWolf, J. T. (2001). Mechanics of materials. New York: McGraw-Hill, 2002.

Berg, M., Cheong, O., Kreveld, M., & Overmars, M. (2008). Computational Geometry. [electronic resource]: Algorithms and Applications. Berlin, Heidelberg: Springer Berlin Heidelberg, 2008, 1-8.

Boone, F., J. (1994). Tailgate Enclosed Telescopic Ramp Structure. U.S. Patent No. US5312149 A. Washington, DC: U.S. Patent and Trademark Office.

Breslin, W., P. & Shoen, M., V. (1998). Telescoping Truck Loading Ramp Assembly. U.S. Patent No. US5813071 A. Washington, DC: U.S. Patent and Trademark Office.

Brown, T. (2008). Design thinking. Harvard Business Review, 84-93. Retrieved 10 May, 2014, from http://www.ideo.com/images/uploads/thoughts/IDEO_HBR_Design_Thinking.pdf

Brown, T. (2009). Change by design: How design thinking transforms organizations and inspires innovation. New York: Harper Business.

Carlsson, L. A., Kardomateas, G. A. (2011). Structural and Failure Mechanics of Sandwich Composites. Dordrecht: Springer.

Carter, C. D. (2011). Multi Tread Segmented Self Deploying Roll Up Ramp. Patent No. US7958586

Chen, S., & Venkatesh, A. (2013). An investigation of how design-oriented organisations implement design thinking. Journal of Marketing Management, 29(15/16), 1680-1700.

Çınar, H. T., & Erdem, H. T. (2008). Yaşam hakkı: tekerlekli sandalye kullanıcılarının konut iç mekan donatı elemanları ve mobilya kullanımı. Politeknik Dergisi, 11(2), 169.

Daniel, I. M., & Abot, J. L. (2000). Fabrication, testing and analysis of composite sandwich beams. Composites Science and Technology, 602455-2463. doi:10.1016/S0266-3538(00)00039-7

Frost, K. L., Bertocci, G., & Smalley, C. (2015). Ramp-Related Incidents Involving Wheeled Mobility Device Users During Transit Bus Boarding/Alighting. Archives of Physical Medicine And Rehabilitation, (5), 928.

Ingle, B. R. (2013). Introduction to Design Thinking. Design thinking for entrepreneurs and small businesses: putting the power of design to work: Apres, 2-15.

Jarvis, R. (1973). On the identification of the convex hull of a finite set of points in the plane. Information Processing Letters, 218-21.

Jones, R. P. (2002). Stowable load ramp for Vehicles. U.S. Patent No. 6,378,927 B1. Washington, DC: U.S. Patent and Trademark Office.

Justak, J. (2013). Telescoping and Magnetic Tailgate Ramp. U.S. Patent No. 20,130,028,693 A1. Washington, DC: U.S. Patent and Trademark Office.

Kaufman, J. G. (2000). Introduction to aluminum alloys and tempers. Materials Park, OH: ASM International, 9-22.

Kenny, M. (2011). Extendable ramp for storage in a tailgate or flat bed. U.S. Patent No. 20,110,072,596 A1. Washington, DC: U.S. Patent and Trademark Office.

Kim, C. S., Lee, D., Kwon, S., & Chung, M. K. (2014). Effects of ramp slope, ramp height and users' pushing force on performance, muscular activity and subjective ratings during wheelchair driving on a ramp. International Journal of Industrial Ergonomics, 44636-646.

Lockwood, T. (2009). Design Thinking: Integrating Innovation, Customer Experience, and Brand Value. New York, NY: Allworth Press.

Martinez, J. (2002). Portable Ramp With Transport Facilitators. U.S. Patent No. 20,020,108,190 A1. Washington, DC: U.S. Patent and Trademark Office.

Mathew, D. (2016). GrabCAD - CAD library. Retrieved September 10, 2016, from https://grabcad.com/library/wheelchair-18.

Meyers, A. R., Anderson, J. J., Miller, D. R., Shipp, K., & Hoenig, H. (2002). Barriers, facilitators, and access for wheelchair users: substantive and methodologic lessons from a pilot study of environmental effects. Social Science & Medicine, 551435-1446.

Mootee, I. (2013). Design thinking for strategic innovation: What they can't teach you at business or design school. Hoboken, NJ: John Wiley & Sons, 16-69.

O'Sullivan, B. (2002). Constraint-aided Conceptual Design. London: John Wiley and Sons, Inc, 9.

Pahl, G., Beitz, W., Feldhusen, J., & Grote, K. (2007). Engineering Design. [electronic resource]: A Systematic Approach. London: Springer London: Imprint: Springer, 2007, 74-184.

Rana. S., R., Rajesh, P., & S, D. (2012). Reviews on the Influences of Alloying elements on the Microstructure and Mechanical Properties of Aluminum Alloys and Aluminum Alloy Composites.

Schmaltz, D. et al. (2002). Loading ramp device which rolls up for storage. U.S. Patent No. 20,020,088,065 A1. Washington, DC: U.S. Patent and Trademark Office.

Schmaltz, D. et al. (2003). Loading ramp device which rolls up for convenient storage. U.S. Patent No. 6,643,878 B2. Washington, DC: U.S. Patent and Trademark Office.

Sheldon, S., & Jacobs, N. A. (2007). Report of a consensus conference on wheelchairs for developing countries: Bengaluru, India 6-11 November 2006.

Silva, N., Kanuwana, N., Bandara, P., Jayalath, S., Mendis, R., & Costa, S. (2015). Assessment of the suitability of ramps for wheel chair access among public buildings in Colombo Sri Lanka. Physiotherapy, 719.

Skyum, S. (1991). A simple algorithm for computing the smallest enclosing circle. Information Processing Letters, 37(3), 121-125.

Songmene, V., Djebara, A., Zaghbani, I., Kouam, J., & Khettabi, R. (2011). Machining and Machinability of Aluminum Alloys. INTECH Open Access Publisher (377-398).

Vianna, M., Vianna, Y., Adler, I. K., Lucena, B., & Russo, B. (2012). Design Thinking: Business Innovation. Rio de Janeiro: MJV Press.

Winter, A., & Hotchkiss, R. (2006). Mechanical Principles of Wheelchair Design. Retrieved January 5, 2016 from http://web.mit.edu/sp.784/www/DOCUMENTS/Wheelchair Manual-Final.pdf.

Wong, V. (2009). How Business Is Adopting Design Thinking. Retrieved October 24, 2014, from http://www.businessweek.com/stories/2009-11-03/how-business-is-adopting-design-thinkingbusinessweek-business-news-stock-market-and-financial-advice.